CHARACTERIZATION OF A SACRAL DORSAL COLUMN PATHWAY ACTIVATING AUTONOMIC AND HINDLIMB MOTOR PATTERN GENERATION

A Dissertation
Presented to
The Academic Faculty

by

JoAnna Todd Anderson

In Partial Fulfillment
of the Requirements for the Degree
Doctor of Philosophy in the
Interdisciplinary Bioengineering Graduate Program
Department of Biomedical Engineering

Georgia Institute of Technology
December 2011

CHARACTERIZATION OF A SACRAL DORSAL COLUMN PATHWAY ACTIVATING AUTONOMIC AND HINDLIMB MOTOR PATTERN GENERATION

Approved by:

Dr. Shawn Hochman, Advisor
Department of Physiology
Emory University School of Medicine

Dr. Stephen P. DeWeerth, Advisor
Department of Biomedical Engineering
Georgia Institute of Technology

Dr. Robert Butera
School of Electrical and Computer Engineering
Georgia Institute of Technology

Dr. T. Richard Nichols
School of Applied Physiology
Georgia Institute of Technology

Dr. Peter Wenner
Department of Physiology
Emory University School of Medicine

Date Approved: September 28, 2011

ACKNOWLEDGEMENTS

I would like to thank the many people who have supported me throughout my time as a graduate student. Thank you to my advisors, Dr. Shawn Hochman and Dr. Stephen P. DeWeerth, for their encouragement and guidance in shaping this research. Thank you to my committee, Dr. Robert Butera, Dr. T. Richard Nichols, and Dr. Peter Wenner, for their thoughtful input. Being a part of two research groups, I have had the pleasure to work with so many wonderful people, whom I would like to thank for their advice and camaraderie: Edgar Brown, Dr. Stefan Clemens, Dr. Elizabeth Gozal, Dr. Liang Guo, Gareth Guvanasen, Dr. Heather Hayes, Michelle Kuykendal, Dr. Kathleen Meacham, Dr. Shane Migliore, Dr. Jeremiah Mitzelfelt, Donald Noble, Brannan O'Neill, Michael Sawchuk, Jacob Shreckengost, Sarah Steinmetz, Dr. Kartik Sundar, Christopher Tuthill, Jason White, and Amanda Zimmerman. Thank you to Chris Ruffin, Shannon Sullivan, and Sally Gerrish for being wonderfully helpful resources in the Bioengineering program and the Biomedical Engineering department. Thank you to the National Science Foundation for five years of research support through the IGERT and GRF programs. Finally, thank you to my family—especially my parents, Joel and Elaine Todd, my brother, Gregory Todd, and my grandmother, Ann Turner—and my husband, Doug, for their unconditional love and many years of unwavering support.

TABLE OF CONTENTS

LIST OF TABLES

Page

LIST OF FIGURES

Page

LIST OF ABBREVIATIONS

5-HT	serotonin or 5-hydroxytryptamine
ACh	acetylcholine
aCSF	artificial cerebrospinal fluid
ANS	autonomic nervous system
AR	adrenergic receptor
ATP	adenosine triphosphate
atr	atropine
BTX	α-bungarotoxin
c	contralateral
CAP	compound action potential
CNS	central nervous system
CPG	central pattern generator
DA	dopamine
DHBE	dihydro-β-erythroidine
DR	dorsal root
EDRO	edrophonium
EMG	electromyographic
GABA	gamma-aminobutyric acid
HLR	hypothalamic locomotor region
i	ipsilateral

IML	intermediolateral
LG	lateral gastrocnemius, ankle extensor
LLA	locomotor-like activity
mAChR	muscarinic acetylcholine receptor
mec	mecamylamine
MLA	methyllycaconitine
MLR	mesencephalic locomotor region
NA	noradrenaline
nAChR	nicotinic acetylcholine receptor
NMDA	N-methyl-D-aspartate
P	postnatal day
praz	prazosin
SCA	sacrocaudal afferent
SCI	spinal cord injury
sDC	sacral dorsal column
sDR	sacral dorsal root
SM	semimembranosus, knee flexor
SNS	somatic nervous system
SPN	sympathetic preganglionic neuron
STFT	short-time Fourier transform
TA	tibialis anterior, ankle flexor
TRPV1	transient receptor potential vanilloid-1
TTX	tetrodotoxin

tub	d-tubocurarine
VL	vastus lateralis, knee extensor
VR	ventral root
xT	times afferent volley recruitment threshold
yoh	yohimbine

SUMMARY

Spinal cord injuries (SCI) sever communication between supraspinal centers and the central pattern generator (CPG) responsible for locomotion. Because the CPG is intact and retains the ability to initiate locomotor activity, it can be accessed electrically and pharmacologically. The goal of this thesis was to identify and characterize a novel spinal cord surface site along the sacral dorsal column (sDC) for electrically evoking locomotor-like activity in the neonatal rat spinal cord. Stimulation of the sDC robustly activated rhythmic left–right alternation in flexor-related ventral roots that was dependent on the activation of high-threshold C fiber afferents. The C fibers synapsed onto spinal neurons, which project to the lumbar segments as part of a pathway dependent on purinergic, adrenergic, and cholinergic receptor activation. In ventral roots containing only somatic efferents, rhythmic activity was rarely recruited. However, in ventral roots containing both autonomic and somatic efferents, sacral dorsal column stimulation recruited autonomic efferent rhythms, which subsequently recruited somatic efferent motor rhythms. The efferent rhythms revealed a half-center organization with very low stimulation frequencies, and the evoked alternating bursts entrained to the stimuli. Similar entrainment was seen when sDC stimuli were applied during ongoing neurochemically-induced locomotor rhythms. The rhythmic patterns evoked by sDC stimulation operated over a limited frequency range, with a discrete burst structure of fast-onset, frequency-independent peaks. In comparison, neurochemically-induced locomotor bursts operated over a wide frequency range and had slower time to peaks that varied with burst frequency. The overall findings support the discovery of an autonomic

efferent pattern generator that is recruited by sacral visceral C fiber afferents. It is hoped that this research will advance the understanding of afferent activation of the lumbar central pattern generator and potentially provide insight useful for future development and design of neuroprosthetic devices.

CHAPTER 1

INTRODUCTION

Spinal cord injuries (SCIs) impair the function of body below the level of the injury because the brain can no longer communicate with the neurons below this level. However, the neuronal circuits located below this injury may still be functional; they are just no longer receiving descending commands to operate and modify them. Understanding the inner-workings of the spinal cord is critical to developing efficient methods for regaining lost functionality for spinal cord injury patients. One circuit of interest for functional recovery is the locomotor central pattern generator (CPG). Electrical stimulation of the spinal cord is one method that has proven itself as a viable option for recovering locomotor function (Dimitrijevic et al. 1998; Gerasimenko et al. 2002; Gerasimenko et al. 2008) and blocking the transmission of pain (Lindblom and Meyerson 1975; Oakley and Prager 2002). However, little emphasis has been placed on understanding how this stimulation results in functional recovery. Instead, the spinal cord is viewed as a hypothetical "black box" where only inputs and outputs were important.

This research aims to identify a potential site on the spinal cord surface suitable for evoking the lumbar central pattern generator, study the afferent inputs required for generating the rhythm, dissect the spinal components involved in the transmission pathway, and characterize the efferent outputs resulting from the electrical stimulation. By systematically investigating each portion of the pathway, the capabilities of the spinal

cord after injury will be better understood with the potential to apply this newfound knowledge to the design and implementation of future neuroprosthetic devices.

1.1 The spinal cord

The spinal cord is a part of the central nervous system (CNS). It acts as a connection for information transfer between the brain and the rest of the body while also serving as a processing center to coordinate complex sensory, motor, and autonomic functions. It is organized into gray and white matter areas. The gray matter, which contains the neuronal cell bodies organized into laminae (Figure 1.1a), is interior to the white matter, which contains axon tracts organized topographically. Furthermore, the spinal cord is organized into segments: cervical, thoracic, lumbar, and sacral (Figure 1.1b). Cervical segments contain circuitry for controlling the neck, diaphragm, and forelimb function. Thoracic segments control trunk musculature. The caudal thoracic segments and lumbar segments of the spinal cord contain spinal circuits that control hindlimb function. The sacral segments contain circuitry controlling bladder, bowel, and sexual function along with musculature of the tail. Sensory information enters the spinal cord through dorsal roots, which can either synapse onto spinal neurons, largely within the dorsal horn, or project rostrocaudally via white matter axon tracts (Figure 1.1c). The ventral horn and intermediate zone contain neural elements associated with motor output. These neurons receive input from both sensory systems as well as descending signals from the brain. Motoneurons axons exit the spinal cord via ventral roots to innervate various muscles throughout the body.

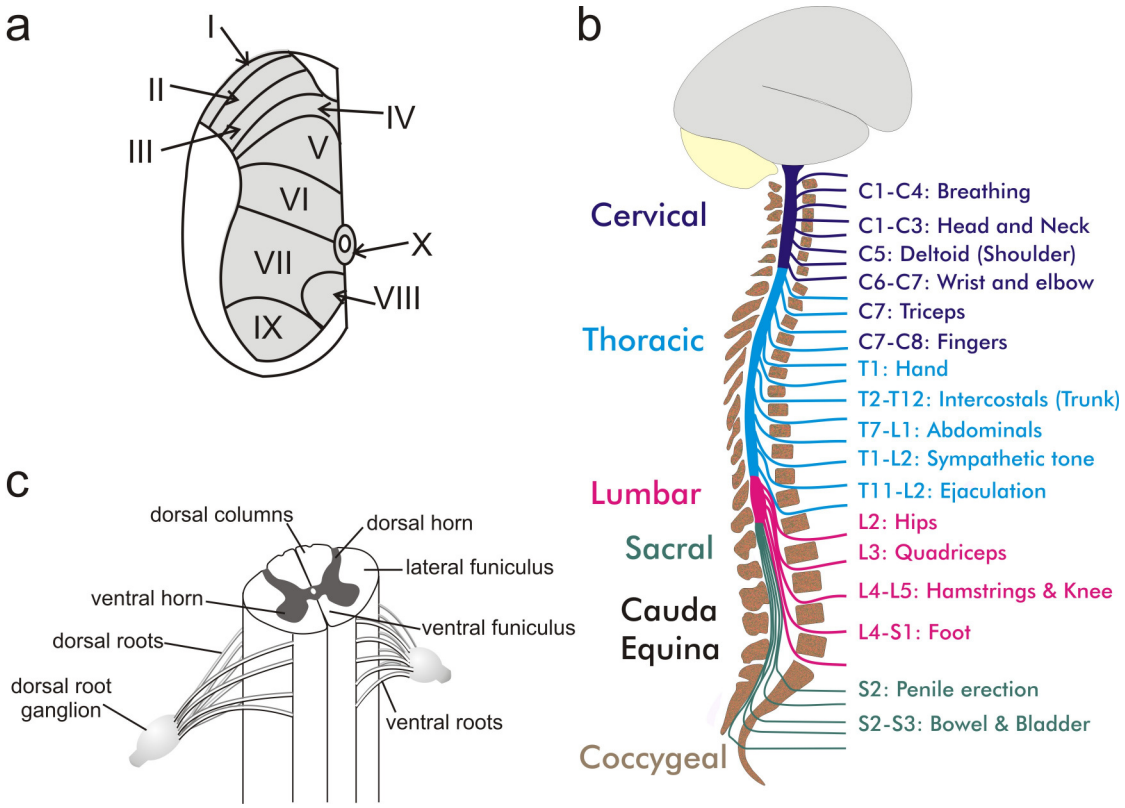

Figure 1.1: Anatomy of the spinal cord

(a) Laminar divisions of the spinal cord gray matter. Laminae I-VI are dorsal horn; laminae VII-X are ventral horn. (b) Segmental divisions of the human spinal cord. The spinal cord is divided into cervical, thoracic, lumbar, sacral and coccygeal segments. The cauda equina consists of the bundle of nerve roots, which descend within the spinal column after exiting the spinal cord but before traveling through vertebral segments. (c) Transverse view of spinal cord with major anatomical features labeled including dorsal and ventral roots, dorsal and ventral horn, and the dorsal column white matter tract.

1.1.1 Somatic and autonomic nervous systems

The nervous system is divided into two components: the central nervous system, which is composed of the brain and spinal cord, and the peripheral nervous system, which is composed of the nerves and ganglia outside the brain and spinal cord, including dorsal root ganglia. The peripheral nervous system is further divided into the somatic and autonomic nervous systems. The somatic nervous system (SNS) is associated with voluntary movements and controls skeletal muscle and its sensations. The autonomic nervous system (ANS) is associated with involuntary actions and controls smooth muscle, cardiac muscle, and exocrine glands, which are involved in subconscious actions such as respiration, digestion, and circulation. While these two systems seem quite disparate, there is convergence of autonomic and somatic innervation on some target organs, such as the bladder, which has autonomic innervation to help identify bladder fullness and somatic innervation of the sphincter to aid in voiding. These two systems work in parallel with the ANS acting continuously, but rarely at a conscious level (Kandel et al. 2000).

1.1.2 Divisions of the autonomic nervous system

The ANS is further divided into the sympathetic, parasympathetic and enteric nervous systems. The sympathetic nervous system is responsible for the classic "fight or flight" phenomenon, while the parasympathetic nervous system is responsible for "rest and digest" actions. The sympathetic and parasympathetic nervous systems (Figure 1.2), in general, exert opposing actions on many bodily organs, such as the heart. They work to maintain a balance within the body and regulate involuntary functions in response to

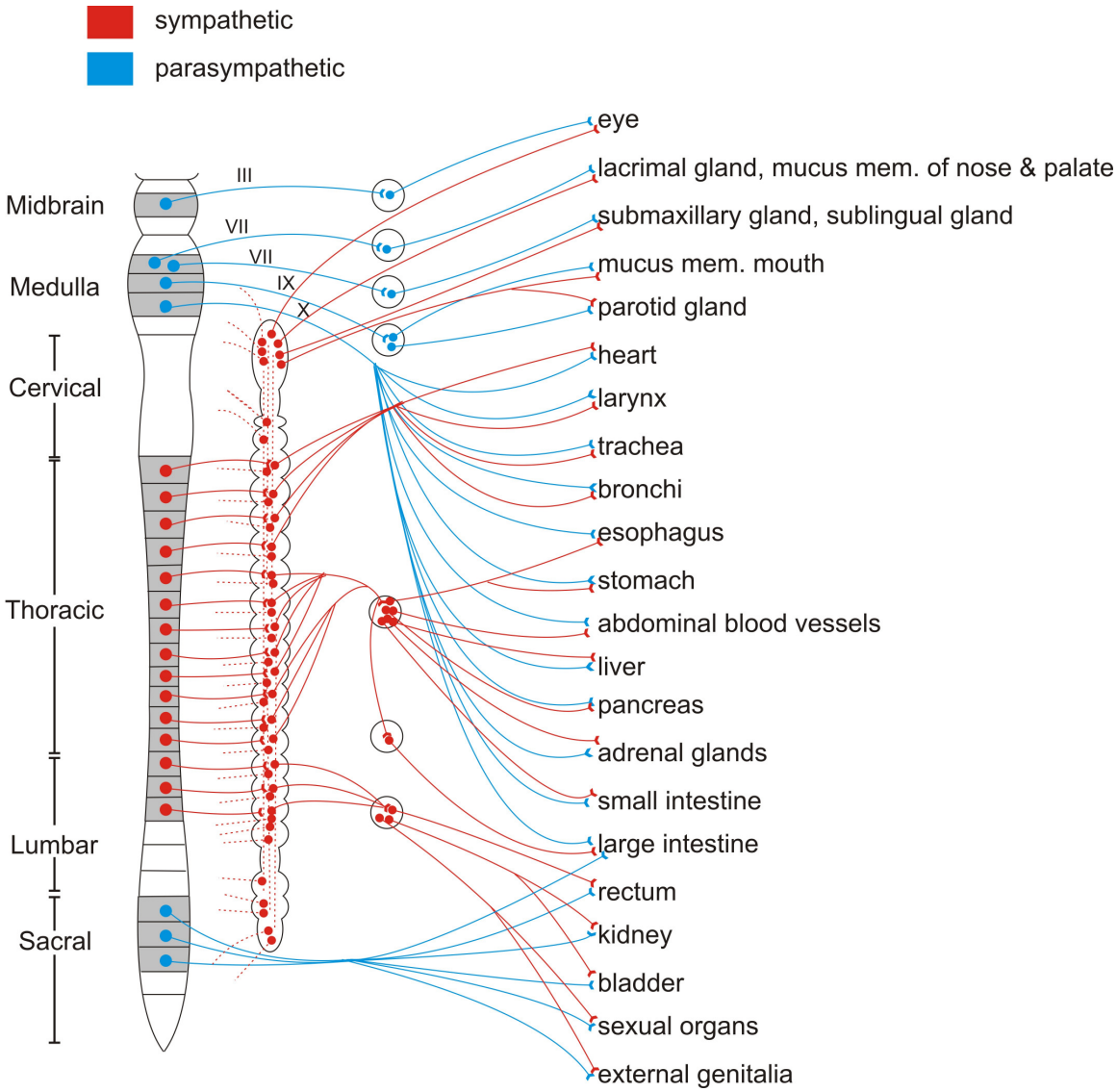

Figure 1.2: Organization of the autonomic nervous system
The autonomic nervous system organization with red indicating the sympathetic nervous system and blue indicating the parasympathetic nervous system. The sympathetic chain located adjacent to the spinal cord contains the SNS postganglionic neurons while parasympathetic postganglionic neurons are located near the target organ. Adapted from Gray's Anatomy, 20th edition (Gray 1918).

continually changing external conditions in order to maintain a stable internal stable environment (Kandel et al. 2000).

The sympathetic and parasympathetic divisions of the autonomic nervous system both use pre- and postganglionic neurons for transmission of signals to peripheral targets, but are organized in distinctly different ways. The sympathetic nervous system's preganglionic neurons are located within the spinal cord in the intermediolateral (IML) cell column within. These neurons are arranged in a ladder-like formation reaching from the lateral funiculus through the IML to the central canal (Strack et al. 1988). Sympathetic nervous system preganglionic neurons have short axons that form cholinergic synapses onto postganglionic neurons housed within the sympathetic chain. The sympathetic chain lies outside of the spinal vertebral column along the ventral surface of the rib cage and extends from thoracic segment T1 to the upper lumbar segment L2 in the rat (Strack et al. 1988). Postganglionic neurons, with few exceptions, release norepinephrine to act on adrenergic receptors on the target organ (Kandel et al. 2000).

The sympathetic chain contains one ganglion per sympathetically innervated spinal segment. Sympathetic preganglionic efferents exit the spinal cord in the ventral root, which also contains somatic efferents. The sympathetic efferents split off from the somatic efferents, forming white rami that innervate the sympathetic postganglionic neurons either at the same spinal segment or by traveling rostrocaudally in the sympathetic cord to neighboring segments (Janig 2006).

The parasympathetic nervous system's preganglionic neurons have origins in cranial nerves VII, IX, and X as well as lower lumbar and upper sacral segments L6-S1 in

the rat (Contreras et al. 1980; Nadelhaft and Booth 1984). Parasympathetic preganglionic neurons project distally with long axons to the parasympathetic postganglionic neurons located close to the target organ of innervation. Both the preganglionic and postganglionic parasympathetic neurons use acetylcholine as their neurotransmitter. The preganglionic neurons release acetylcholine that acts on nicotinic receptors on the postganglionic neurons, which then release acetylcholine to act on muscarinic receptors on the target organ (Kandel et al. 2000).

1.1.3 Acetylcholine receptors

Acetylcholine is an essential neurotransmitter to both somatic and autonomic function. Acetylcholine is released from motoneurons to act at the neuromuscular junction causing muscle contraction, and it is a major neurotransmitter in the autonomic nervous system, both for sympathetic and parasympathetic branches. Acetylcholine acts on receptors divided into two classes: nicotinic acetylcholine receptors (nAChRs) and muscarinic acetylcholine receptors (mAChRs) (Kerlavage et al. 1986).

1.1.3.1 Nicotinic acetylcholine receptors

Nicotinic cholinergic receptors are a class of well-studied ionotropic receptors found throughout the nervous system. They are a member of the Cys-loop family of ligand-gated receptors, which also includes $GABA_A$, strychnine-sensitive glycine, and 5-HT_3 receptors (Alexander et al. 2008; Millar and Gotti 2009). There are five classes of nicotinic subunits—alpha, beta, gamma, delta, and epsilon—which combine into a pentameric configuration containing various configurations of these subunits. In the vertebrate nervous system, 17 nAChR subunits have been identified: $\alpha_{1\text{-}10}$, $\beta_{1\text{-}4}$, γ, δ, and ε (Itier and Bertrand 2001; Graham et al. 2002; Kalamida et al. 2007; Alexander et al.

2008). These subtypes are divided into neuronal-type and muscle-type subunits based on their proclivity to form receptors on specific cell types. Nicotinic receptors are non-selective cation channels permeable to sodium, potassium, and calcium depending on the subunit configurations (Kerlavage et al. 1986; Fucile 2004).

Nicotinic receptors forming in the membranes on neurons are composed only of alpha and/or beta subunits (Itier and Bertrand 2001; Alexander et al. 2008). They may either form homomeric or heteromeric pentamers with the configuration determining the biophysical properties of the channel. Receptors containing α_7, α_9, or $\alpha_9\alpha_{10}$ subunits are sensitive to α-bungarotoxin, while other nAChRs are insensitive to α-bungarotoxin (Johnson et al. 1995; McIntosh et al. 2009). Of the dozens of possible subunit combinations, combinations containing $\alpha_4\beta_2$, $\alpha_3\beta_2$, and α_7 subunits have been found in the spinal cord of the rat (Millar and Gotti 2009) and localized to the IML cell column, the ventral horn, and central gray (Wada et al. 1989). In the spinal cord, cholinergic interneurons have been identified which receive synapses from myelinated and unmyelinated primary afferent fibers (Olave et al. 2002). Cholinergic interneurons have also been implicated to have direct effects on the lumbar CPG and motoneurons in the neonatal rat spinal cord (Deuchars 2007; Anglister et al. 2008).

1.1.3.2 Muscarinic acetylcholine receptors

Muscarinic receptors are members of a class of 7TM, or G-protein coupled, metabotropic receptors (Alexander et al. 2008). Largely associated with the autonomic nervous system, this receptor is associated with functions of the eye, airway, heart rate, smooth muscle, and glandular secretions (Kerlavage et al. 1986). Currently, there are five distinct muscarinic subtypes, M1-M5. Muscarinic receptors possess two allosteric

binding sites, one defined by binding gallamine, strychnine, and brucine, while the other binds KT5720; WIN62,577; WIN71,708; and staurosporine (Lazareno et al. 2000, 2002; Alexander et al. 2008). The M2-M4 mAChR subtypes have been identified in the rat spinal cord (Hoglund and Baghdoyan 1997) and are found in white and gray matter of the spinal cord (Oguz Kayaalp and Neff 1980). M2 and M3 receptors are distributed in the dorsal horn where nociceptive Aδ and C fibers terminate (Hoglund and Baghdoyan 1997) and play a role in mediating antinociceptive effects (Naguib and Yaksh 1997).

1.1.4 Adrenaline/noradrenaline receptors

Like the acetylcholine receptors, adrenergic receptors (ARs) are important receptors in the autonomic nervous system. The monoamine neurotransmitters adrenaline and noradrenaline both bind to adrenergic receptors (Berecek and Brody 1982; Alexander et al. 2008). Adrenaline is released from postganglionic sympathetic neurons and acts to increase heart rate and increase blood pressure as part of the classic fight-or-flight response. Adrenergic receptors are G-protein coupled and are divided into two classes, alpha and beta (Berthelsen and Pettinger 1977; Alexander et al. 2008). Noradrenergic projections reach the spinal cord through descending projections originating in the pons (Westlund et al. 1983).

1.1.4.1 Alpha-adrenergic receptors

There are two types of α-adrenergic receptors, α_1 and α_2. The α_1-adrenergic receptors are typically located on the effector organ, and α_2-adrenergic receptors are typically located presynaptically to regulate neurotransmitter release (Civantos Calzada and Aleixandre de Artiñano 2001). Both are found on smooth muscle and have opposing effects on vascular tone with α_1-ARs causing vasoconstriction and α_2-ARs causing

vasodilation (Civantos Calzada and Aleixandre de Artiñano 2001). Subtypes of α-adrenergic receptors found on neurons include both α_1 and α_2 subtypes (Jones et al. 1982). Specifically, α_{1a}-ARs are found in the rat spinal cord in areas related to motor function; α_{1b}-ARs are distributed throughout the ventral and dorsal horns; and α_{1d}-ARs are distributed in the spinal cord, but their levels are very low compared to other α_1-ARs (Wada et al. 1996; Day et al. 1997). The α_{2A}- and α_{2C}-ARs are also found in spinal cord, with α_{2A}-ARs located on the terminals of capsaicin-sensitive, substance P-containing afferent fibers and α_{2C}-ARs found in spinal interneurons (Stone et al. 1998).

Similar to the nAChRs, α_2-ARs, particularly the α_{2A} subtype, mediate antinociception in the spinal cord (Reddy et al. 1980; Gordh et al. 1989; Millan 1992); however, the α_1-ARs, particularly the α_{1a} subtype, are more associated with potentiating nociceptive perception (Hedo and Lopez-Garcia 2001). It has been proposed that the adrenergic system's involvement in nociception may involve "volume transmission" as opposed to traditional synapses due to the scarcity of noradrenergic boutons in the dorsal horn, but the adrenergic modulation of complex motor activities, such as locomotion, may occur through traditional synapses (Rajaofetra et al. 1992). The influence of the adrenergic system on locomotor tasks was first suggested due to the activation of neuronal circuits responsible for locomotion by noradrenergic agents (Jankowska et al. 1967). It has been demonstrated that noradrenergic drugs, particularly α_2 agonists, are the most effective at initiating locomotion in chronic spinal cats (Barbeau and Rossignol 1987). The α_2 agonists also modulate established locomotor rhythms by increasing step cycle, increasing the amount of foot drag, and decreasing cutaneous sensation (Chau et al. 1998). In the rat spinal cord, α_1 agonists successfully initiate bouts of locomotor activity

(Sqalli-Houssaini and Cazalets 2000) and "fast" alternating left–right rhythms (Gabbay and Lev-Tov 2004), while in the cat they do not (Chau et al. 1998).

1.1.5 *In vitro* spinal cord preparation

Spinal cords from neonatal rats (zero to five days old) are easily isolated, and they can survive *in vitro* for extended periods of time (six to eight hours) in a solution of artificial cerebrospinal fluid (aCSF) (Cazalets et al. 1998; Kiehn and Butt 2003). This preparation has been used to study various aspects of motor behavior in mammals (Cazalets et al. 1998). Due to the isolated conditions, exquisite control over the extracellular environment is possible, lending itself to pharmacological studies. Another advantage to this animal model is the absence of the blood-brain barrier. Because of this, all applied neurochemicals have direct access to all neuronal structures. Additionally, specific segments of the spinal cord can be targeted using split bath methods. In this way, the extracellular medium can be tightly controlled in order to manipulate the motor activity (Cazalets et al. 1994).

While *in vitro* preparations have many advantages over *in vivo* preparations due to the controllability of the environment and ability to record intracellularly, sacrifices are made in observing more "physiologically relevant" behaviors. For example, with the *in vitro* spinal cord preparation, the view of locomotor activity is incomplete as there are no limbs to observe. As a result, more intact preparations have been developed where innervation to target organs, such as the bladder (Sugaya and De Groat 1994) or lung (Mellen and Feldman 2000), or muscles, such as those in the hindlimbs (Kiehn and Kjaerulff 1996; Hayes et al. 2009), are left intact. These hybrid preparations attempt to

combine the advantages of both *in vitro* and *in vivo* preparations by retaining an observable, physiological output.

The research presented here used the *in vitro* spinal cord preparation and two preparations with efferent targets left intact: one with hindlimbs attached and one with the sympathetic paravertebral chain attached.

1.2 The central pattern generator

Within the spinal cord there is a network of neurons capable of generating coordinated locomotor activity without descending commands or sensory feedback (Kiehn and Butt 2003). This CPG has been studied in many species including lamprey, rodent, and human (Buchanan and Grillner 1987; Dimitrijevic et al. 1998; Kiehn and Butt 2003). Central pattern generators are not restricted to the production of locomotion; CPGs for respiration and sexual function have also been identified (Richter 1982; von Euler 1983; Chung et al. 1988).

The exact location and interneuronal makeup of the locomotor CPG has not been identified in mammals. Studies attempting to isolate putative CPG interneurons have been performed using genetically modified mice to selectively abolish individual populations of interneurons (Goulding 2009). The most heavily studied interneuron subclasses, called V0, V1, V2, and V3, are genetically similar to motor neurons due to their development in the ventral half of the neural tube and arise from intermediate/ventral progenitors (Goulding 2009). These putative "core" CPG interneurons each correspond to unique phenotypes of interneurons, and all have influence over the locomotor pattern produced; however, no one subclass is wholly

responsible for the generation of motor patterns (Lanuza et al. 2004; Gosgnach et al. 2006; Crone et al. 2008; Wang et al. 2008; Zhang et al. 2008).

1.2.1 Central pattern generator models

1.2.1.1 Half-center oscillator

Locomotion takes many forms including swimming, slithering, quadrupedal stepping, and bipedal stepping with each presenting its own set of challenges. Each CPG works to coordinate the movements of the muscles to propel the animal in its environment. However, at the most basic level, the CPG is an oscillator. Studies on the mammalian CPG began one hundred years ago by T. Graham Brown where he noted the alternation between flexors and extensors in cat muscles during walking experiments (Brown 1911). Based on these observations, the half-center oscillator model for generating rhythms was formed (Brown 1914; Jankowska et al. 1967). At its simplest, a half-center oscillator is composed of two cells, which receive reciprocal inhibition from one another (Figure 1.3a). In this configuration, only one cell can be active at a time, producing an alternating pattern between the cells. A two-cell half-center model is far too simple to describe the complicated coordination of terrestrial quadrupedal or bipedal locomotion given the multi-joint coordination that is required. Because of this, several models have been presented to describe this coordination. Here, two popular models will be discussed.

1.2.1.2 Unit burst generator

The unit burst generator model allows for complex, coordinated patterns by connecting several half-center oscillators together, for example, one for each joint in a

limb. Each joint's half-center dictates the alternation between antagonistic muscles, but the inter-coordination of each unit burst generator forms the overall locomotor pattern (Grillner 1981). This configuration allows for the production of a variety of motor patterns by changing the relative strengths of the connections to affect the phasing between the joints (Figure 1.3b).

1.2.1.3 Multi-level model

A potential limitation of the unit burst generator model would be how it deals with feedback from the environment and incorporates that into the rhythm. For example, if the CPG is only composed of interconnected half-centers, a perturbation that shortened or lengthened a burst would disrupt and offset all subsequent bursts from what was anticipated. However, based on observations in the cat hindlimb, this is not always the

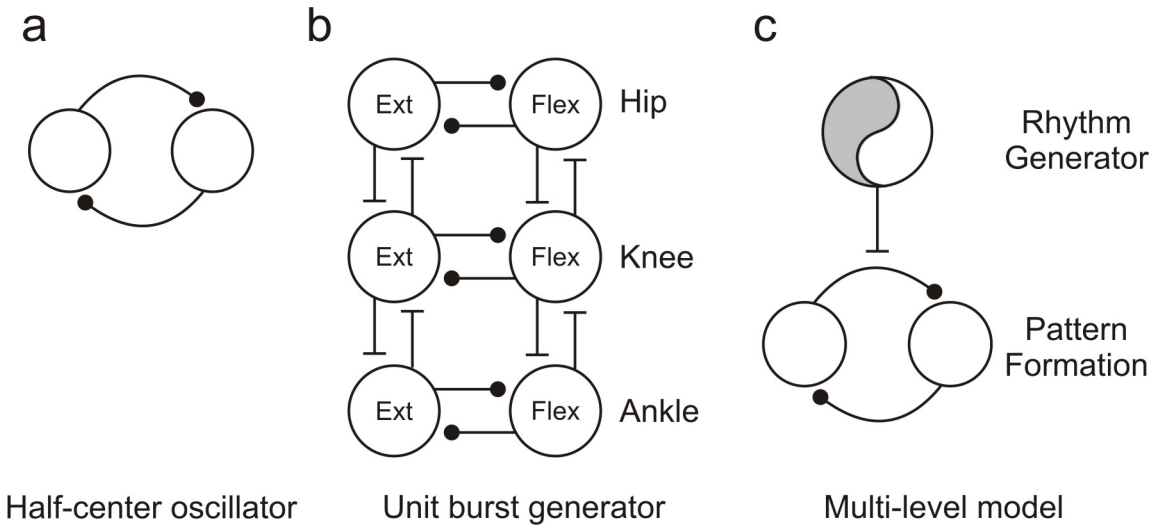

Figure 1.3: Central pattern generator models
Three proposed models for production of alternating rhythms. At its simplest, (a) a two neurons network connected by mutual inhibition may produce alternating patterns. (b) The unit burst generator combines half-center oscillators, one per limb joint, to produce a variety of rhythms. (c) A proposed two-level model with the rhythm generator "clock" connected to the network responsible for motor output patterning.

case; perturbations lengthening the flexion phase may be followed by a shortened extension phase, resulting in no step cycle duration change and leaving timing in subsequent cycles unchanged from what it was (Guertin et al. 1995). Thus, a two-level model was developed incorporating a rhythm generator and a pattern formation circuit to account for data such as this (Figure 1.3c). The rhythm generator acts as a clock, and the pattern formation circuit coordinates the individual muscle patterns (Rybak et al. 2006). Using a two-level model allows for other locomotor phenomena, such as deletions, to be explained as well since in this model, the clock would continue to keep time as the pattern formation circuit copes with sensory perturbations (Lafreniere-Roula and McCrea 2005; Duysens et al. 2006).

1.2.2 Locomotor-like activity

Locomotion is the fundamental behavior that allows organisms to move around in and interact with their environments. As discussed previously, the CPG is a specialized network of neurons capable of autonomously generating rhythms. Descending inputs from the brain are necessary to initiate and adapt the locomotor output, but are not needed for the CPG to produce basic motor patterns. In patients with spinal cord injury, descending pathways are severed, and communication between the brain and the spinal cord segments below the lesion is either limited or no longer possible.

1.2.2.1 Pharmacological induction of locomotor-like activity

In the 1980's the isolated spinal cord preparation was used to demonstrate that N-methyl-D-aspartic acid (NMDA) application resulted in rhythmic alternating activity in hindlimb motor neurons (Kudo and Yamada 1987; Smith et al. 1988). This alternating activity can be measured via ventral roots—in which case it is termed locomotor-like

activity (LLA)—or via muscles. The resulting LLA spatiotemporally resembles the locomotion of the intact hindlimb (Kiehn and Kjaerulff 1996). In the isolated neonatal rat spinal cord preparation, motor output recorded from the lumbar ventral roots L2 and L5 corresponds to the activity in flexor and extensor muscles, respectively, and has alternating flexor–extensor combined with alternating left–right rhythms (Kiehn and Kjaerulff 1998).

The pharmacological induction of LLA can be achieved by bath application of various neurotransmitters (Cazalets et al. 1992) as well as excitatory amino acids (Kudo and Yamada 1987; Smith et al. 1988; Cazalets et al. 1992). All of these chemicals have an excitatory effect on the CPG. In the neonatal rat, a combination of 5-HT and NMDA is used to elicit a LLA, which has been described as resembling either walking or swimming (Cowley and Schmidt 1994; Kiehn and Kjaerulff 1996), but with unrestrained hindlimbs, it is kinematically consistent with overground locomotion (Hayes et al. 2009). While this pharmacological method provides a strong and sustained locomotor pattern, it is not translatable into a neuroprosthetic device to control locomotion in spinal cord-injured individuals due to widespread actions of both 5-HT and NMDA on numerous neural systems. In addition to 5-HT and NMDA, other neurochemicals also produce rhythmic motor patterns in neonatal rodent spinal cords. Acetylcholine (ACh) in combination with an acetylcholinesterase inhibitor, edrophonium (EDRO), produces rhythmic motor patterns as recorded from peripheral nerves in the neonatal rat spinal cord; however, the combination of ACh and EDRO rarely produces locomotor-like activity. Instead, these motor patterns were typified by in-phase activation of ipsilateral flexor and extensor nerves alternating with the contralateral side (Cowley and Schmidt

1994). Neurochemicals used for inducing locomotion are not universal across species. Applying 5-HT/NMDA to the mouse spinal cord does not normally induce locomotor rhythms. Rather, dopamine must be added to the cocktail for sufficient activation of locomotor rhythms (Jiang et al. 1999; Whelan et al. 2000).

1.2.2.2 Afferent evoked induction of locomotor-like activity

Another technique for inducing LLA is applying electrical stimuli to the spinal cord in various locations. It has been shown that low-threshold (1.2-6 times threshold) electrical stimuli can activate the hindlimb locomotor CPG in the neonatal rodent spinal cord (Lev-Tov and Pinco 1992; Bonnot et al. 1998; Lev-Tov et al. 2000; Marchetti et al. 2001; Gabbay et al. 2002; Gordon and Whelan 2006). The different areas that have been shown to induce LLA include the ventrolateral funiculus (Magnuson and Trinder 1997), lumbar dorsal roots (Marchetti et al. 2001), sacral dorsal roots (Kremer and Lev-Tov 1997; Strauss and Lev-Tov 2003), and the cauda equina (Whelan et al. 2000). Stimulation of sensory afferents is beneficial for electrical induction of LLA because it utilizes the inherent feedback onto the motor system and may create a more physiologically relevant motor pattern.

1.2.2.2.1 Dorsal root stimulation

Stimulation of sacral and lumbar dorsal roots has been shown to evoke rhythmic motor patterns in both neonatal mouse and neonatal rat spinal cords (Bonnot et al. 1998; Whelan et al. 2000; Marchetti et al. 2001; Strauss and Lev-Tov 2003). Stimulation of the coccygeal dorsal roots, often referred to as the cauda equina, can also produce rhythmic motor output in both sacral and lumbar segments of the spinal cord in the mouse (Whelan et al. 2000; Gordon and Whelan 2006; Zhong et al. 2007; Mandadi et al. 2009). These

rhythms are qualitatively similar to those produced by pharmacological means previously discussed at the level of the ventral root; however there are noticeable differences in muscle activation patterns produced by 5-HT/NMDA and cauda equina activation of the CPG. For example, during stimulation of the cauda equina, rectus femoris was active during extension and semitendinosus was active during flexion, but during 5-HT/NMDA rhythms, the phases during which these muscles were active switched (Klein et al. 2010).

Afferent evoked rhythms differ significantly from pharmacologically evoked rhythms with respect to the duration the rhythm. Afferent evoked rhythms can last tens of seconds, generally thirty to sixty seconds (Delvolve et al. 2001), while pharmacologically induced rhythms persist for minutes at a time (Kjaerulff and Kiehn 1996). It has been proposed that the afferent evoked rhythms end because the afferents fail to sustain a steady rhythmic drive (Delvolve et al. 2001), which may be the result of many mechanisms. A likely mechanism to explain this would be prolonged synaptic depression, which may result in decreased transmitter output due to the inability of the immature, developing synapses of the neonates to produce sustained transmitter release even during moderate stimulation rates (Lev-Tov and Pinco 1992). Other mechanisms include action potential failure at afferent terminals, branch point blockade, neurotransmitter depletion, and inactivation of presynaptic release sites (Lev-Tov and O'Donovan 1995; Kremer and Lev-Tov 1998).

Stimulation of the sacral dorsal roots to evoke LLA has been shown to depend on activation of sacral cord relay neurons projecting rostrally into the lumbar segments. These sacral segments are mainly associated with tail, bladder, and colon innervation, and activation of sacral rhythmic activity (tail movements) is not necessary for activation

of lumbar rhythmic activity (Strauss and Lev-Tov 2003). Furthermore, the sacral dorsal root evoked lumbar rhythm is not impaired by blockade of sacral NMDA and adrenoceptors (Strauss and Lev-Tov 2003). In the mouse, monoamines have been shown to have modulatory effects on afferent evoked lumbar rhythms. Application of noradrenaline (NA) or dopamine (DA) both completely blocked the afferent evoked rhythm; in contrast, 5-HT only slowed the rhythms with no effect on the phasing (Gordon and Whelan 2006). These effects were mimicked by application of selective receptor agonists, with α_2-adrenoceptors mimicking the effects of NA; D_1, D_2, or D_3 dopamine receptors mimicking the effects of DA; and 5-HT_2 receptors mimicking the effects of 5-HT on the afferent evoked rhythms (Gordon and Whelan 2006).

1.2.2.2.2 Epidural stimulation

Along with the study of afferent evoked means of activating the lumbar CPG, previous research has demonstrated that epidural stimulation can induce locomotor-like movements in cats, rats, and humans with complete spinal cord transections (Iwahara et al. 1992; Dimitrijevic et al. 1998; Gerasimenko et al. 2002; Ichiyama et al. 2005; Lavrov et al. 2006). In these adult preparations and patients, wire electrodes were placed on the dorsal surface of the spinal cord above the intact dura mater, which is the outermost layer of meninges enveloping the CNS, and stimulus trains in the 30-50 Hz range are applied to induce stepping patterns. The location of effective stimulation varies from species to species. In the cat segments L1, L4 and L5 are effective at inducing stepping patterns (Iwahara et al. 1992; Gerasimenko et al. 2003), whereas in the rat segments L2 and S1 are the most effective (Ichiyama et al. 2005; Lavrov et al. 2006), and in the human L2 is the most effective (Dimitrijevic et al. 1998). Because of the placement of the epidural

electrodes, it is possible that the stimulation is activating afferents, which then activate the CPG as already discussed.

1.2.2.2.3 Effects of stimulation on on-going rhythms

In the presence of ongoing LLA, stimuli have been shown to have several different effects. Resetting occurs when a stimulus activates the CPG such that the cycle of the locomotor rhythm is shortened or lengthened followed by the return of regular rhythm in the coordinated fashion. For example, flexor reflex afferents, a combination of joint, cutaneous, group II and group III afferents, can reset fictive locomotion in the spinal cat (Hultborn 1998). Entrainment occurs when the frequency of the CPG locomotion is altered by and follows the frequency of the external stimuli. For example, stimulation of group I knee afferents or hip afferents can reset the locomotor rhythms (Conway et al. 1987; Kriellaars et al. 1994).

1.2.2.3 Mutual inhibition in locomotor-like activity

The involvement of inhibitory pathways in CPG activation has been implicated given the alternating oscillatory behavior observed. Gamma-aminobutyric acid (GABA) receptor activation has been shown to suppress the locomotor network and aid in the left–right patterning of the motor output during development (Kiehn and Butt 2003). Upon maturity, the left–right coordination control is replaced by inhibitory glycinergic systems for alternation and by excitatory glutamatergic systems for synchrony (Kiehn and Butt 2003). Glycine is also pivotal for flexor–extensor patterning, and blocking glycinergic receptors results in synchronous activity (Kiehn and Butt 2003). Motoneuron recordings in the neonatal rat have shown that the CPG patterning results from alternating

glutamatergic excitation and glycinergic inhibition (Cazalets et al. 1996; Hochman and Schmidt 1998).

1.2.2.4 Rostrocaudal gradient of the central pattern generator

Many studies have been performed in the rodent dissecting the locomotor CPG, and based on these studies, the rhythmogenic center for the hindlimb locomotor CPG has been established. Initially, it was believed that the rodent locomotor CPG was restricted to the L1 and L2 segments of the lumbar cord with these segments driving the more caudal lumbar segments rhythmically (Cazalets et al. 1996). However, subsequent studies revealed that the lower lumbar segments, too, could produce rhythmic motor outputs when separated from L1 and L2 by a transverse cut through L3 (Kremer and Lev-Tov 1997) suggesting that the hindlimb CPG extended beyond L1 and L2. The idea of a more distributed CPG was supported by other lesioning studies (Kjaerulff and Kiehn 1996). The rhythms in the lower lumbar spinal cord were not as robust as in the L1/L2 segments and required the application of extra neurochemicals to aid in their induction, suggesting that while the system is widely distributed longitudinally, the more rostral segments possess a higher rhythmogenic capacity.

Additionally, partitioned bath experiments also supported the hypothesis that the rostral lumbar segments were more rhythmically suited than the lower segments. Using partitions separating T13-L2 from L3-L6 segments, a cocktail of serotonin (5-HT) and NMDA was applied to the individual baths. When applied to T13-L2, rhythmic activity was seen in the lower lumbar segments; however, when applied to just L3-L6, only tonic activity was observed in the these segments (Cazalets et al. 1995). These results differ from those previously discussed in that no rhythmic activity was observed in the lower

lumbar segments. This can be explained by differences in the concentration of neurochemicals used and the variability of post-synaptic receptor distribution in the neonatal rodents (Schmidt and Jordan 2000; Liu and Jordan 2005).

Further lesioning studies revealed that the components responsible for the rostrocaudal coordination require the ventral funiculus to be present, and that left–right coordination is distributed along the length of the cord, but is more dominant in rostral lumbar segments (Kjaerulff and Kiehn 1996; Kremer and Lev-Tov 1997). The location identified by these studies has been supported by activity-dependent labeling in both the cat and the rat (Kjaerulff et al. 1994; Carr et al. 1995).

1.2.2.5 Dorsoventral localization of the central pattern generator

The distribution of neurons involved in rhythmogenesis has also been investigated in the dorsoventral axis. Both activity dependent labeling and lesioning studies have been performed in order to isolate these neurons. Using sulphorhodamine as an activity dependent marker during 5-HT/NMDA-induced locomotion in the neonatal rat spinal cord, labeled neurons were found in the medial intermediate gray and around the central canal in lumbar and lower thoracic segments (Kjaerulff et al. 1994; Cina and Hochman 2000). Some of the activity-dependent labeling in the cord may be false positive labeling from application of NMDA; however, with just 5-HT used for inducing locomotor-like activity, the localization of labeling is similar, but the number of labeled neurons is reduced (Cina and Hochman 2000). Immunoreactive c-fos labeling in the cat during fictive locomotion was also seen in the intermediate gray and around the central canal of the lumbar spinal cord, consistent with the rodent studies (Dai et al. 2005). Lesioning studies revealed that removal of the dorsal horns to a level just ventral to the central canal

still resulted in rhythmic bursting induced by 5-HT/NMDA with no change in cycle period but with a decrease in burst duration (Bracci et al. 1996; Kjaerulff and Kiehn 1996).

1.2.2.6 Sympathetic outflow with CPG activity

The majority of studies on the spinal cord and the CPG have revolved around somatic motor patterns, which have somewhat overshadowed the importance of studying the autonomic interactions with the CPG. As previously discussed, the autonomic nervous system regulates and adapts functions such as blood pressure and respiration, and as an animal moves in its environment, many autonomic changes must also occur. In the cat, sympathetic efferent activity from the cardiac and cervical nerves was phase coupled to hindlimb, forelimb, and trunk muscle efferents during L-DOPA induced fictive locomotion (Schomburg et al. 2003). These studies suggest the presence of an additional CPG controlling autonomic outflow that coordinates with the locomotor CPG or the possibility that the central CPG coordinates both somatic and autonomic actions.

1.2.2.7 Lesion studies

In the context of afferent activation of the CPG, it is also important to understand which portions of the spinal cord are essential connections between those afferents and the CPG network. Thus, white matter lesioning studies were performed to identify axon tracts responsible for transmitting afferent information to the CPG. Lesions of individual and groups of axon tracts were performed in the neonatal rat spinal cord in conjunction with sacral dorsal root activation of the CPG. Lesions to the dorsal columns had no effect on the evoked rhythms; however, lesions to the dorsolateral funiculi, lateral/ventrolateral funiculi, or ventral funiculi weakened the evoked rhythms but did not

block them completely (Etlin et al. 2010). Additionally, lesions leaving the dorsal column's white matter tracts intact were not able to produce rhythmic activity in the lumbar segments by dorsal root stimulation, but when individually leaving any of the other white matter tracts intact, locomotor-like activity could be elicited by sacral dorsal root stimulation (Etlin et al. 2010). These results suggest that the fibers projecting to the lumbar CPG are distributed in many white matter tracts but are not contained within the dorsal columns at the level of the spinal cord that was lesioned.

1.3 Afferents

Afferents are the means by which sensory organs transmit information back to the spinal cord and brain for processing and integration into motor and autonomic tasks. Afferents enter the spinal cord through dorsal roots where they bifurcate and synapse in the spinal gray matter to form reflex pathways, which do not involve any additional spinal or supraspinal processing. Other afferent branches travel to higher centers for further processing and sensory integration. Afferents come in a range of diameters and degrees of myelination. Larger, more heavily myelinated fibers are referred to as low-threshold afferents, and smaller, less myelinated fibers are referred to high-threshold afferents. Low-threshold afferents generally transmit non-pain information from the periphery, such as limb position or cutaneous information. High-threshold afferents generally transmit pain information, but they may also transmit visceral pain and non-pain information. The terms "low-threshold" and "high-threshold" relate to the amount of current or voltage required to activate that fiber subtype (Kandel et al. 2000). These thresholds also correlate to the fibers' conduction velocities, with low-threshold fibers generally conducting at rates much faster than high-threshold fibers. However, in

neonatal rodents, the conduction velocities vary a great deal from the adult animal because the systems are still maturing and the myelination of the fibers is not complete (Fulton 1987). The myelinated fibers increase in diameter as the animal grows to adult (Nussbaumer et al. 1989). For example, in the rat tibial nerve, fiber diameter increases from approximately 0.5-1.5 μm at P1 to 1.5-12.5 μm at P30, due to thickening of the myelin sheath (Vejsada et al. 1985). This corresponds to an increase in the fastest conduction velocities increasing from 1.4 m/s at P1 to 35 m/s at P30 (Vejsada et al. 1985). Similarly, in rat dorsal root ganglia (DRGs), conduction velocities of the low- and high-threshold fibers are hardly distinguishable, with all having conduction velocities of less than 1 m/s at P0, but by P14 the groups of afferent fibers are separable by conduction velocity with the fastest traveling at 15 m/s and the slowest traveling at 1.5 m/s (Fitzgerald 1987).

1.3.1 Visceral sympathetic afferents

Visceral afferents aid in maintaining homeostasis within the body and provide information about the internal state of the body as part of the autonomic nervous system. These afferents transmit information from the periphery to the spinal cord through nerves which then synapse and either form reflex pathways or travel rostrally to the nucleus tractus solitarus in the brain through both the spinothalamic tract and the dorsal columns (Katter et al. 1996; Al-Chaer et al. 1998; Kandel et al. 2000). The mechanism of perception arising from visceral afferents is much less well understood than their somatic counterparts, partly because sensations such as visceral pain are not well localized due to their signals' convergence with somatic inputs in the dorsal horn (Kirkup et al. 2001). Understanding autonomic sensory signaling is of particular importance because in

patients with SCIs, the autonomic reflex pathways may remain intact, depending on the level and severity of the injury, but the supraspinal control over actions such as micturition is lost and thus no longer voluntary. Autonomic afferents release a variety of neurochemicals, including substance P and calcitonin gene-related peptide (CGRP) (Kawatani et al. 1986; Kandel et al. 2000). In the sacral level of the spinal cord, the pelvic and pudendal nerves play an important role in autonomic function for the bowel, bladder, and sexual organs (Kawatani et al. 1986). These afferents project to the spinal cord's Lissauer's tract and the dorsal columns tract (Kawatani et al. 1986; McKenna and Nadelhaft 1986).

1.3.2 Nociceptive afferents

Nociception is the neural process of encoding and decoding noxious stimuli. Classically, it has been thought that visceral input to higher centers of the CNS is mediated by the spinothalamic tract and the spinoreticular tract (Al-Chaer et al. 1996). However, more recently, it has been shown that the dorsal column pathway is involved in the process of pain perception, more specifically that of visceral pain (Al-Chaer et al. 1996). Visceral pain encompasses pain originating from organs, such as the colon, stomach, pancreas, and ureter (Palecek 2004). Lesions of the dorsal column have been shown to dramatically reduce the sensation of pelvic pain in cancer patients (Hirshberg et al. 1996), and the lesioning has been used as a last resort for treating intractable visceral pain (Hitchcock 1974; Gildenberg and Hirshberg 1984).

Several different compounds mediate nociceptive signaling, and the signaling involves different receptor subtypes for the different pain modalities. Both capsaicin and ATP, among others, activate nociceptive signaling pathways (Gu and Heft 2004;

Nakatsuka and Gu 2006) and are involved in the transmission of visceral pain (Kirkup et al. 2001). Capsaicin activates the transient receptor potential vanilloid-1 (TRPV1) receptor and ATP activates the family of purinergic P2X receptors (Su et al. 1999; Gu and Heft 2004; Nakatsuka and Gu 2006). The TRPV1 receptor, a thermo- and chemoreceptor, is found in peripheral free nerve endings as well as on presynaptic afferent terminals in the dorsal horn (Julius and Basbaum 2001; Levine and Alessandri-Haber 2007; Willis Jr 2007; Mandadi et al. 2009). Similar to TRPV1 receptors, ionotropic P2 purinoceptors (P2X receptors) localize on primary afferent terminals in the dorsal horn, but they are also found on dorsal horn interneurons throughout the spinal segments (Nakatsuka and Gu 2006).

Dorsal root ganglion (DRG) neurons expressing TRPV1 usually express $P2X_3$ receptors as well; therefore, capsaicin-sensitive afferents are usually also ATP-sensitive (Nakatsuka and Gu 2006). These neurons convey information to the superficial lamina of the spinal cord; however, many DRG neurons express $P2X_3$ but not TRPV1, and these neurons project into the deep dorsal horn (Gu and Heft 2004; Nakatsuka and Gu 2006). These two subpopulations converge in the deep dorsal horn lamina V, with the capsaicin-sensitive/ATP-sensitive neurons synapsing on interneurons in lamina I. The capsaicin-sensitive/ATP-sensitive neurons play an important role in the pain mechanism because many of them directly relay nociceptive information to the brain (Nakatsuka and Gu 2006). Additionally, TRPV1 containing neurons have a tetrodotoxin (TTX) resistant component to their voltage gated Na^+ channel current indicating that the application of TTX should not block transmission of pain (Su et al. 1999).

1.3.3 Dorsal column pathway

The dorsal columns pathway is a white matter tract located on the dorsal midline of the surface of the spinal cord. Primary afferents enter the dorsal columns from the dorsal root ganglia, bifurcate, and travel rostral and caudally. The dorsal columns contain short, intermediate, and long projecting fibers. The distance traveled by the fibers is related to the afferent's sensory modality, and only about 25% of the dorsal columns primary afferent fibers reach the medulla; all others terminate in the spinal cord gray matter (Willis and Coggeshall 1991). The dorsal columns are divided into the funiculus gracilis and funiculus cuneatus. The afferents originating from segments caudal to T6 are found in the more medial funiculus gracilis, while afferents originating from segments rostral to T6 populate the funiculus cuneatus. The dorsal columns transmit information regarding discriminative aspects of tactile sensations, such as cutaneous touch, kinesthesia, and viscerosensory information, including pain information (Al-Chaer et al. 1996, 1996; Al-Chaer et al. 1998; Willis et al. 1999). Lesions of the dorsal columns diminish the activation of thalamic neurons by innocuous mechanical stimuli and also lead to a reduction of activity of the thalamic neurons evoked by visceral stimuli (Palecek 2004). Moreover, high frequency (>30 Hz) stimulation of the dorsal columns has been used for the treatment of neurogenic pain syndromes by inducing paresthesia and pain associated with ischemia (Meyerson et al. 1995; Oakley and Prager 2002).

Other higher-order fibers enter the dorsal columns from neurons within the gray matter of the spinal cord. These fibers, called the post-synaptic dorsal column tract, transmit propriospinal information and visceral pain information more rostrally and have cell bodies originating from lamina III, IV, and V (Giesler et al. 1984; Enevoldson and

Gordon 1989; Willis and Coggeshall 1991; Palecek 2004). Post-synaptic dorsal column neurons are unique in that they receive input from a variety of low- and high-threshold afferent subtypes, including low- and high-threshold cutaneous, low- and high-threshold mechanoreceptors, and group I and II muscle afferents (Jankowska et al. 1979; Brown et al. 1983; Noble and Riddell 1988).

1.4 Aims and objectives

The objective of this dissertation is to gain insight into the role of sacral dorsal column (sDC) stimulation in activating pattern generating circuitry and to characterize it in terms of afferent populations recruited, interneuronal pathways activated, and efferent output generated. First, I identified a site along the sacral dorsal columns capable of recruiting lumbar rhythms mediated by C fiber activation (Chapter 3). The rhythms generated were largely inconsistent with locomotor-like activity, but did maintain left-right alternation. Second, I demonstrate a dependence on nociceptive and autonomic related neurotransmitters with specific sensitivity of α_1-adrenergic receptor to sacral segments and sensitivity of cholinergic receptors to lumbar segments (Chapter 4). In addition, this research shows activation of autonomic and somatic efferent circuits by sDC stimulation with a rhythmic activity noticeably absent in lower lumbar (L3-L5) segments but present in all other recorded segments (T11-S2) (Chapter 5). Lastly, I demonstrate that sDC stimulation can activate and entrain rhythms alone and entrain ongoing pharmacological rhythms with very slow stimulation frequencies (Chapter 5).

CHAPTER 2

GENERAL METHODS

In order to accomplish the goals of this research, several different spinal cord preparations were necessary, including an isolated spinal cord preparation for evaluation of sacral dorsal column (sDC) and sacral dorsal root (sDR) evoked central pattern generator (CPG) activity, a partitioned bath isolated spinal cord preparation for selective application of pharmacological agents, a hindlimbs attached preparation for evaluation of muscle activity, and a sympathetic chain attached preparation for evaluation of sympathetic output. All procedures were approved by the Emory University Institutional Animal Care and Use Committee (IACUC).

2.1 Isolated spinal cord preparation

Experiments were performed on the isolated spinal cord preparation as described previously (Hochman and Schmidt 1998; Machacek and Hochman 2006). Spinal cords were isolated from postnatal day (P) zero to P4 Sprague Dawley rats by decapitating and eviscerating the animal. The animal was then transferred to a recording chamber containing a static bath of cooled (4°C), continuously oxygenated (95% O_2, 5% CO_2) artificial cerebral spinal fluid (aCSF) containing (in mM): 128 NaCl, 1.9 KCl, 1.2 KH_2PO_4, 26 $NaHCO_3$, 2.4 $CaCl_2$, 1.3 $MgSO_4$, and 10 glucose, pH of 7.4 (Hochman and Schmidt 1998; Machacek et al. 2001; Machacek and Hochman 2006; Hayes et al. 2009). Using a ventral vertebrectomy to expose the spinal cord from thoracic segment T1 to the

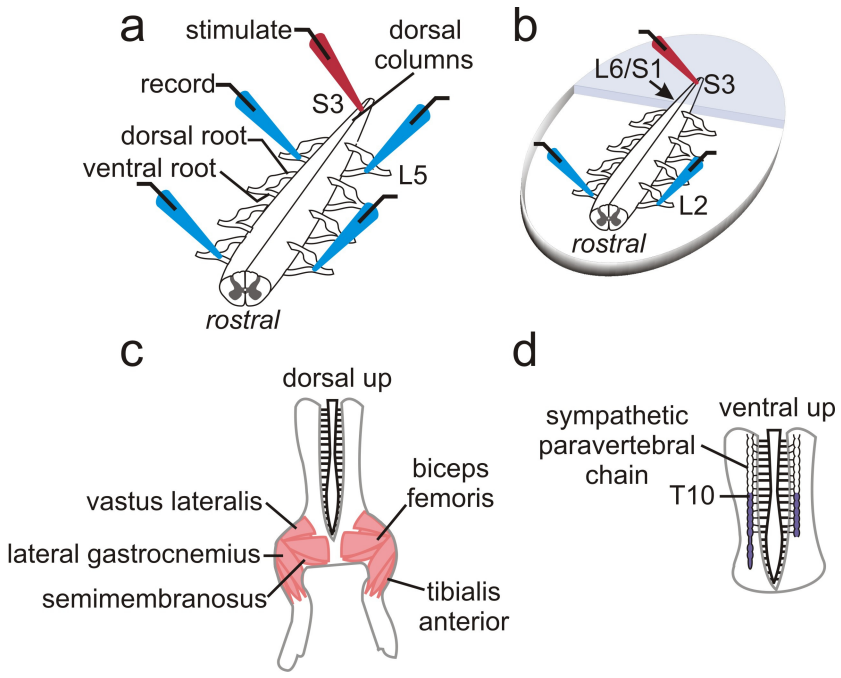

Figure 2.1: Schematics of general experimental preparations

Schematic of (a) whole bath isolated spinal cord preparation, (b) split bath isolated spinal cord preparation, (c) hindlimbs-attached spinal cord preparation, (d) sympathetic chain-attached spinal cord preparation. All preparations had recordings from ventral roots. Accessible hindlimb muscles (c) were those on the lateral aspect of the limbs due to positioning the spinal cord dorsal up in order to access the dorsal column for stimulation. (d) Recordings from the sympathetic paravertebral chain were taken from segments T10-L2 (shaded).

cauda equina, the spinal cord was then isolated by severing nerve roots and removing it from the vertebral column. The cord was stabilized with insect pins to the Sylgard bottom of the recording chamber with the dorsal aspect of the cord facing up and allowed to reach room temperature.

Glass suction electrodes were applied to ventral lumbar roots (L2s and L5s) *en passant* for recording, and a glass suction electrode with tip diameter averaging 30 µm was applied to the surface of the cord along the sacral dorsal column (dorsal surface midline) between sacral segments S2 and S4 (Figure 2.1a). In some instances, dorsal column stimulation-evoked volleys were recorded in contiguous dorsal roots between T13 and S4 to determine the distribution of afferent fibers activated by the sacral dorsal column (sDC) stimulus. In most cases, neurograms were digitally recorded at 5 kHz (Digidata 1320A, Axon Instruments), amplified (10,000x), and high-pass filtered at 30 Hz.

2.1.1 Stimulation techniques

Rhythmic activity was induced by repetitive stimulation of the sacral dorsal columns or the lumbar or sacral dorsal roots. Trains of stimuli between 0.2 and 10 Hz were used at intensities of 50-500 µA and durations of 200-500 µs. Stimulus trains as long as fifty seconds were delivered once every three minutes to allow for sufficient recovery of the prolonged motoneuron depolarization occurring throughout the stimulation trains (Lev-Tov et al. 2000; Whelan et al. 2000). Unless otherwise indicated, stimulus trains of 40 s at 2 Hz with an intensity of 200 µA/200 µs were applied.

For studies using threshold as a measure of afferent fiber recruitment, threshold was defined as the minimum current amplitude pulse with 200 μs duration required to evoke a detectable compound action potential of the lowest threshold afferents in the dorsal root (for dorsal root stimulation) or in the dorsal columns white matter tract (for dorsal columns stimulation).

2.1.2 Evaluation of current spread

Given that another ascending afferent pathway, Lissauer's tract, which transmits mechanosensory and nociceptive information (Ranson 1914; Willis and Coggeshall 1991), is located adjacent to the dorsal column pathway on either side, I sought to establish the extent of stimulation current spread along the surface of the cord. The spinal cord's surface was stimulated at S3 along the dorsal column midline, and recording electrodes were moved mediolaterally along the dorsal surface at the L6/S1 segment junction to record any compound action potentials recruited in the white matter tracts. In two experiments, little to no current spread from a 200 μA/200 μs pulse was detected at sites 100 μm lateral to the dorsal column midline indicating that the stimulation electrode's current selectively activated dorsal columns fibers.

2.1.3 Pharmacological induction of locomotor-like activity

Application of the monoamine serotonin (5-HT) and the excitatory amino acid N-methyl-D-aspartate (NMDA) to the isolated rat spinal cord typically activates the locomotor CPG (Kudo and Yamada 1987; Smith et al. 1988). In select experiments, 50 μM 5-HT combined with 5 μM NMDA was applied to the isolated spinal cord to induce locomotor-like activity in the ventral roots. These rhythms were typified by alternating left–right and alternating flexor–extensor activity.

2.1.4 Lesions to the dorsal columns

Lesions to the dorsal columns were made by cutting the midline of the dorsal surface of the spinal cord with fine iris scissors or sharp glass probes. Lesions were located one-half to one whole segment rostral to the sacral dorsal column stimulation site and allowed to recover for forty-five minutes to an hour before evaluating the effect on sDC evoked lumbar rhythms. All cords were subsequently preserved using 4% paraformaldehyde and stored in 15% sucrose at 4°C. Lesioned cords were embedded in agar and sectioned in a transverse orientation on a Vibratome into 100 μm thick sections to evaluate the extent of the lesion. Slices were then Nissl stained to discriminate white and gray matter (Nissl 1894; Weiss and Greep 1977) and imaged using a Nikon microscope and software.

2.2 Split bath technique

In select experiments studying pharmacological interactions with sDC-stimulation, a partitioned bath was used to apply various pharmacological agents to specific segments of the spinal cord. A plastic partition was placed around the cord and sealed with petroleum jelly (Figure 2.1b). Dyes were used to verify the seal's integrity.

2.3 Hindlimbs-attached preparation

In order to differentiate the ventral root effects into more specific actions, a hindlimbs attached preparation was utilized. Rather than isolating the spinal cord, as in earlier experiments, the hindlimbs and their associated nerves were left intact as in Hayes et al (Hayes et al. 2009). To achieve this, P0-3 rats were decapitated and eviscerated, similar to other preparations described previously, in circulating low-calcium, high-magnesium aCSF (in mM: 128 NaCl, 1.9 KCl, 1.2 KH_2PO_4, 26 $NaHCO_3$, 0.85 $CaCl_2$,

6.5 $MgSO_4$, and 10 glucose, pH of 7.4) to chemically restrict limb movement. In addition to the ventral vertebrectomy as performed for the isolated cord preparation, a subsequent dorsal laminectomy was also added in order to provide more exposed surface area of the spinal cord for diffusion of oxygen. With the dorsal side of the spinal cord exposed for stimulation, the hindlimbs were pinned with their medial side down, exposing the lateral aspect muscles for recording (Figure 2.1c). The limbs were pinned in order to restrict movement for recording via suction electrode. This was accomplished by positioning insect pins through the hip, knee, and ankle joints as well as the toes; dorsal roots of thoracic and lumbar segments were rhizotomized prior to pin insertion to curtail nociceptive sensory feedback. The remaining ribs were also pinned at each segment to restrict movement along the thorax. Fascia and fatpads were removed from the musculature to provide access to individual hindlimb muscles. Electromygraphic (EMG) recordings were obtained by applying large (>100 μm diameter) glass suction electrodes to identified flexor and extensor muscles lying along the lateral aspect of the hindlimb. The bath was transitioned to a perfusion system circulating oxygenated regular aCSF to maximize oxygenation to the hindlimb musculature.

2.4 Sympathetic chain-attached preparation

In addition to somatic efferents destined for skeletal muscle, ventral roots also contain autonomic efferents. Because the sympathetic chain runs alongside the exterior of the vertebral column, it is possible to record pre- and/or postganglionic sympathetic activity concurrently with ventral root recordings. To achieve this, P0-3 rats were decapitated and eviscerated, similar to other preparations described previously, in circulating low-calcium, high-magnesium aCSF. A dorsal laminectomy was completed

from T1 to the tail in order to expose the dorsal surface of the spinal cord for oxygenation. A ventral vertebrectomy was also added with careful consideration taken to not damage the sympathetic chain. The preparation was positioned ventral up to allow for recording from the sympathetic chain and ventral roots concomitantly with insect pins into a recording chamber continuously perfused with regular aCSF (Figure 2.1d). Hindlimbs were then removed, leaving only the spinal cord, ribcage, and sympathetic chain. The sympathetic ganglia were identified and freed from surrounding connective tissue while maintaining continuity with the ventral roots (Figure 2.2).

Sympathetic chain segments from T12 to L2 ventral roots were used for recordings. Glass suction electrodes were applied either *en passant* or to cut ends of the sympathetic chain running between the sympathetic ganglia. Recordings from the sympathetic chain were verified by stimulating the homonymous ventral root to evoke a volley in the sympathetic recording electrode. Glass suction electrodes were also positioned on the L2 ventral roots for recordings of rhythmic lumbar activity. Sacral dorsal roots S2-S4 were stimulated to produce rhythmic activity in the lumbar ventral roots as described in Section 2.1.1.

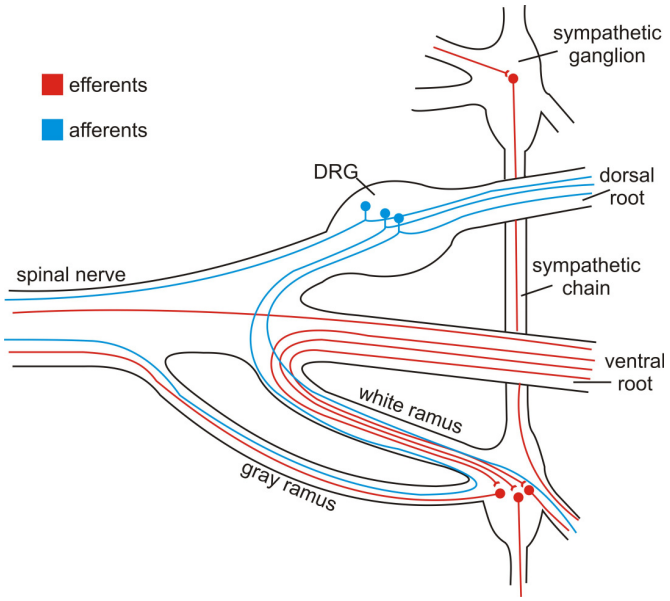

Figure 2.2: Sympathetic chain and its relationship to dorsal and ventral roots
The sympathetic chain's orientation with respect to spinal nerves. Efferents exit the spinal cord, and either enter the spinal nerve or travel in the white ramus to the sympathetic ganglia. In the sympathetic ganglia, efferents synapse onto sympathetic post-ganglionic neurons or travel to neighboring sympathetic ganglia through the sympathetic chain. Post-ganglionic axons exit the ganglia via the gray ramus to join the spinal nerve or through sympathetic nerves. Afferents enter the dorsal root ganglion (DRG) directly, after traveling in the gray and white rami, or through the sympathetic nerves via the white ramus. Adapted from Gray's Anatomy, 20th edition (Gray 1918).

2.5 Pharmacology

Neurochemicals used were obtained from Sigma-Aldrich (St. Louis, MO). All neurochemicals were stored in stock solutions of 1-100 mM at -20°C and then added to the bath to reach the desired concentration. The neurochemicals used and sites of action are summarized in Table 2.1.

Table 2.1: Summary of neurochemicals and concentrations used

Neurochemical	*Site of Action*	*Concentration*
Serotonin (5-HT)	5-HT receptor agonist	50 μM
N-methyl-D-aspartate (NMDA)	Glutamate receptor agonist	5 μM
Bicuculline methiodide (bic)	$GABA_A$ receptor antagonist	1 μM
N-vanillylnonanamide	TRPV1 receptor agonist	500 nM
Suramin	$P2X_{1-3}$ receptor antagonist	100 μM
Pancuronium	nAChR antagonist	25 μM
Yohimbine (yoh)	α_2-AR antagonist	2 μM
Prazosin (praz)	α_1-AR antagonist	2 μM
Dihydro-β-erythroidine (DHBE)	α_{2-4}-nAChR antagonist	50 μM
Atropine (atr)	mAChR antagonist	5 μM
Mecamylamine (mec)	$\alpha_{3,6,7,9}$-nAChR antagonist	50 μM
Methyllycaconitine (MLA)	α_7-nAChR antagonist	100-500 nM

2.6 Analysis techniques

The neural signals recorded were analyzed with a combination of techniques and software packages including MATLAB (The Mathworks, Inc.) and pClamp 10.2 software (Molecular Devices).

2.6.1 Burst analysis

Analysis of bursting patterns was performed in custom software, SpinalMOD (Gozal 2010), modified to suit the needs of this project. Stimulus artifacts were removed from signals for analysis and display by setting data points coinciding with stimulus pulses to zero. Data were then rectified and filtered using a low-pass Chebyshev Type II filter (2^{nd} order, 2.5 Hz stopband edge frequency, -20 dB stopband ripple) for burst identification. Once burst onsets and offsets were identified, burst duration, frequency, duty cycle, and phase between signal pairs were calculated. The phase between two signals was defined as the time from burst midpoint of the first signal to burst midpoint of the second divided by the cycle period, with 0 being exactly in-phase and 0.5 being 180° out-of-phase. The mean phase and mean resultant vector, r, which ranges from 0 to 1, were plotted on circular plots as previously demonstrated (Kjaerulff and Kiehn 1996). Angular deviation, which is closely related to the resultant vector, was calculated as

$$SD_{\phi} = \sqrt{2(1-r)} \quad (1)$$

where SD_{φ} is the angular deviation (Zar 1999). Burst intensity was defined as the rectified integral of the burst, defined by burst onset and offset time-points, divided by the burst duration (Gillis 1998). Locomotor-like activity was defined as left–right alternation combined with flexor–extensor alternation. Average bursting waveforms for

each signal were also calculated by extracting the low-pass filtered burst envelopes normalized for cycle period and finding the mean for each percent of the normalized cycle period, giving 100 points along the average waveform. Values for the bursting parameters are reported as means±S.D. unless otherwise indicated.

2.6.2 Quantification of pharmacological effects

In several studies presented here, pharmacological agents were used to modulate rhythmic patterns produced by sacral afferent stimulation. To assess these modulatory effects, bursting parameters taken from the SpinalMOD analysis were compared for various conditions. These bursting parameters included instantaneous burst frequency, burst duration, and burst intensity. Bursts were defined as multiple, non-reflex, events in a given time window detected by the rectified, low-pass filtered data. Bursting parameters were compared across conditions using a one-sample t-test comparing percent changes to a mean of zero. Statistical significance was set at $\alpha=0.05$. Strong but not statistically significant changes were also determined with $\alpha=0.1$. Two-sample, unpaired t-tests were used to compare pharmacological effects to time-matched control experiments for irreversible pharmacological effects.

2.6.3 Frequency domain analysis

In some instances, visualization of bursting activity in both the time and frequency domains were beneficial for comparing activity in different roots or activated by different methods. Spectrograms of short-time Fourier transforms (STFTs) and wavelet transforms were used for visualizing data in the time and frequency domains. These two methodologies were suitable for analysis of nonstationary data, such as biological data (Mor and Lev-Tov 2007). For the STFTs, data were divided into 256

overlapping windows (50% overlap) and Fourier transforms were repeatedly applied to each window across the signal. Wavelet transforms utilized the complex Morlet wavelet. Continuous wavelet transforms were taken as the sum of the signal multiplied by scaled, shifted versions of the Morlet wavelet (Goupillaud et al. 1984; Torrence and Compo 1998; Mor and Lev-Tov 2007). Both methods have been described in detail in the context of rhythmic spinal patterns in previous research (Mor and Lev-Tov 2007). Initial MATLAB code for wavelet transforms was written and provided by A. Grinsted, J. C. Moor, and S. Jevrejeva at http://www.pol.ac.uk/home/research/waveletcoherence/. Short-time Fourier transforms were computed in MATLAB using the "spectrogram" command.

2.6.4 Phase response curves

Phase response curves (Winfree 1980; Glass and Mackey 1988; Vogelstein et al. 2005) were generated for experiments in which stimulation of the sDC occurred during ongoing 5-HT/NMDA LLA. Each stimulus pulse generates a pair of "old" and "new" phases (φ_{old}, φ_{new}) depending on the calculated phase at which the stimuli occurred. If the stimulus has no effect on the ongoing rhythm, then the old phase will equal the new phase. When plotted as old phase vs. new phase, phase advances will lie above the equality diagonal, and phase delays will lie below. The onset of bursting was defined as the zero phase marker. At the time of stimulation, the old phase, φ_{old}, was calculated as

$$\varphi_{old} = \frac{t_{stim} - t^N}{\bar{T}} \tag{2}$$

where t_{stim} is the time of stimulation, t^N is the time of the most recent burst onset, and $\bar{T}$ is the mean cycle length measured during unperturbed bursting. After the stimulus occurs, the new phase φ_{new}, was calculated as

$$\varphi_{new} = 1 - \frac{t^{N+1} - t_{stim}}{\bar{T}} \tag{3}$$

where t^{N+1} is the time of the next burst onset after stimulation.

CHAPTER 3

SACRAL C FIBER AFFERENTS ARE REQUIRED FOR GENERATING LUMBAR VENTRAL ROOT RHYTHMS USING ELECTRICAL STIMULATION

The central pattern generator (CPG) responsible for locomotion can be accessed either pharmacologically or electrically, and it has been extensively studied in the isolated spinal cord of neonatal rats (Kudo and Yamada 1987; Smith et al. 1988) and mice (Hernandez et al. 1991; Bonnot et al. 1998). Activation of the CPG produces alternating rhythms, including locomotor-like activity, when activated by monoamines combined with N-methyl-D-aspartate (NMDA) or by acetylcholine (Kudo and Yamada 1987; Smith et al. 1988; Cowley and Schmidt 1994). Electrical stimulation has also been shown to activate the hindlimb locomotor central pattern generator in the neonatal rodent via dorsal root stimulation (Lev-Tov and Pinco 1992; Bonnot et al. 1998; Lev-Tov et al. 2000; Marchetti et al. 2001; Gabbay et al. 2002; Gordon and Whelan 2006) and the adult rat, cat, and human via epidural stimulation of the dorsal surface of the spinal cord (Dimitrijevic et al. 1998; Gerasimenko et al. 2005; Ichiyama et al. 2005; Gerasimenko et al. 2006; Gerasimenko et al. 2008).

Epidural stimulation has been shown to be effective at activating the locomotor CPG at multiple sites on the spinal cord. Stimulation of the sacral cord, in particular, has been shown to evoke locomotion in the adult spinal rat presumably by activation of

primary afferents (Edgerton and Roy 2002; Gerasimenko et al. 2006). Similarly, stimulation of the upper thoracic ventrolateral funiculus can activate locomotor-like activity in the neonatal rat by surface electrodes (Magnuson and Trinder 1997). Additionally, stimulation of the lumbar ventrolateral funiculus or the dorsal columns by penetrating electrodes through the ventral surface of the spinal cord also activates locomotor-like activity in the neonatal rat (Iwahara et al. 1991). In earlier research, our group developed a conformable multi-electrode array for epidural spinal cord stimulation and used it to stimulate the thoracic spinal cord with the ultimate goal of producing a neuroprosthetic device for restoring function to spinal cord injury (SCI) patients (Meacham et al. 2008; Guo et al. 2010). In an SCI patient with loss of locomotor ability, however, a preferred therapeutic stimulation site for restoring function would be caudal to the location of the lumbar CPG—which is predominantly localized in rostral lumbar segments (Cazalets et al. 1996; Kjaerulff and Kiehn 1996; Dimitrijevic et al. 1998)—to limit activation of unwanted spinal circuits and to ensure that the injury will not separate the stimulation from accessing the CPG.

For this research, we have selected the sacral dorsal column as a potential surface stimulation site for evoking locomotor-like activity in the neonatal rat spinal cord. The dorsal column is an afferent fiber pathway positioned along the midline of the spinal cord's dorsal surface, and it was selected based on the conclusions that the epidural-stimulation (Edgerton and Roy 2002; Gerasimenko et al. 2006) and dorsal root (DR)-stimulation (Lev-Tov and Pinco 1992; Bonnot et al. 1998; Lev-Tov et al. 2000; Gabbay et al. 2002; Gordon and Whelan 2006) studies commonly activated primary afferents in the sacral spinal cord. The dorsal column contains short and long projecting primary

afferent fibers which travel both rostrally and caudally, with most fibers terminating in the spinal gray, and only 25% reaching the medulla (Willis and Coggeshall 1991). The dorsal column transmits information regarding discriminative aspects of tactile sensations, kinesthesia, and viscerosensory pain information (Al-Chaer et al. 1996, 1996; Al-Chaer et al. 1998; Willis et al. 1999), and the distance traveled by the fibers is related to the afferent's sensory modality (Willis and Coggeshall 1991). The involvement of nociceptive input in the facilitation of locomotion has been appreciated in decerebrate cat preparations as noxious cutaneous stimuli applied to the perineum trigger locomotor patterns (Belanger et al. 1996; Chau et al. 2002). These perineal afferents, which originate in sacral segments, travel through the dorsal column before terminating in spinal cord gray matter or the nucleus gracilis (Al-Chaer et al. 1996). More recent research in mice by Whelan and colleagues directly demonstrated a contribution of nociceptive pathways in the modulation of SCA evoked locomotor rhythms via activation of the heat-sensitive transient receptor potential vanilloid-1 (TRPV1) receptor. They demonstrated that application of TRPV1 receptor agonists to sacral spinal segments blocked the production of lumbar motor rhythms by desensitizing nociceptive afferents (Szolcsányi 2004; Tominaga and Tominaga 2005; Mandadi et al. 2009). TRPV1 receptors are preferentially expressed in cutaneous and visceral nociceptive fibers (Kirkup et al. 2001; Gu and Heft 2004; Nakatsuka and Gu 2006). Conclusive studies for determining the fiber populations required for sacral afferent evoked CPG patterns have not been performed.

In the present work, I focused on characterizing the sacral dorsal column stimulation parameters required for activating the hindlimb motor CPGs including

identifying the afferent populations required. I demonstrate that TRPV1 receptor activation-sensitive, slowly-conducting afferent fibers are both necessary and sufficient for recruitment of sacrally-mediated lumbar motor rhythmogenesis.

3.1 Sacral dorsal column stimulation recruits lumbar rhythm generators

Initial studies using the isolated spinal cord preparation were performed to characterize the rhythmic patterns evoked by sDC stimulation. Rhythmic patterns induced by the stimulation of the sDC were studied in 53 experiments using recordings from the lumbar ventral roots associated with flexor (L2) and extensor (L5) projecting motoneurons (Kiehn and Kjaerulff 1998). Stimulation of sDC afferents with pulses at an amplitude of 200 μA, duration of 200 μs, and frequency of 2 Hz reliably induced periods of alternating activity in the left and right L2 ventral roots. The activity had a mean phase shift between the two roots of 173.3±26.16° (mean phase ± angular deviation, n=53) indicating that the two roots were out of phase regardless of activity produced in L5 ventral roots. The stimulus-induced L2 motor pattern deteriorated with stimulation trains longer than approximately forty seconds. I varied the stimulation frequency (0.2 to 2 Hz) and found the rhythm depressed within a relatively constant timeframe (36.6±9.9 s; n=26) independent of stimulation frequency; however, there was a tendency for motor pattern depression to occur more quickly with increased stimulation frequency, with an average motor pattern lasting 33.3 s for 0.2 Hz and 29.1 s for 2 Hz stimulation.

3.2 Variability in extensor-related L5 ventral root output

To establish the extent that sDC stimulation-induced rhythmic motor pattern generation represents expression of the locomotor CPG, recordings from L2 and L5 ventral roots were conducted. Both rhythmic and reflex pathways were recruited by sDC

stimulation. Rhythmic activity was observed in 53 of 59 experiments, and in all 53 experiments rhythmic alternating activity in the L2 ventral roots was observed. In comparison, rhythmic L5 ventral root activity was not reliably expressed and was never observed in the absence of rhythmic activity in L2 ventral roots. In 28 out of 53 experiments only time-locked, stimulation-evoked reflexes were observed in L5 roots (Figure 3.1a). These stimulus-evoked reflexes began 39.6±10.8 ms after the stimulus pulse and 6.9±12.3 ms prior to stimulus-evoked reflexes observed in L2 ventral roots. In the remaining 25 experiments, sDC stimulation was capable of recruiting rhythmic bursting events in the L5 ventral roots. For the purpose of these experiments, locomotor-like activity (LLA) was defined as alternating left–right rhythms coupled to alternating flexor (L2)–extensor (L5) rhythms (Kjaerulff and Kiehn 1996). In cases where L5 ventral roots were rhythmically active, the initiation of L5 rhythmicity began with the L2 bursting in 14 out of 25 cases and was delayed by an average of 1.8±0.83 cycles for the remaining cases. Most commonly, the activity pattern was that of left–right alternation, with rhythmic L5 bursting in-phase with its ipsilateral L2 (Figure 3.1b; n=17/53). This pattern is distinct from LLA because the ipsilateral flexors and extensors co-contract. A pattern consistent with locomotor-like activity was observed in only a small fraction of the animals, and in these cases L5 bursting and coupling were comparatively weak (Figure 3.1c; n=8/53). Rhythms were categorized based on mean phase relationships among root pairs with root pairs categorized as either in-phase or out-of-phase (see Figure 3.1 phase diagrams).

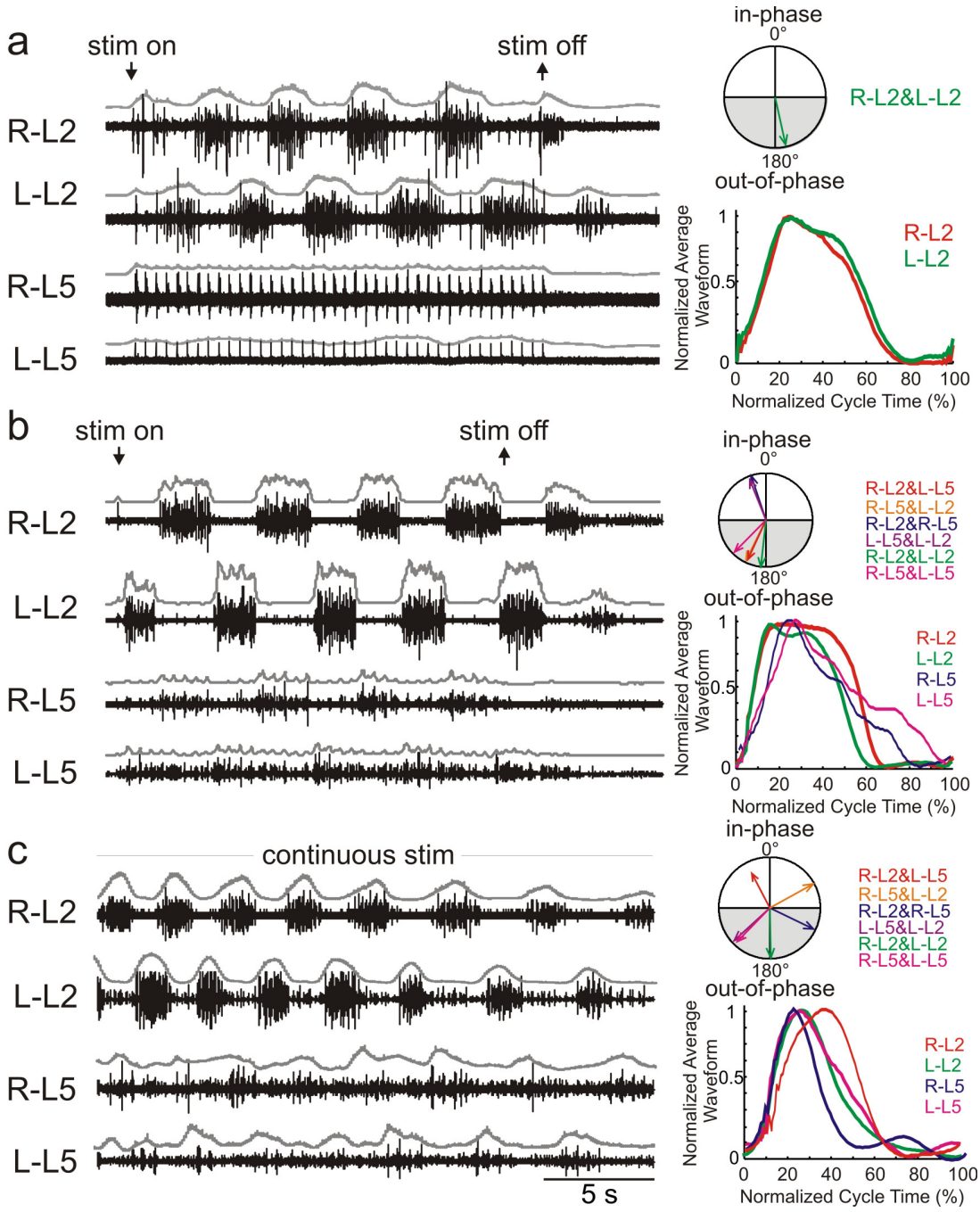

Figure 3.1: Sacral dorsal column stimulation evoked various rhythmic motor patterns
Stimulation of the sDC consistently produced rhythmic alternation in the L2 ventral roots. However, the pattern of activity produced in the L5 ventral roots varied. Evoked L5 activity was classified as either (a) reflexive, (b) rhythmic but in-phase with the ipsilateral L2, or (c) locomotor-like. Root pairs were classified as either in-phase (white region of phase plot) or out-of-phase (shaded region of phase plot) by their mean phase value represented by resultant vectors. Resultant vector length, (shown on the phase plots) represents concentration of phase values around the mean. Rhythms with ipsilateral L2-L5 pairs in-phase were classified as in (b) while rhythms with ipsilateral L2-L5 pairs out-of-phase were classified as in (c). Raw neurograms are displayed below their rectified filtered waveforms. Average filtered waveforms, normalized for cycle and amplitude are displayed for each root to show variation in burst shapes.

A summary of phase relationships for experiments with L5 bursting activity is shown in Table 3.1. Overall, phase relationships with L5 roots were less consistent due to the considerable variability in L5 rhythmicity and weak bursting levels in general. For example, note that for locomotor-like activity, L2 pairs were clearly out-of-phase, but L5 pairs were shifted by about 25% of the cycle out of phase. Interestingly, with flexor–extensor co-contraction, the cross-coupling between L2 to the contralateral L5 segment appeared more tightly coupled than for the ipsilaterally-coupled L5. The phase relationships, particularly those comparing L2 to L5 ventral roots, had a large amount of variability. To confirm the existence of two distinct populations, a histogram of the phase relationships between L2 and its contralateral L5 was plotted for all experiments. This histogram clearly shows that there are two populations of bursting rhythms consistent with the above categorization (Figure 3.2).

In total, these results are consistent with other reports of stronger rhythmogenic capacity in more rostral lumbar segments (Kjaerulff and Kiehn 1996; Cowley and Schmidt 1997; Kremer and Lev-Tov 1997). The variability in the patterns expressed by the L5 ventral roots may be accounted for by the subtle differences in afferent populations recruited with sacral dorsal column stimulation or by the weaker rhythmogenic capacity of the lower lumbar segments. The stimulation electrode placement on the midline may result in recruitment of slightly different afferent populations in each experiment, which may result in variability in the patterns produced. The patterns produced in L5 were universally weak compared to L2 demonstrating a weaker coupling between the L2 and L5 segments, which might allow for a variety of patterns to be produced.

Table 3.1: Comparison of phase relationships for rhythmic patterns produced via sDC stimulation

	Flexor–extensor co-contraction		***Locomotor-like activity***	
root pair	*observed*	*predicted*	*observed*	*predicted*
iL2-cL2	170.1 ± 26.7° (n=17)	180°	178.7 ± 23.3° (n=8)	180°
iL2-cL5	168.7 ± 51.5° (n=17)	180°	30.4 ± 53.3° (n=8)	0°
iL2-iL5	27.3 ± 45.8° (n=17)	0°	175.2 ± 64.7° (n=8)	180°
iL5-cL5	142.4 ± 48.7° (n=4)	180°	90.8 ± 27.1° (n=1)	180°

Phase relationships for L2 and L5 ventral roots from animals categorized as either having flexor–extensor co-contraction or locomotor-like activity. Values are presented as angular mean ± angular deviation. Predicted phase values for stereotypical coupling are provided for reference.

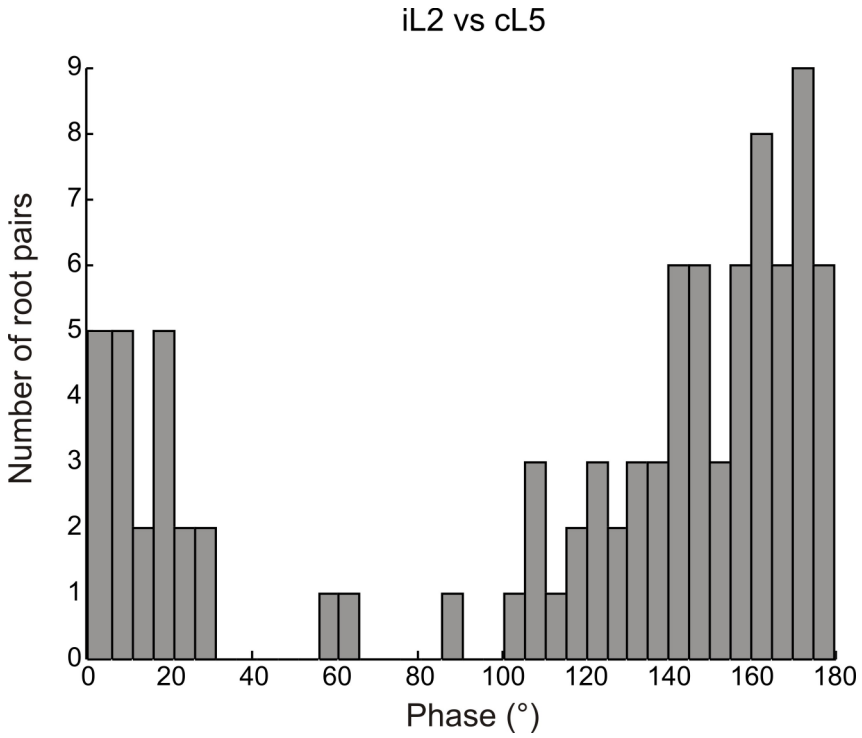

Figure 3.2: Histogram of phase relationships between L2 and contralateral L5 ventral roots
Histogram of calculated phase relationships for L2 vs. contralateral L5 ventral root pairs for all experiments. Bin width of 5.0° was used to count number of occurrences. The histogram shows two clear populations of phase relationships corresponding with the flexor-extensor co-contraction (100-180°) and locomotor-like activity (0-30°). Additionally, there were a few intermediate pairs (50-90°) which, when categorized, would contribute to increasing the variance of the population.

3.3 Afferent fiber populations involved

3.3.1 Sacral dorsal root and sacral dorsal column stimulation recruit overlapping pathways

While it is assumed that sDC stimulation evoked observed actions via recruitment of primary afferents, direct evidence is required. I first identified the rostrocaudal distribution of afferents recruited by sDC stimulation. I stimulated the sDC while recording antidromic volleys in dorsal roots T11-S3. Antidromic volleys were detected in segments ranging from T11 to S3 with volley size generally diminishing with increased distance from the stimulating electrode indicating that recordings more distal to the stimulation site had fewer afferent fibers traveling that distance (Figure 3.3a; n=2/2). Complementary orthodromic stimulation of S2-S4 dorsal roots also generated afferent volleys when in S3 sDC recordings (n=5/5; not shown). Together these results demonstrate that the sDC contains afferent axon collaterals that originate from many spinal segments.

Strauss and Lev-Tov (2003) showed that, like sDC stimulation, SCA stimulation also undergoes a depression of similar duration that is likely due to afferent transmission fatigue since subsequent stimulation of contralateral SCAs reinstates the motor rhythm. I took advantage of the observed stimulation-induced rhythm depression to determine whether sDC-evoked rhythms involved afferent recruitment, and if so, to identify the segmental origins. Stimulus trains applied to the sDC or to the corresponding sacral dorsal roots (S2-S4) induced comparable rhythmic L2 motor activity that underwent similar time-dependent depression. Rhythm deterioration produced by trains of stimuli applied to the sDC at S3 prevented subsequent evoked rhythms by sDR stimulation at S4,

and the converse was true when stimulation order was reversed (Figure 3.3b; n=4/4). These results demonstrate that sDC stimulation requires recruitment of dorsal column sacral afferents to activate lumbar motor patterns. However, as with stimulation of contralateral SCAs, an increase in stimulus intensity to recruit additional populations of afferents was able to reinstate sDC and sDR evoked rhythms and will be discussed in a later section (see Section 3.3.5). In comparison, stimulation of lumbar dorsal roots never interfered with sDC evoked rhythmic activity (n=2/2) and lumbar DC stimulation never evoked a bursting pattern (n=3/3). Therefore the sacral afferent population activated by sDR stimulation is one that travels through the sDC and is sufficient for activating the CPG.

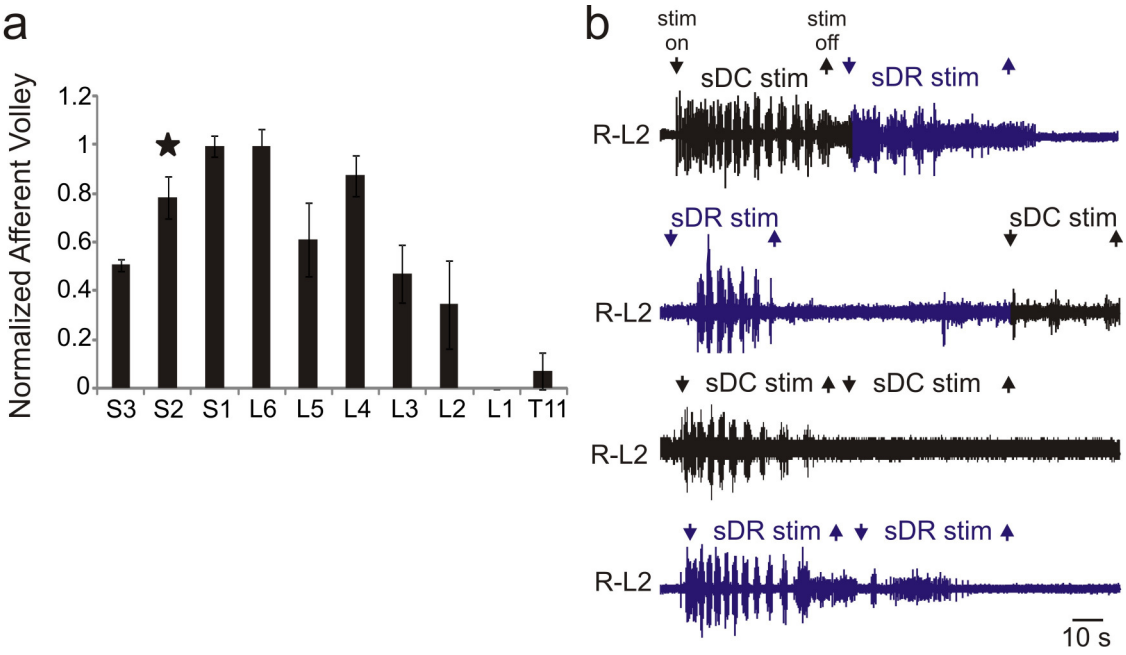

Figure 3.3: Rhythms evoked by sDC stimulation require sacral afferents in the sDC
(a) Stimulation of the sDC at S2 (denoted by star) recruited measurable afferent volleys in roots from T11-S3, with maximal volley amplitude in the sacral segments (mean±S.D.). Star denotes stimulation of the dorsal columns at S2. (b) Stimulation of the sDC until it deteriorates immediately followed by stimulation of sDR could not reinstate the rhythm, suggesting sDC and sDR stimulation are activating overlapping populations of afferent fibers. The reverse stimulation protocol (sDR stimulation followed by sDC stimulation) also could not reinstate the alternating rhythm. Examples showing repeated sDC or sDR stimulation are also shown demonstrating that repeated stimulation of the same site at the same stimulus intensity do not reinstate rhythms.

3.3.2 Dorsal column lesions

To establish that the axons travelling in the dorsal columns were indeed the population of fibers activating the lumbar CPG, lesions were made to the isolated spinal cord on the midline of the dorsal surface before and after attempting to activate the lumbar CPG by sDC stimulation. In five experiments, the dorsal columns were lesioned approximately one segment rostral to the site of stimulation. Even though some dorsal column lesions were incomplete, all affected the sDC-evoked rhythm (Figure 3.4). Values for observed reductions in burst intensity, duration and frequency are provided in Table 3.2. This data suggests the sacral afferent population activated by sDC stimulation includes a population that travels rostrally in the dorsal column.

Table 3.2: Effects of lesions to the dorsal column on sDC-evoked rhythms

	Burst Intensity (μV)	*Burst Frequency (Hz)*	*Burst Duration (s)*	*Number of Bursts*
Before Lesion	3.25 ± 2.51	0.23 ± 0.09	2.99 ± 2.09	7.70 ± 2.21
After Lesion	1.19 ± 1.74	0.17 ± 0.15	1.04 ± 0.94	4.00 ± 3.71
Percent Change	-60.6 ± 52.4%*	-35.3 ± 58.4%$^{+}$	-46.5 ± 50.9%*	-40.4 ± 57.0%$^{+}$

Lesions to the dorsal column were variable and depended on the severity of the lesion. Pooled data for five experiments (10 L2 ventral roots) along with percent changes are shown here (mean±S.D.). Plus signs ($^{+}$) indicate statistical significance with $0.05<p<0.1$, and asterisks (*) indicate statistical significance with $p<0.05$ using one-sample t-test comparing percent changes to a mean of zero.

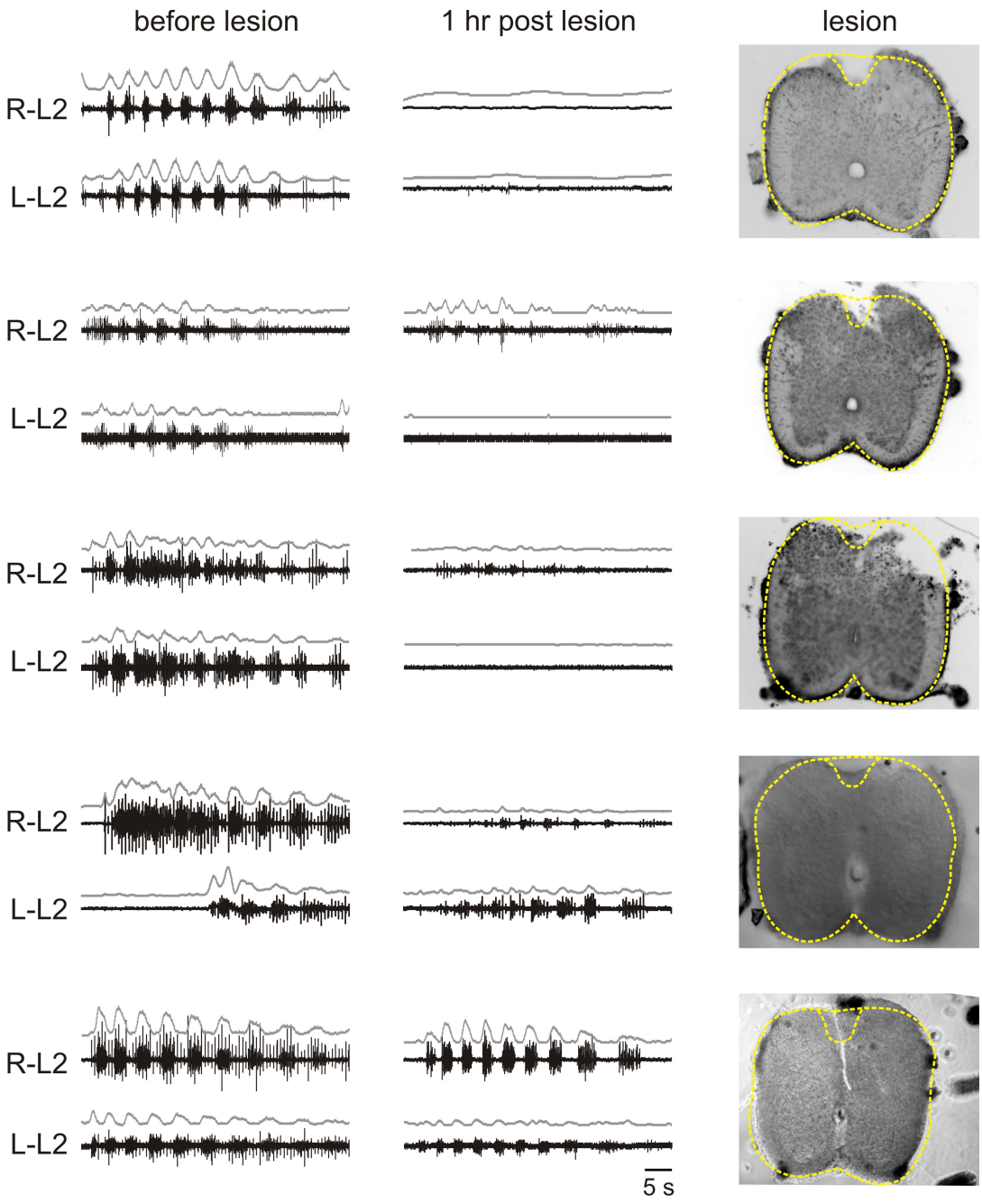

Figure 3.4: Lesions to the dorsal column affected sDC-evoked lumbar rhythms
Lesions were made to the dorsal columns approximately one segment rostral to the site of stimulation. Recordings from the L2 ventral roots uniformly diminished after lesioning and depended on the severity of the lesion. Lesions eliminating portions of the dorsal column reduced sDC-evoked rhythmic activity 1 hr post lesion in 4 out of 5 cases. In the last case, the lesion was slight and only affected tonic firing superimposed on rhythmic bursting. Gray-scale Nissl-stained images of the lesion for the first three examples are shown. The tissue integrity for the remaining two examples deteriorated prior to Nissl staining; thus gray-scale phase contrast images are displayed. Dashed outlines for preceding, unlesioned sections are shown with the dorsal column white matter tract outlined for reference.

3.3.3 Comparison of afferent volley to L2 reflex recruitment

To directly determine the relationship between L2 reflex recruitment and recruitment of afferent fiber populations, compound action potentials (CAPs) were recorded in a sacral dorsal root and/or the dorsal column while monitoring L2 ventral root activity during sDR or sDC stimulation. The experimental configuration is shown in Figure 3.5a. Stimulation electrodes were placed on the sDC and an sDR between S1 and S4. Recording electrodes were placed more proximal to the spinal cord on the homonymous dorsal root and on the dorsal columns at L5. The electrical stimulus intensity that straddled minimal recruitment of afferents was defined as threshold. Current intensity was then increased until L2 ventral root activity was observed for comparison. The threshold for evoking an afferent volley by either sDR or sDC stimulation is shown in Table 3.3. In general, the current required to activate volleys via sDC stimulation was higher and more variable than that required via sDR stimulation. DC volley thresholds for sDR stimulation were not calculated due to the interposed DR recording electrode between sDR stimulation and DC recording electrodes, which may have hindered conduction of the volley.

Table 3.3: Comparison of threshold current values for evoked afferent volleys

	DR Volley Threshold	*DC Volley Threshold*
sDR stimulation	4.3 ± 1.8 μA (n=18)	N/A
sDC stimulation	8.0 ± 5.3 μA (n=3)	18.8 ± 11.4 μA (n=5)

Current values for threshold were established as the minimum current required for presence of the indicated volley. Values are presented as mean±S.D. Overall, DR volley thresholds were lower than DC volley thresholds and had lower variability.

The threshold current intensities required to recruit afferent volleys were less than those required for evoking activity in the L2 ventral root. When expressed as multiples of dorsal root afferent volley threshold, reflexes were observed at 1.9±0.4 times the afferent volley threshold (xT) (n=15), and for sDC stimulation, L2 reflexes were observed at 2.7±1.6xT (n=11). The two populations were not statistically different (unpaired t-test, $p>0.05$) indicating that the thresholds were comparable and consistent independent of the site of stimulation.

Since the threshold for recruiting reflex activity in the L2 ventral root was greater than that for recruiting the afferent volleys, L2 recruitment may be the result of recruitment of higher-threshold fibers (i.e. Aδ or C fibers) or interneuronal populations. Moreover, the use of threshold as a measure of recruitment of distinct fiber populations is likely blurred in this preparation as myelination of axons is incomplete at birth (Fulton 1987). Thus, distinctions between low-threshold Aβ, higher-threshold Aδ, and unmyelinated C fibers become more difficult both in terms of threshold for recruitment and conduction velocity. Multiple component compound action potentials were observed following both sDC and sDR stimulation in P2 and P3 isolated spinal cords, and conduction velocities for these components were calculated based on the time elapsed from stimulation to the apex of the specified component divided by the distance between the electrodes (n=4; Figure 3.5b). Even though conduction velocity measurements change greatly in the first postnatal week (P0-7), differences between P2 and P3 conduction velocities for the different fiber populations are slight (Fulton 1987) but clearly separable (Nussbaumer et al. 1989). Conduction velocity measurements of later sDC components were excluded due to branching of afferents as they travel in the dorsal

column. The branching of afferents in the dorsal column reduces the axon diameter, which lowers the conduction velocity of the fibers. These reductions are unpredictable in the experimental setup used, which makes the later sDC components unreliable. Since supramaximal stimulation (>50T) did not recruit additional components, it was determined that the CAP components represented A and C fiber populations, with C fibers comprising the slowest conducting population (Figure 3.6a and b). Histograms reporting the range and incidence of conduction velocities for identified components are shown in Figure 3.5c and d. These data are also summarized in Table 3.4.

Table 3.4: Conduction velocities of afferent fibers

	1st component	*2nd component*	*3rd component*
DR conduction velocity	0.89 ± 0.44 m/s	0.37 ± 0.09 m/s	0.19 ± 0.07 m/s
DC conduction velocity	0.50 ± 0.09 m/s	N/A	N/A

Conduction velocities of afferent volleys in the DR and the DC were calculated as the time to signal deflection, represented in (Figure 3.5a), over the measured distance between stimulating and recording electrodes. Values are presented as mean±S.D.

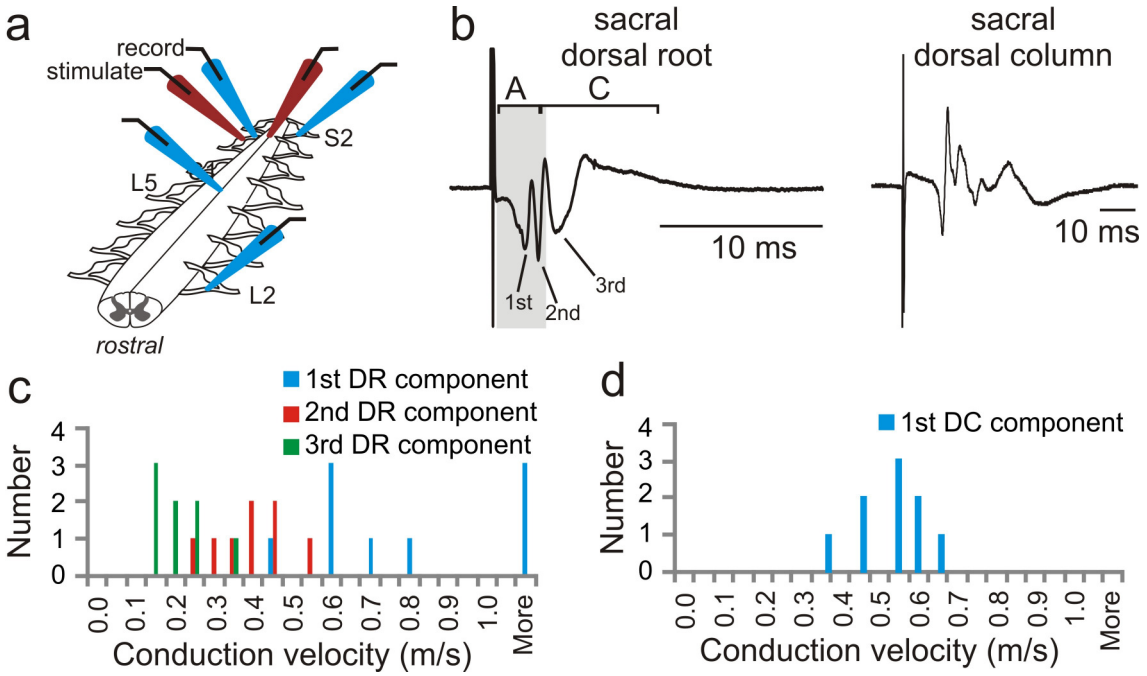

Figure 3.5: Conduction velocities of afferent fiber populations
(a) Recoding setup for afferent volley studies. (b) Representative example of afferent volleys with multiple components being recruited via sDR and sDC stimulation. (c) Histogram of sDR CAPs conduction velocities separated by component. (d) Histogram of sDC CAPs 1st component conduction velocities. Bin size 0.05 m/s. Histograms contain pooled data from four animals (14 CAPs total).

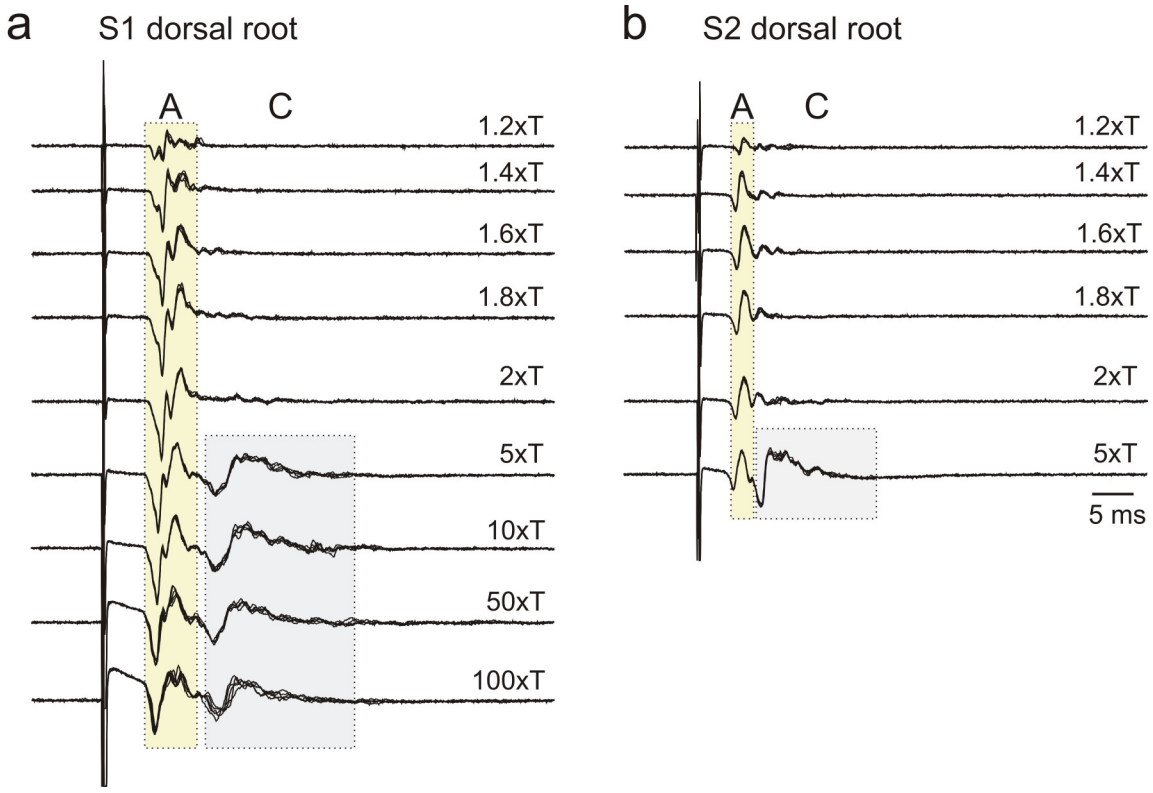

Figure 3.6: Relation of afferent volleys components to threshold afferent recruitment in sacral dorsal roots

Recordings are from a P2 animal in the S1 dorsal root (a) and S2 dorsal root (b). Stimuli were delivered with 0.2 ms pulse width at positive polarity. Recording and stimulating electrodes were placed most proximally and distally for each root, respectively. Displayed episodes represent 5 sweeps superimposed. Values are expressed in multiples of threshold of the first detectable deflection in the afferent volley. (a) For the S1 root, stimuli were tested at strengths up to 100xT. Note that in this root the slowest conducting volley was near-maximally recruited between 2xT and 5xT. The lack if subsequent recruitment if any additional volleys even at 100xT confirms that these are C fibers, that in the neonate are recruited at low threshold values. (b) In the S2 dorsal root, separation of A from C fiber components was less due to smaller inter-electrode distance and consequent reduced conduction time. The C fiber volley was recruited between 2xT and 5xT in this root as well. A and C fiber volleys components are highlighted and designated A or C.

3.3.4 High-threshold afferents are necessary and sufficient for sacral dorsal column evoked rhythms

To establish if recruitment of select afferent fiber populations were sufficient for motor pattern generation, afferent volleys were recorded at stimulus intensities below and at those required for their recruitment. Based on reflex recruitment as defining threshold, previous studies indicated that low-threshold stimuli could be used to activate the hindlimb locomotor CPG via low-threshold, large diameter sacrocaudal afferents (Lev-Tov and Pinco 1992; Bonnot et al. 1998; Lev-Tov et al. 2000; Marchetti et al. 2001; Gabbay et al. 2002; Gordon and Whelan 2006). Here, using afferent volley recruitment to define threshold, I found that lumbar motor rhythms recruited using either sDR or sDC stimulation was relatively low, at less than or equal to 2xT for most experiments (n=14/17). However, afferent volley recordings demonstrated that a low threshold did not correspond to the recruitment of only the fastest conducting low-threshold afferent fibers. Rather, this intensity also recruited slower conducting high-threshold fibers (Figure 3.7a and b). Critically, it was only when the slower conducting high-threshold afferents, clearly recruited at stimulus intensity defined as low-threshold, was rhythmic motor activity recruited. Importantly, the threshold value required to recruit these high-threshold fibers was highly variable and ranged from 1.1-4xT (2.0±0.8xT, n=11). Thus, at least for sacral afferents, at this stage in development, it is clear that threshold values cannot be used to discriminate between afferent fiber populations.

To determine if high-threshold fibers are not only required but also sufficient for recruiting the CPG, the contribution of the low-threshold fibers must be eliminated. A

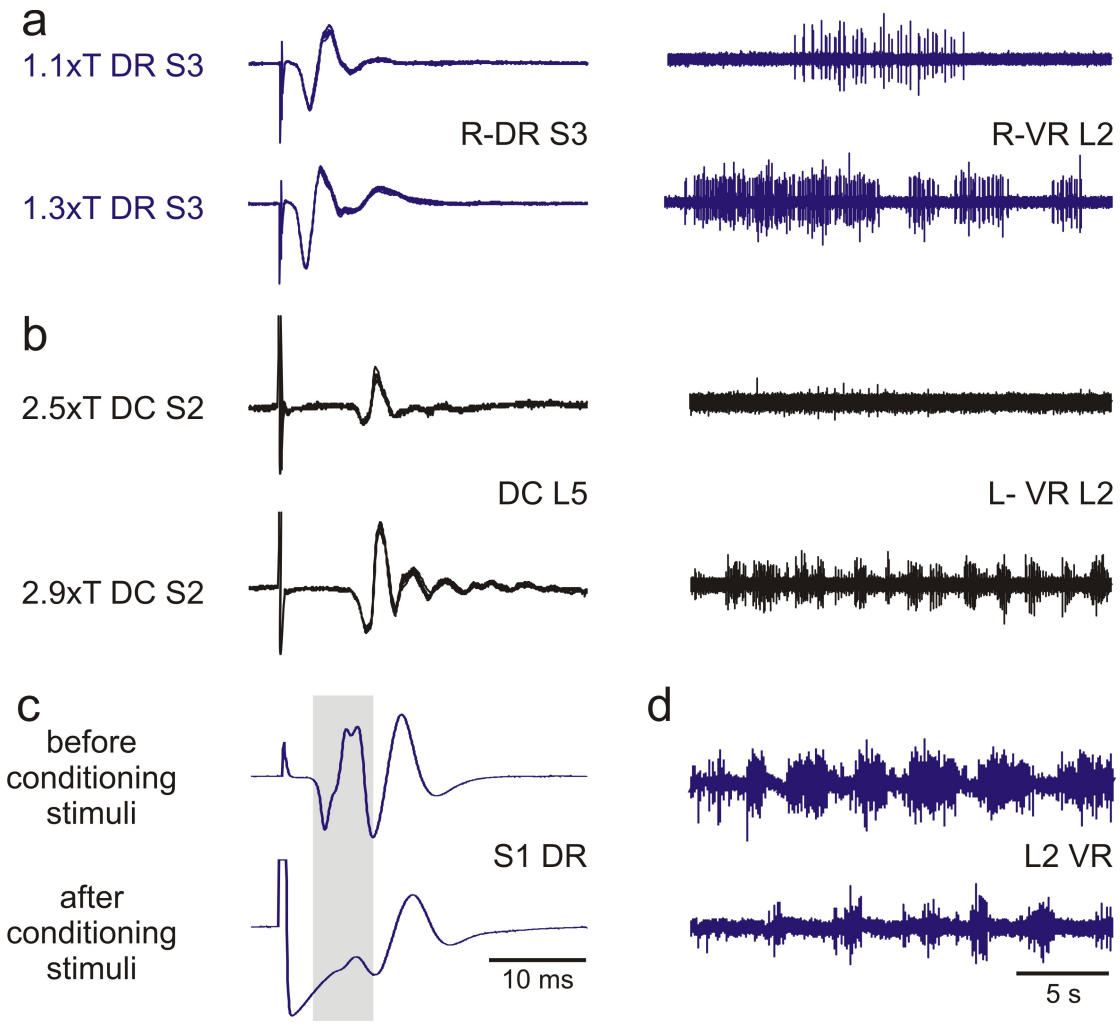

Figure 3.7: Recruitment of rhythmic motor output requires activation of high-threshold afferents Stimulation of (a) sacral dorsal roots or (b) sacral dorsal columns at intensities that recruit high-threshold afferents activates lumbar motor rhythms, demonstrating that high-threshold fibers are necessary for activating the CPG. (c,d) High-threshold (50xT), negative polarity stimulation at 50 Hz prior to the typical 2 Hz stimulus train blocks low-threshold afferents selectively (c), but does not block recruitment of lumbar motor rhythms (d), demonstrating that high-threshold fibers are sufficient for activating the CPG.

short, train of high intensity, negative polarity stimulus pulses (50 Hz, 20 pulses, 200xT) was used to temporarily block conduction in the faster conducting low-threshold, A fiber afferents (Russo et al. 2000; Quevedo 2011). The mechanism behind these conditioning stimuli is unknown at this time (Quevedo 2011) but may be related to high-intensity stimuli selectively blocking certain fiber populations (Changfeng and Dazong 1994). The conditioning stimuli affected propagation of both A and C fiber populations, but more profoundly affected the A fibers by reducing the amplitude of the CAP volley (Figure 3.7c). Applying this conditioning stimulation to the sacral dorsal root weakened but did not block activation of the L2 rhythmic motor activity (Figure 3.7c and d), indicating that C fiber afferent activation was sufficient for recruiting the lumbar CPG (n=2/2). However, it is still possible that the remaining A fibers being recruited are involved in the rhythmogenesis, but the weakened rhythm could also be explained by fewer C fibers being recruited post-conditioning stimuli. In conjunction with the aforementioned results demonstrating that the slower conducting C fiber afferents were required for the expression of the rhythmogenesis, these slower conducting afferents are both necessary and sufficient for recruiting lumbar CPG rhythms. Conversely, faster conducting A fibers are neither necessary nor sufficient.

3.3.5 Depressed rhythms resulting from submaximal activation of afferents can be reinstated with increased stimulation intensity

In order to determine the extent to which recruitment of additional fiber populations could reinstate deteriorated motor rhythms, lower intensity stimuli, which eventually depressed the motor rhythm, were followed by higher intensity stimuli. Submaximal 2xT stimulation of the S2-S4 sDR at 2 Hz evoked rhythmic alternation in

the L2 ventral roots, as previously discussed, which eventually deteriorated. Immediately stimulating at 2xT again (Figure 3.8a) did not reinstate the rhythm, but the afferent volley recorded remained unchanged, showing that conduction failure of afferent fibers did not contribute to the observed depression (n=3/3). However, if 2xT stimulation induced depression was immediately followed with increased intensity between 3-5xT, the rhythm always reinstated (Figure 3.8b). Thus, recruiting a distinct population of afferent fibers from the same root, as evidenced by an increase in afferent volley amplitude, was able to circumvent motor rhythm depression. This supports the view that synaptic depression of primary afferent transmission leads to deterioration of motor rhythm generation and demonstrates that subpopulations of C fiber afferents sacral dorsal root recruited by the higher intensity stimulation are capable of activating motor rhythms.

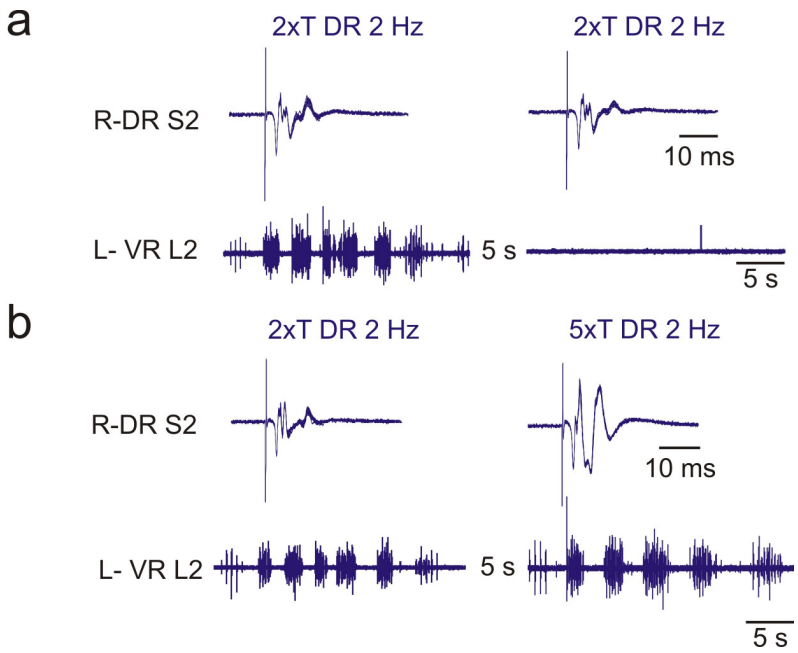

Figure 3.8: Reinstatement of depressed rhythms by recruiting non-fatigued afferents
(a) Activation of the sDR recruits L2 rhythms, which deteriorates and cannot be reinstated with the same stimulation intensity a short time later; however the afferent volley remains unchanged. (b) Stimulation at a higher intensity of the same dorsal root after depression reinstates the L2 ventral root motor pattern by recruiting additional populations of non-fatigued afferents.

3.3.6 Transient receptor vanilloid-1 receptor agonists selectively eliminate recruitment of C fiber afferents and afferent evoked lumbar rhythms

To determine more fully which C fiber afferents mediate sDC-evoked CPG activation, studies using agonists and antagonists of known nociceptive pathways were performed. I tested the actions of agonists acting on transient receptor potential vanilloid-1 (TRPV1) receptors, which are known to be associated with nociceptive afferent information processing, on sDC and sDR evoked rhythmic motor output

TRPV1 receptors are activated by capsaicin and localize primarily on primary afferents terminals in superficial dorsal horn of neonatal rodent, activation of these receptors has been shown to initially increase locomotor frequency followed by a suppression of locomotion activated by sacrocaudal afferent stimulation in neonatal mice (Mandadi et al. 2009). In this work, application of the TRPV1 receptor agonist N-vanillylnonanamide, a synthetic capsaicin, similarly affected sDR and sDC evoked lumbar rhythms in the neonatal rat, irreversibly blocking the activity if left applied for greater than five minutes (Figure 3.9a and b; n=3/3 and n=5/5, respectively). Additionally, recordings of the slower conducting component of the afferent volleys in the sacral dorsal root were correspondingly blocked (n=3/3). Blockade of these later, slower conducting volleys supports their identity as high-threshold C fibers and supports the earlier data that C fibers are necessary for recruitment of rhythmic motor patterns. Afferent volleys in the dorsal columns were also affected, with a global decrease in DC volley amplitude, which was difficult to interpret given the complex multi-segmental composition of dorsal column fibers with various degrees of branching, which would affect the conduction velocities of fibers (n=4/5). Nonetheless, selective blockade of the

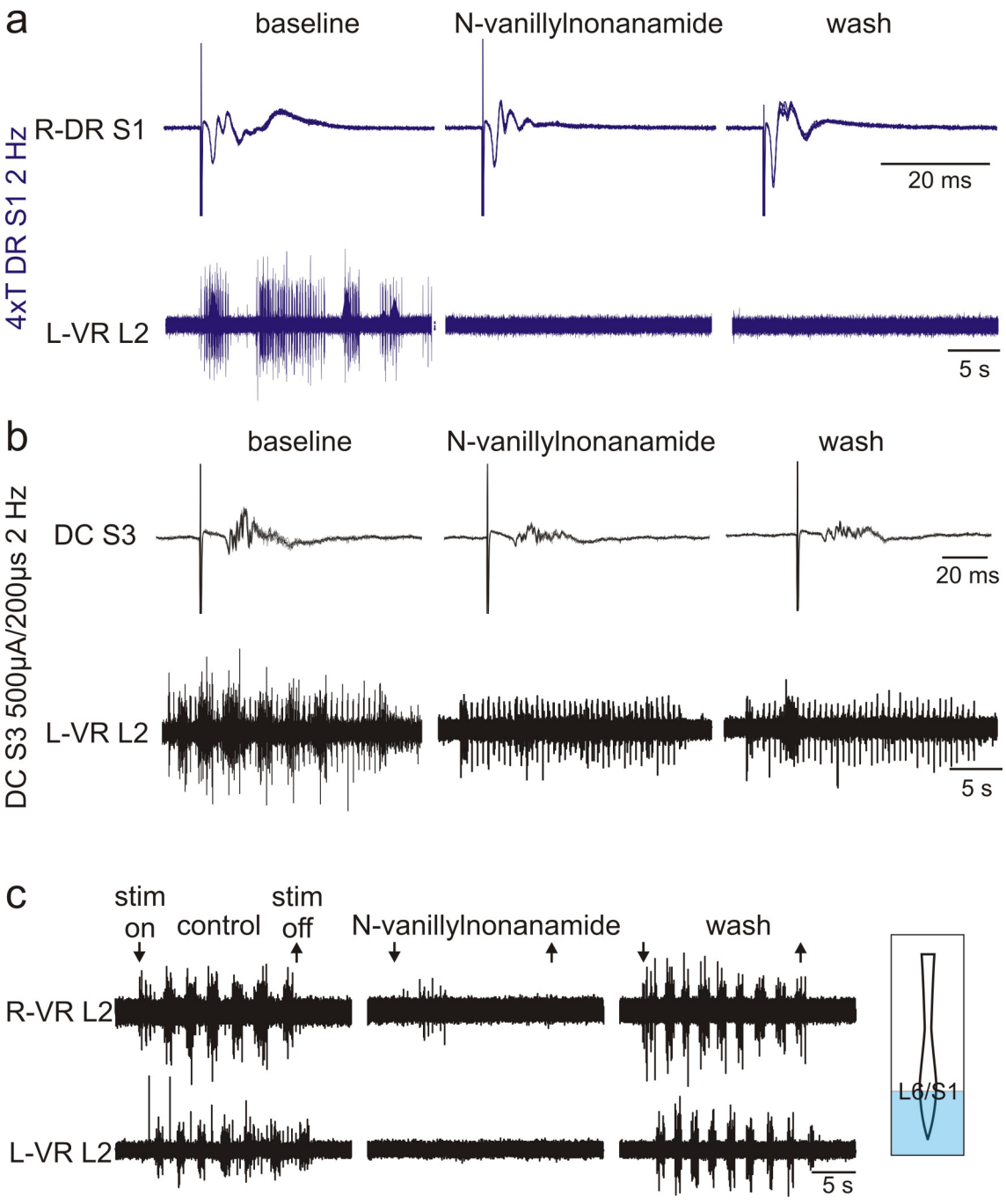

Figure 3.9: High-threshold afferents sensitive to TRPV1 agonists block rhythmic output
Application of the TRPV1 receptor agonist N-vanillylnonanamide desensitizes high-threshold afferents activated by (a) sDR stimulation resulting in a loss in the later volley components and loss of rhythmic lumbar activity. (b) N-vanillylnonanamide had similar effects of sDC stimulation evoked lumbar rhythms, but had a global decrease of dorsal column compound action potentials due to extensive axon branching and multisegmental components. (c) Selective application of N-vanillylnonanamide to sacral segments blocks rhythmic lumbar output activated by sDC stimulation, similar to that reported in Mandadi et al (2009) for sacrocaudal afferent stimulation.

C fibers in dorsal roots combined with block of sDC stimulation evoked actions strongly suggests that visceral afferents alone are capable of activating the observed lumbar motor rhythms.

To determine if TRPV1 agonist actions were selective to sacral segments, the experimental bath was divided into thoracolumbar and sacral segments using a transverse partition. Application of 500 nM N-vanillylnonanamide to the sacral chamber abruptly and transiently activated lumbar rhythmic motor activity but then completely abolished stimulation induced rhythmic activity (n=7/7) presumably through receptor desensitization. This effect was reversible, and rhythmic activity returned upon washout if accomplished within 5 minutes of application (Figure 3.9c). These results demonstrate that the TRPV1 receptors located on sacral primary afferents can eliminate sDC-evoked lumbar ventral root activity.

3.4 Summary and perspective

The overall findings suggest sacral visceral C fiber afferents access the lumbar CPG. The following observations support this conclusion. Selective tonic stimulation of the sDC robustly activated rhythmic alternating L2 ventral root activity that deteriorated, usually in under a minute, consistent with actions arising from afferents. Sacral dorsal column stimulation-evoked ventral root rhythms required activation of sacral afferents with C fibers identified as both necessary and sufficient. The rhythm encoding complement of C fibers in the sDC arise from viscera, and comprise a population of nociception encoding TRPV1 afferents.

CHAPTER 4

PHARMACOLOGICAL DISSECTION OF SPINAL PATHWAYS INVOLVED IN AFFERENT EVOKED RHYTHMS

Sacrocaudal afferent (SCA) stimulation has revealed that both short and long multifunicular projecting propriospinal neurons play a role in SCA induced rhythms, suggesting that many different spinal tracts play a role in the generation of lumbar rhythms by SCA afferents (Etlin et al. 2010). These results correspond with research indicating that many propriospinal white matter tracts in the ventral cord are active during locomotion (Jankowska 1992; Jankowska and Edgley 1993). For this research, surface stimulation of the sacral dorsal column (sDC) was used for recruitment of afferent fibers that activate the lumbar pattern generating network in the neonatal rat spinal cord. Similar to SCA activated lumbar rhythms, sDC activated rhythms are mediated by sacral afferents traveling briefly in the dorsal column before synapsing onto interneurons (Strauss and Lev-Tov 2003; Etlin et al. 2010).

The recruitment of multifunicular pathways also suggests that many pathways may be acted upon by SCAs to generate motor rhythms. The involvement of nociceptive afferents and pathways in SCA induced rhythmogenesis was also supported with the involvement of heat-activated TRPV1, cold-activated TRPM8 and analgesia-inducing μ-opioid receptors, supporting an involvement of nociceptive afferents in modulation of SCA generated rhythms (Blivis et al. 2007; Mandadi et al. 2009). In the last chapter, I

demonstrated that sacral TRPV1 receptor-expressing C fiber afferents are necessary and sufficient for activation of the lumbar pattern generator, and moreover, within the sDC, these afferents are visceral C fibers. TRPV1 receptors, along with ATP-sensitive purinergic P2X receptors, are preferentially expressed in cutaneous and visceral nociceptive fibers (Kirkup et al. 2001; Gu and Heft 2004; Nakatsuka and Gu 2006). However, unlike the TRPV1 receptor, P2X receptors are also found post-synaptically on interneurons throughout the spinal cord.

The descending monoaminergic neurotransmitters serotonin (5-HT), noradrenaline (NA), and dopamine (DA) are well known for modulating spinal cord locomotor function (Sillar et al. 1998; Kiehn et al. 1999; Schmidt and Jordan 2000; Sqalli-Houssaini and Cazalets 2000; Ballion et al. 2002; Branchereau et al. 2002; Jordan and Schmidt 2002; Allain et al. 2005; Liu and Jordan 2005). Additionally, the monoamines modulate SCA-induced rhythms in the neonatal mouse with NA and DA depressing rhythms and 5-HT increasing burst amplitude and cycle period (Gordon and Whelan 2006). Specifically, α_1-adrenoceptor, 5-HT_2-receptor, and D_1 receptor agonists increased burst amplitude, and α_1-adrenoceptor and 5-HT_2-receptor agonists also increased cycle period whereas α_2-adrenoceptor and 5-HT_7 receptor agonists depressed or disrupted the SCA-evoked rhythms (Gordon and Whelan 2006). In contrast, studies have demonstrated that α_2-adrenoceptor agonists can aid in the initiation of stepping in chronic spinal cats (Forssberg and Grillner 1973; Chau et al. 1998; Marcoux and Rossignol 2000; Barthelemy et al. 2006), and studies in the neonatal rat demonstrated that α_1-adrenoceptor agonists can generate lumbar rhythms (Gabbay and Lev-Tov 2004), but it has also been shown that α-adrenoceptor antagonists have no effect on SCA induced lumbar rhythms in

the rat (Strauss and Lev-Tov 2003). These variable effects of α-adrenoceptor antagonists may be dependent on the species of animal being studied and the method for activating locomotor activity.

Acetylcholine and cholinergic interneurons have also been implicated in CPG activation based on a host of studies, which have focused on cholinergic axons modulating locomotor activity and identifying essential properties for CPG-related interneurons (Cowley and Schmidt 1997; Deuchars 2007; Miles et al. 2007; Brownstone and Wilson 2008; Kwan et al. 2009; Zagoraiou et al. 2009). However, it has been suggested that sacral, cholinergic relay interneurons ascending through the ventral and ventrolateral funiculi may play a role in SCA induced rhythms (Strauss and Lev-Tov 2003; Anglister et al. 2008; Lev-Tov et al. 2010).

In this work, the role of adrenergic and cholinergic receptor containing interneurons in the expression of sDC-evoked lumbar rhythms is explored.

4.1 Nociceptive related purinergic receptor pathways also alter sacral afferent evoked lumbar rhythms

Similar to TRPV1 receptors, ionotropic P2 purinoceptors (P2X receptors) localize on primary afferent terminals in the dorsal horn, but they are also found on dorsal horn interneurons throughout the spinal segments (Nakatsuka and Gu 2006). Because TRPV1 receptor agonists had effects on the afferent volley, effects of the P2X receptor antagonist suramin were also studied. Using 100 μM suramin, which would block $P2X_{1,2,3}$ receptors (Lambrecht 2000), afferent volleys were recorded in the sacral dorsal roots of the isolated neonatal rat spinal cord along with the lumbar ventral root activity in L2. Suramin had no effect on the amplitude of the afferent volley; however, suramin irreversibly blocked

rhythmic lumbar patterns in the ventral root (Figure 4.1a and b). These results indicate that P2X receptor activation is required for the production of sDC-evoked lumbar rhythms.

The experimental bath was again partitioned to isolate the bathing media of thoracolumbar segments from sacral segments. Suramin (100 μM) blocked rhythmic motor output when applied to either sacral (Figure 4.1c; n=4/5) or thoracolumbar baths (n=3/3, data not shown). Suramin's actions were irreversible only in the thoracolumbar bath, but they were reversible in the sacral bath. This difference in reversibility may be a result of suramin acting on different P2X receptor subtypes in thoracolumbar versus sacral spinal segments since $P2X_3$ receptors are found presynaptically on primary afferent terminals whereas $P2X_2$ receptors are found postsynaptically on spinal neurons in all segments (Chizh and Illes 2001). Thus, sacral bath effects could be due to $P2X_3$ receptor activation while thoracolumbar segment effects could be due to $P2X_2$ receptor activation alone. The reversibility seen in the sacral cord application of suramin may be due to the fast desensitization of $P2X_3$ receptors, while the irreversibility of suramin in thoracolumbar segments may be explained by the $P2X_2$ receptor's slow desensitization (Chizh and Illes 2001). In combination with the TRPV1 receptor results in the previous chapter, one potential afferent fiber population that could be responsible for sDC-evoked rhythms is the population of visceral C fibers since P2X receptors and TRPV1 receptors colocalize on visceral C fibers (Gu and Heft 2004; Christianson et al. 2009).

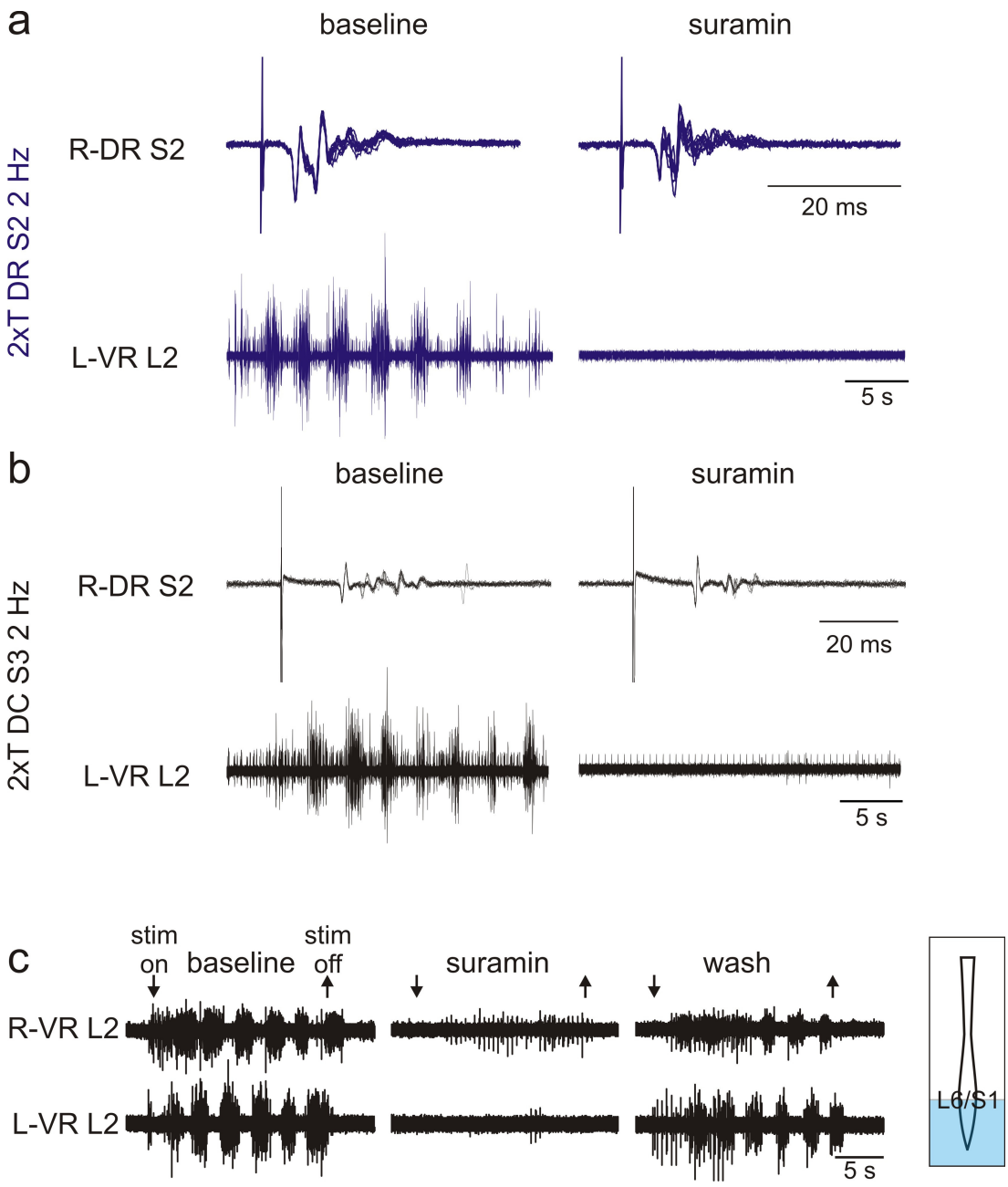

Figure 4.1: P2X receptors are activated during sacral afferent stimulus-evoked lumbar rhythms Application of the P2X receptor antagonist suramin blocks rhythmic activity induced by (a) sDR and (b) sDC stimulation; however, suramin does not affect the size of the afferent volley, indicating its actions are postsynaptic. (c) Selective application of suramin to sacral segments abolished sDC evoked rhythmic activity, indicating P2X receptor containing interneurons are located in the sacral segments. Additionally, selective application of suramin to thoracolumbar segments also abolish sDC evoked rhythms, indicating additional populations of P2X receptor containing interneurons involved in CPG activation are widely distributed (data not shown).

4.2 Alpha-adrenergic involvement in sDC-evoked rhythms

Previous research suggested that α-adrenergic receptors (α-ARs) are involved in rhythmogenesis in the sacrocaudal cord via application of NA/NMDA (Gabbay et al. 2002; Gabbay and Lev-Tov 2004) but are not involved in sDR-induced lumbar rhythmogenesis in the rat (Strauss and Lev-Tov 2003) implying that there are multiple, independent means for accessing the lumbar CPG. Other research in the spinal cat has indicated that noradrenergic agents initiate locomotor bouts better than other monoamines (Barbeau and Rossignol 1987; Chau et al. 1998). Here I sought to identify the involvement of α-ARs in sDC-evoked lumbar rhythms.

4.2.1 Whole bath experiments

Initial experiments evaluating the effects of α-AR antagonists were done in the isolated spinal cord preparation with the α-AR antagonists individually applied to the whole cord. Whole bath application of the α_2-adrenergic receptor antagonist, yohimbine (2 μM), did not block the stimulus-evoked rhythmic motor output in the L2 ventral roots (n=3/3; Figure 4.2a). Yohimbine's effects on bursting properties, summarized in Table 4.1, were slight and not statistically significant with burst intensity, frequency, and number slightly decreased and burst number slightly increased (n=5 experiments, 10 L2 ventral roots). Prazosin (2 μM), an α_1-adrenergic receptor antagonist, blocked (n=2/5) or attenuated (n=3/5) sDC-evoked lumbar rhythms (Figure 4.2a). Prazosin significantly reduced burst intensity ($p<0.05$), and reduction in burst frequency was near significance ($0.05<p<0.01$) (Table 4.1, Figure 4.2c). Burst duration and number were also reduced, but the effects were not statistically significant. In Figure 4.2b and c, normalized changes in burst parameters are displayed for all analyzed roots. Yohimbine's effects were

variable and evenly spread between increases and decreases whereas prazosin's effects have greater tendency to diminish bursting parameters. Because these effects were irreversible, control experiments receiving no drug application were also analyzed and are displayed as mean±S.D. in Figure 4.2b and c, and in subsequent analyses without washout effects, for comparison (n=3). The effects of yohimbine were statistically the same as control experiments (both after 45 minutes) for all parameters ($p>0.05$, unpaired t-test). With prazosin, the effects on burst intensity were statistically significant compared to control experiments ($p<0.05$, unpaired t-test) but were insignificant for all other parameters. From these experiments, it was demonstrated that the α_1-AR antagonist, prazosin, had the clearest effects on the sDC-evoked rhythms. This result is in contrast to work previously reported on SCA-evoked lumbar rhythms (Strauss and Lev-Tov 2003). However, from these experiments it was impossible to distinguish sites of action of the α_1-AR antagonists; thus experiments using a partitioned bath were conducted.

Table 4.1: Comparison of mean values for whole bath application of α-AR antagonists

	Yohimbine (n=5)		*Prazosin (n=5)*	
	0 min	**45 min**	**0 min**	**45 min**
Burst Intensity (μV)	8.54 ± 3.76	6.14 ± 3.66	6.28 ± 3.55	3.53 ± 4.79*
Burst Frequency (Hz)	0.36 ± 0.06	0.33 ± 0.08	0.36 ± 0.06	0.19 ± 0.17^{+}
Burst Duration (s)	1.58 ± 0.30	1.71 ± 0.44	1.84 ± 0.61	1.01 ± 0.94
Number of Bursts	6.50 ± 2.09	5.5 ± 2.12	5.80 ± 1.75	3.5 ± 3.2

Burst intensity, frequency, duration, and number were calculated before and 45 minutes after application of either yohimbine or prazosin. Values are presented as mean±S.D. for 5 experiments. Significant changes ($p<0.05$) from a one-sample t-test comparing percent changes to zero are indicated by an asterisk (*). Changes with $0.05<p<0.1$ are indicated by plus sign (+).

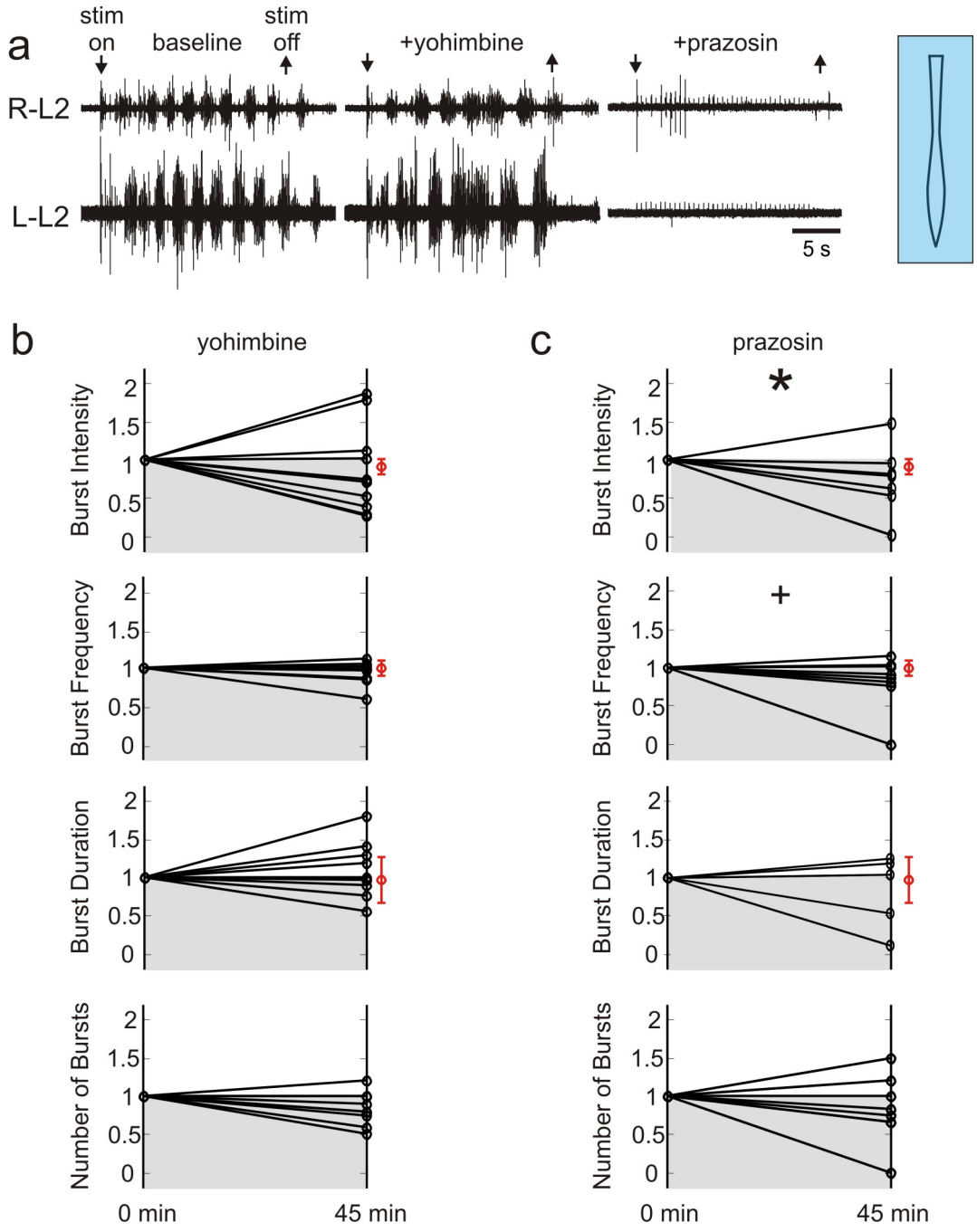

Figure 4.2: Effects of α-AR antagonists on sDC-evoked rhythms

Application of the α_1-AR antagonist, yohimbine, and the α_2-AR antagonist, prazosin, to the spinal cord indicated that prazosin had significant effects on the rhythm whereas yohimbine had no significant effect. A representative electroneurogram example of the effects of yohimbine and prazosin on sDC-evoked lumbar patterns is shown in (a). Normalized changes for each experiment's individual L2 ventral root parameters are shown in (b) for yohimbine and (c) for prazosin (n=5). Significant changes ($p<0.05$) from a one-sample t-test comparing percent changes to zero are indicated by an asterisk (*). Changes with $0.05<p<0.1$ are indicated by plus sign (+). Because these effects were irreversible, control experiments with no drug application were performed and analyzed after 45 minutes, shown as mean±S.D. in red.

4.2.2 Split bath experiments

To simplify the effects of the α-AR antagonists and to further isolate their actions, split bath preparations for selective regional application of prazosin and yohimbine were used. Both prazosin and yohimbine were used in combination as done previously in split bath experiments (Strauss and Lev-Tov 2003). Initially, the partition was situated at the lumbosacral border between L6/S1 segments. Application of both prazosin and yohimbine to the thoracolumbar segments had no significant effect on bursting properties with no effect on burst frequency or number, slight depression of burst intensity, and slight increase in burst duration (n=6/6, 10 L2 roots; Table 4.2; Figure 4.3a and b). These effects were statistically similar to control experiments for all parameters. However, application of yohimbine and prazosin to sacral segments blocked (n=5/10) or attenuated (n=5/10) sDC-evoked lumbar rhythms, resulting in significant decreases in burst intensity, frequency, duration and number ($p<0.05$) (Table 4.2; Figure 4.3a and c). These effects were all statistically significant compared to control experiments over the same period of time ($p<0.05$). The split bath experiments had greater significance than the whole bath α-adrenergic receptor antagonist experiments due to an increased number of experiments.

In Figure 4.3b and c, normalized changes in burst parameters are displayed for all analyzed roots. Rostral application had variable effects, with no clear tendency toward increasing or decreasing bursting parameter values whereas caudal application had a greater tendency to diminish bursting parameters.

Table 4.2: Effects of co-applied α-AR antagonists to split bath with partition at S1

	Rostral to S1(n=6)		*Caudal to S1(n=10)*	
	0 min	**45 min**	**0 min**	**45 min**
Burst Intensity (μV)	5.36 ± 3.79	4.19 ± 3.14	5.47 ± 4.45	1.72 ± 3.23*
Burst Frequency (Hz)	0.37 ± 0.08	0.36 ± 0.07	0.33 ± 0.05	0.16 ± 0.19*
Burst Duration (s)	1.36 ± 0.29	1.55 ± 0.38	1.75 ± 0.377	0.75 ± 0.92*
Number of Bursts	4.58 ± 1.24	4.5 ± 2.17	4.90 ± 1.65	2.28 ± 2.93*

Burst intensity, frequency, duration, and number were calculated before and 45 minutes after application of yohimbine and prazosin to either the rostral or caudal split bath at S1. Statistical significance from a one-sample t-test comparing percent changes to zero ($p<0.05$) is indicated by an asterisk (*).

Figure 4.4 contains summaries of the percent changes from baseline for burst intensity, burst frequency, burst duration, and number of bursts. Significant groups were identified using pooled data and Student's t-test comparing the mean of the percent changes to zero. Overall, the effects seen from bath application of yohimbine and prazosin can be attributed to prazosin alone based on the whole bath application experiments. The actions of prazosin in the sacral segments indicate activation of α_1-ARs in neuronal elements contained in sacral segments, rather than directly on the CPG in lumbar segments, to depress the sDC-evoked rhythm.

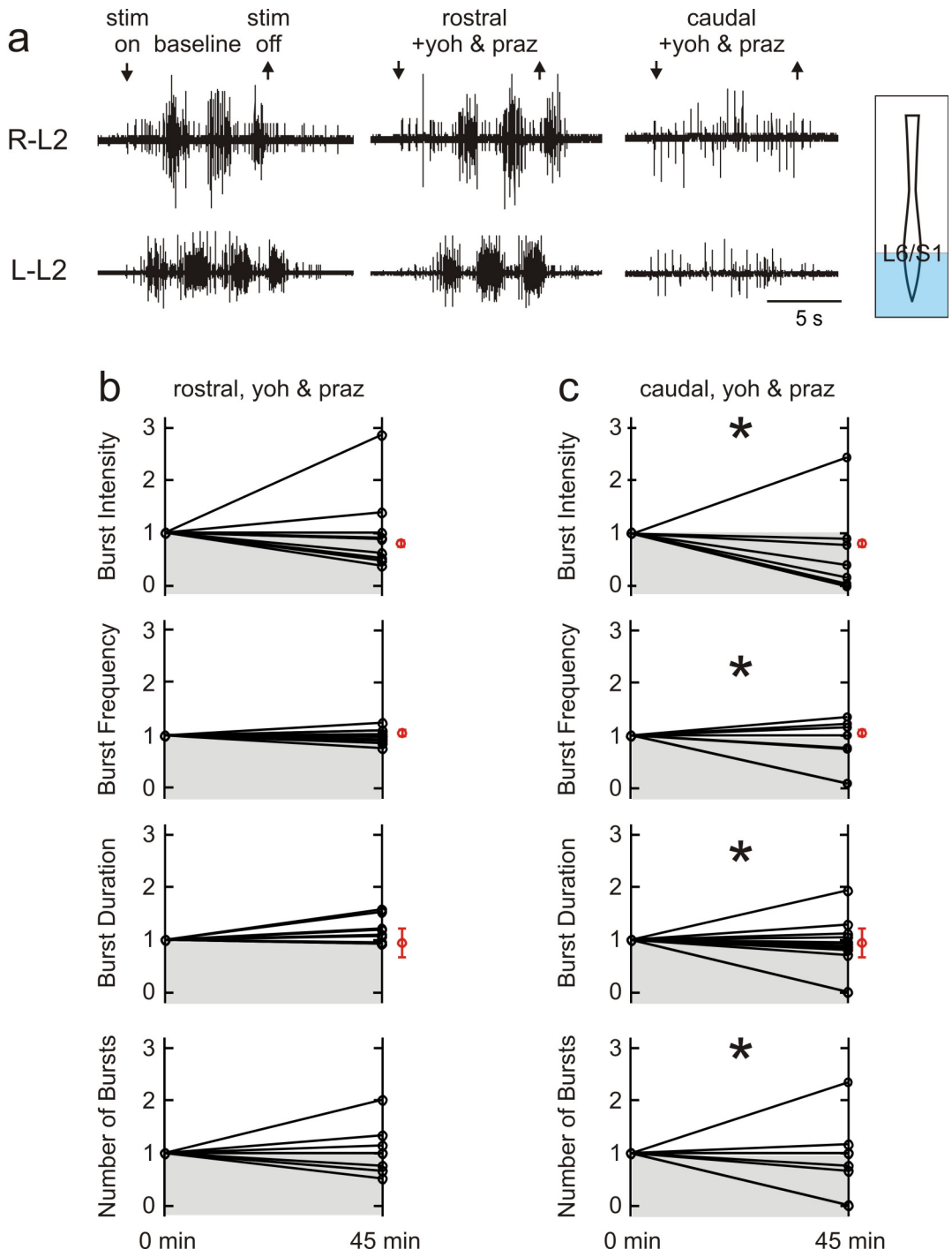

Figure 4.3: Effects of α-AR antagonists on sDC-evoked rhythms using split bath at S1
Application of the α_1-AR antagonist, yohimbine, and the α_2-AR antagonist, prazosin, to the spinal cord indicated that caudal application had significant effects on the rhythm whereas rostral application had no significant effects. A representative example of the effects of yohimbine and prazosin applied to the separate baths is shown in (a). Normalized values for each experiment's individual L2 root parameters are shown in (b) for rostral application and (c) caudal application. Significant changes ($p<0.05$) from a one-sample t-test comparing percent changes to zero are indicated by an asterisk (*). Because these effects were irreversible, time-matched control experiments with no drug application were performed and analyzed, shown as mean±S.D. in red.

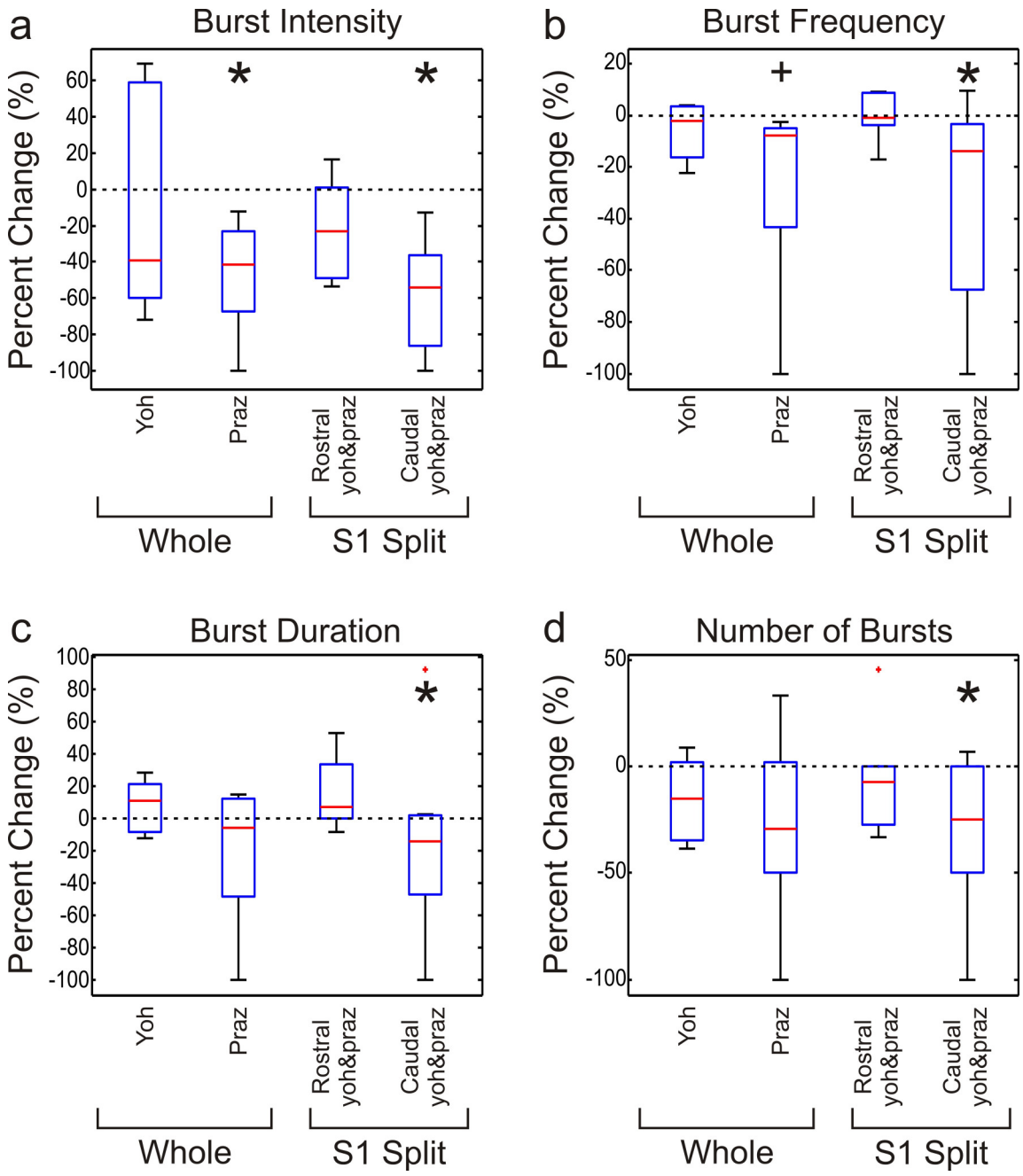

Figure 4.4: Summary of α-AR antagonists' effects based on application condition
Percent changes for each condition and each parameter are presented as box plots. Medians are shown as red lines. Boxes outline the 25th and 75th percentiles with whiskers indicating the range. Extreme outliers are shown individually. Significant changes were only observed in caudal bath application and with application of prazosin. Generally, α-AR antagonists decreased all parameters. Statistical significance, determined by a one-sample t-test comparing percent changes to a mean of zero,with $p<0.05$, is indicated by an asterisk (*), and strong changes with $0.05<p<0.1$ are indicated by a plus sign (+).

4.3 Cholinergic system

Previous research suggested that sacral cholinergic interneurons play a major role in modulation of SCA-induced motor rhythms (Anglister et al. 2008). Moreover, bath application of ACh can produce a rhythm similar to the most prevalent rhythm produced by sDC stimulation where ipsilateral flexors and extensors co-contract but alternate with the contralateral limb (Cowley and Schmidt 1994). Here I sought to evaluate the involvement of ACh receptors in sDC-evoked lumbar rhythms.

4.3.1 Whole bath experiments

Initial experiments evaluating the effects of ACh receptor antagonists were done in the isolated spinal cord preparation with the ACh receptor antagonists DHBE, mecamylamine, and atropine applied in combination. The combined effects reversibly blocked (n=4/5) or attenuated (n=1/5) rhythmogenesis (Figure 4.5a and b). Burst frequency, duration, and number of bursts were all significantly reduced, while burst intensity was strongly depressed (Table 4.3; n=5).

Table 4.3: Summary of combined DHBE, mecamylamine, and atropine effects on sDC-evoked rhythms

	DHBE, mecamylamine, and atropine (n=5)		
	0 min	**45 min**	**wash**
Burst Intensity (μV)	2.90 ± 1.67	1.23 ± 2.76^{+}	4.07 ± 1.71
Burst Frequency (Hz)	0.36 ± 0.09	0.09 ± 0.20*	0.33 ± 0.08
Burst Duration (s)	1.66 ± 0.78	0.14 ±0.31*	1.36 ± 0.67
Number of Bursts	6.30 ± 1.72	0.8 ± 1.79*	4.88 ± 1.61

Burst intensity, frequency, duration, and number were calculated before and 45 minutes after application of DHBE, mecamylamine, and atropine. Values are presented as mean±S.D. for six experiments. Statistical significance from a one-sample t-test comparing percent changes to zero ($p<0.05$) is indicated by an asterisk (*). Strong changes ($0.05<p<0.1$) are indicated by a plus sign (+).

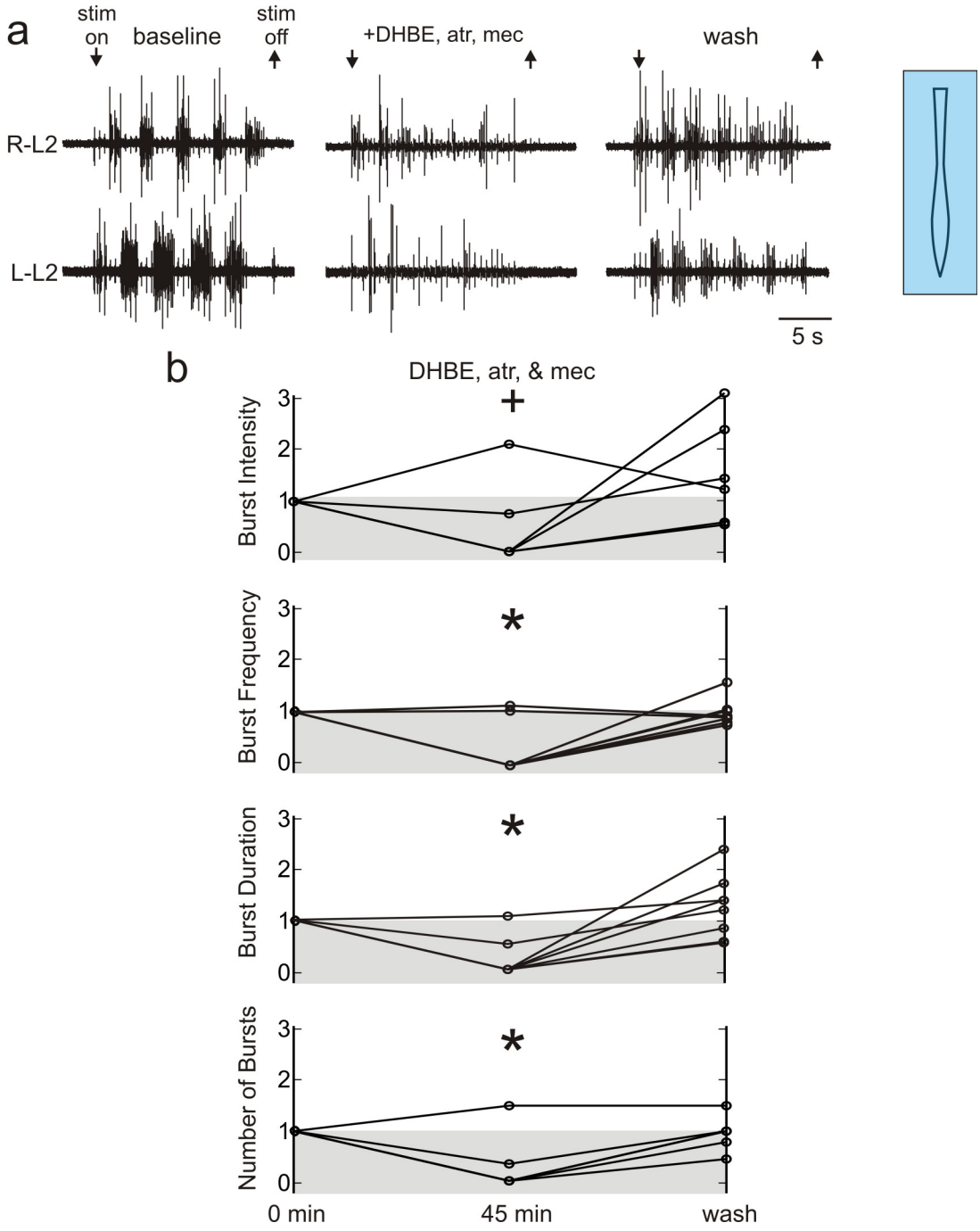

Figure 4.5: Effects of combined nAChR and mAChR antagonists on sDC-evoked rhythms
Application of nAChR and mAChR antagonists significantly reduced all parameters measured when applied in combination. A representative example of the combined effects of DHBE, mecamylamine, and atropine is shown in (a). Normalized changes from baseline values for each experiment's individual L2 root parameters are show in (b) for whole bath application (n=5). Significant changes ($p<0.05$) from a one-sample t-test comparing percent changes to zero are indicated by an asterisk (*). Strong changes with $0.05<p<0.1$ are indicated by plus sign (+).

Individually, whole bath application of dihydro-β-erythroidine (DHBE), an α_{2-4}-nicotinic ACh receptor (nAChR) antagonist, produced no significant changes in sDC-evoked lumbar rhythms for burst intensity (n=3/3; Table 4.4; Figure 4.6a and b). The effects of DHBE were not statistically different from time-matched control experiments. The trend toward a depression in intensity may have become significant with statistical sample size of sufficient power.

Table 4.4: Summary of DHBE effects on sDC-evoked rhythms

	DHBE (n=3)	
	0 min	**45 min**
Burst Intensity (μV)	6.50 ± 4.24	4.23 ± 3.88^{+}
Burst Frequency (Hz)	0.30 ± 0.04	0.30 ± 0.05
Burst Duration (s)	2.10 ± 0.24	1.61 ± 0.78
Number of Bursts	5.33 ± 1.15	5.00 ± 1.00

Burst intensity, frequency, duration, and number were calculated before and 45 minutes after application of DHBE. Values are presented as mean±S.D. No values were statistically significant ($p<0.05$) using a one-sample t-test comparing percent changes to zero; however, parameters with $0.05<p<0.1$ are indicated with a plus sign (+).

Application of atropine, a broad-spectrum muscarinic ACh receptor (mAChR) antagonist, reversibly blocked (n=1/3) or attenuated (n=2/3) sDC-evoked rhythms (Figure 4.6a). Burst intensity, duration, and the number of bursts decreased slightly, but no effects were statistically significant (Figure 4.6c). Results are summarized in Table 4.5. The effects of atropine were reversible, with washout returning to near baseline values. These results suggest an involvement of mAChRs in sDC-evoked rhythms.

Table 4.5: Summary of atropine effects on sDC-evoked rhythms

	Atropine (n=3)		
	0 min	**45 min**	**wash**
Burst Intensity (μV)	4.60 ± 3.64	3.30 ± 3.13	6.02 ± 2.97
Burst Frequency (Hz)	0.35 ± 0.04	0.24 ± 0.23	0.35 ± 0.06
Burst Duration (s)	1.55 ± 0.48	0.37 ±0.44	1.71 ± 0.63
Number of Bursts	6.33 ± 0.58	2.8 ± 2.75	5.17 ± 0.76

Burst intensity, frequency, duration, and number were calculated before and 45 minutes after application of atropine. Values are presented as mean±S.D. for three experiments (5 L2 ventral roots). No statistical significance was found with a one-sample t-test comparing percent changes to zero.

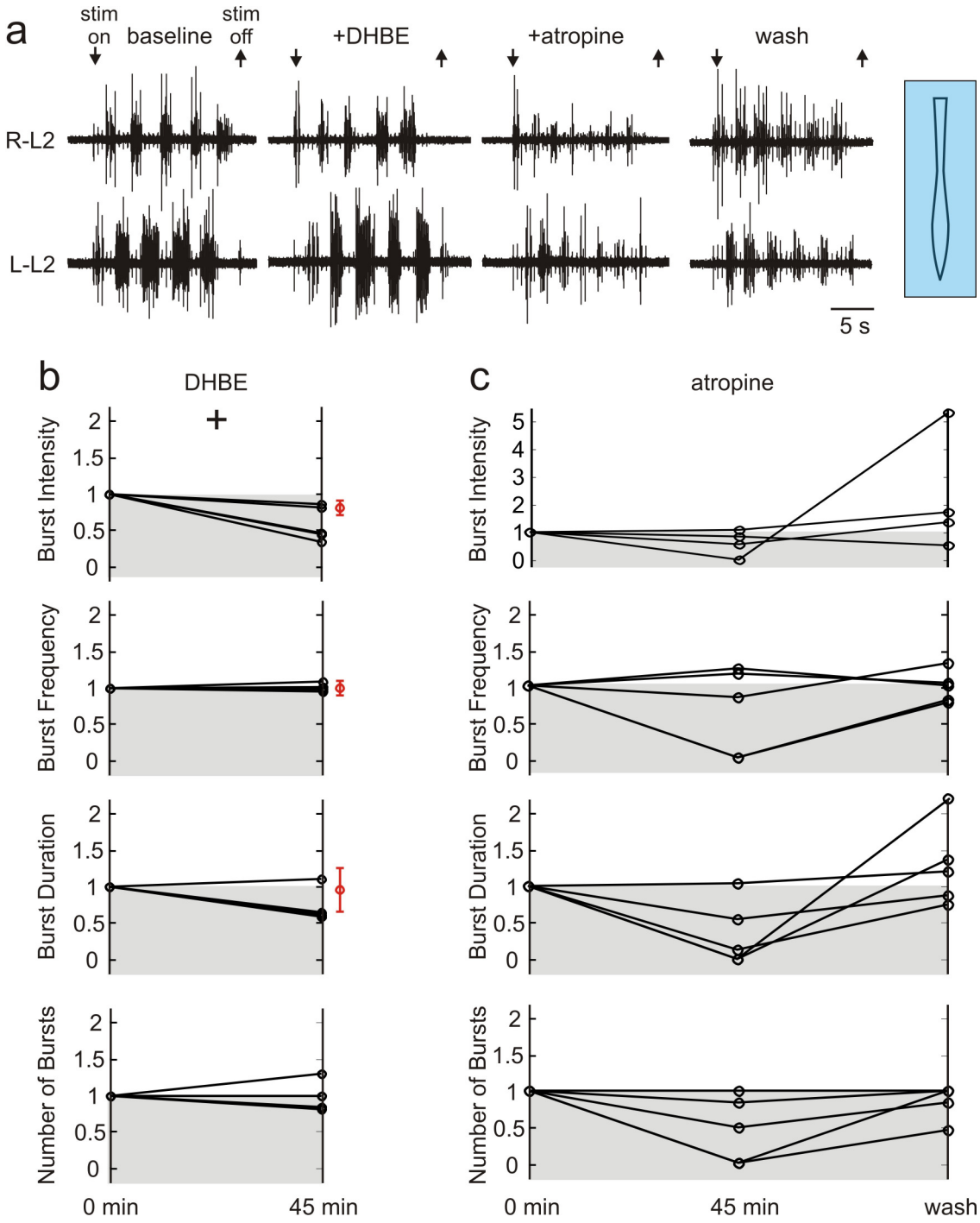

Figure 4.6: Effects of DHBE and atropine on sDC-evoked rhythms

(a) The nAChR antagonist, DHBE, and the mAChR antagonist, atropine, were applied to the spinal cord. (b) DHBE caused no significant effects on the bursting pattern, only slightly decreasing burst intensity and duration in a subset of experiments. (c) Atropine reversibly altered the bursting pattern by significantly affecting the burst duration and slightly decreasing the burst intensity, frequency, and number of bursts in a subset of experiments. Normalized values for each experiment's individual L2 root parameters are shown in (b and c). Strong changes ($0.05<p<0.1$) from a one-sample t-test comparing percent changes to zero are indicated by a plus sign (+). (n=3 for DHBE; n=3 for atropine) For DHBE, control experiments with no drug application were performed and analyzed, shown as mean±S.D. in red for the same time period.

Mecamylamine, an $\alpha_{3,6,7,9}$ nAChR antagonist, reversibly blocked (n=1/3) or attenuated (n=2/3) sDC-evoked rhythms (Figure 4.7a). Slight decreases in burst intensity, frequency and number were seen and burst duration was significantly decreased. Figure 4.7b shows that the effects of mecamylamine were depressive on burst intensity, duration, and number in all but one ventral root recorded, but the depression wasn't statistically significant. Table 4.6 summarizes these results. Combined with the results of DHBE, these results indicate an involvement of $\alpha_{6,7}$ subunit(s) of nAChRs in sDC-evoked lumbar rhythmogenesis since α_9-nAChRs are not found in the CNS (McIntosh et al. 2009).

Table 4.6: Summary of mecamylamine effects on sDC-evoked rhythms

	Mecamylamine (n=3)		
	0 min	**45 min**	**wash**
Burst Intensity (μV)	3.82 ± 0.77	2.05 ± 3.57	5.75 ± 3.41
Burst Frequency (Hz)	0.35 ± 0.09	0.15 ± 0.26	0.37 ± 0.04
Burst Duration (s)	1.86 ± 1.03	0.23 ± 0.40	1.43 ± 0.23
Number of Bursts	4.50 ± 0.87	1.33 ± 2.3	5.50 ± 0.50

Burst intensity, frequency, duration, and number were calculated before and 45 minutes after application of mecamylamine. Values are presented as mean±S.D. for three experiments. No statistical significance was found using a one-sample t-test comparing percent changes to zero.

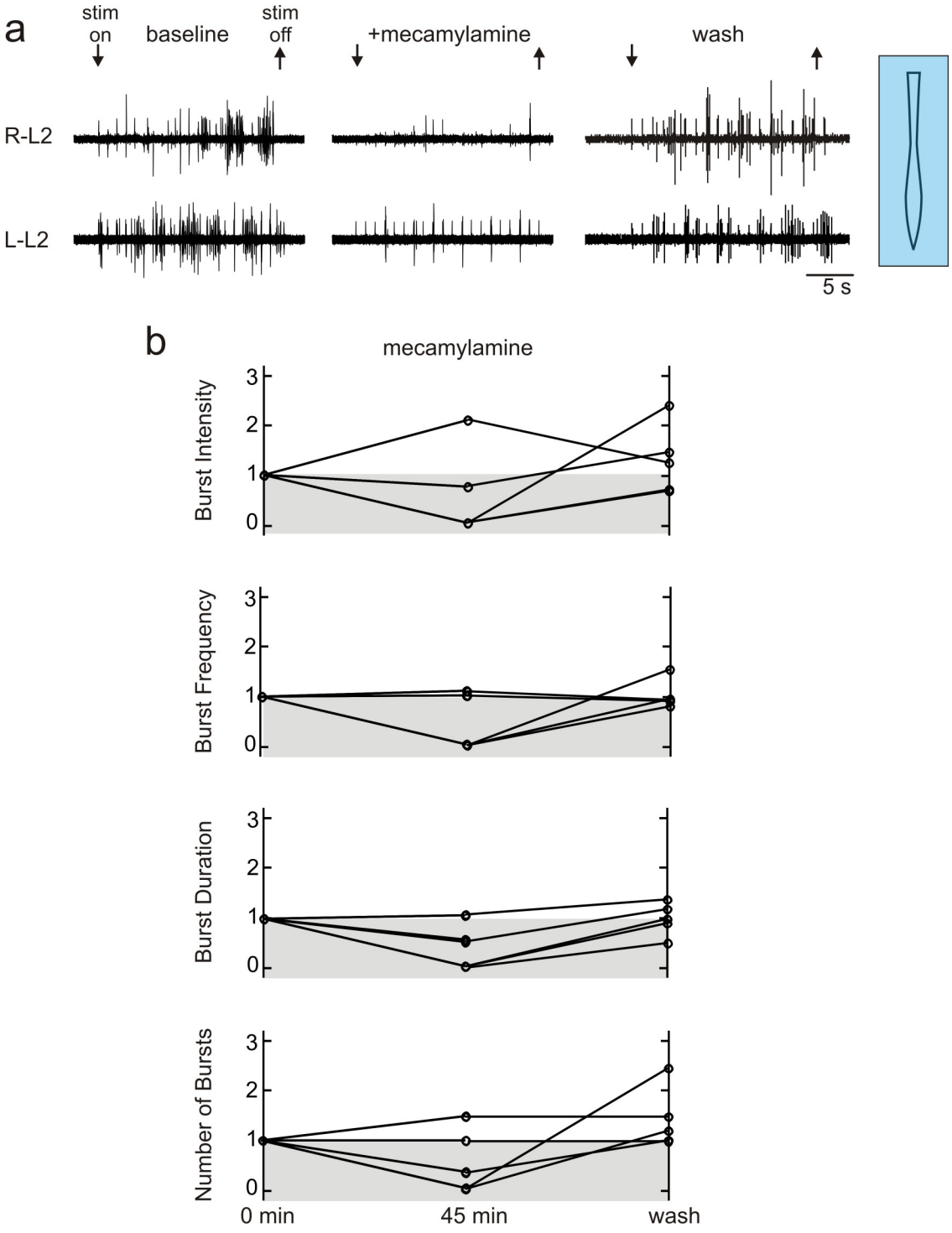

Figure 4.7: Effects of mecamylamine on sDC-evoked rhythms

(a) Application of the nAChR antagonist, mecamylamine, reversibly altered the bursting rhythm. (b) Burst duration was significantly decreased after application of mecamylamine. Effects on burst intensity, frequency, and number of bursts were variable, but generally decreasing. Normalized changes from baseline values for each experiment's individual L2 root parameters are shown in (b) (n=3). No statistical significance was found using a one-sample t-test comparing percent changes to zero.

However, when experiments with the very selective α_7 nAChR antagonist, methyllycaconitine (MLA), were conducted, MLA significantly reduced the mean burst intensity, frequency and number when applied to the whole bath (n=7; Table 4.7). Rhythmic activity was altered in the majority of experiments either completely (n=2/7) or attenuated (n=3/7; Figure 4.8a). MLA significantly reduced burst intensity, frequency, and number of bursts; burst duration was also decreased (Figure 4.8b). These effects required an extremely long amount of time to be observed (average of 3 hours), which is significantly longer than any other drug used in this study, but the effects were greater than control experiments where no drug was applied (n=5). The effects of MLA on burst intensity, frequency, and number of bursts were all statistically different from time-matched control experiments indicating the changes observed were due to actions of MLA (n=3 controls; $p<0.05$). The effects of MLA were shown to be partially reversible in one experiment, which required an additional two hours of washout (n=1/5 where washout was attempted). Based on these experiments, the effects of the nAChR antagonists could, at least partially, be attributed to actions on the α_7-nAChR.

Table 4.7: Effects of MLA on sDC-evoked rhythms

	Methyllycaconitine (n=7)	
	0 min	**180 min**
Burst Intensity (μV)	6.92 ± 3.51	4.57 ± 4.13*
Burst Frequency (Hz)	0.31 ± 0.06	0.17 ± 0.16*
Burst Duration (s)	1.76 ± 0.56	1.34 ± 1.28
Number of Bursts	7.50 ± 2.57	3.50 ± 3.46*

Burst intensity, frequency, duration, and number were calculated before and 180 minutes after application of MLA. Values are presented as mean±S.D. Statistical significance from a one-sample t-test comparing percent changes to zero ($p<0.05$) is indicated by an asterisk (*).

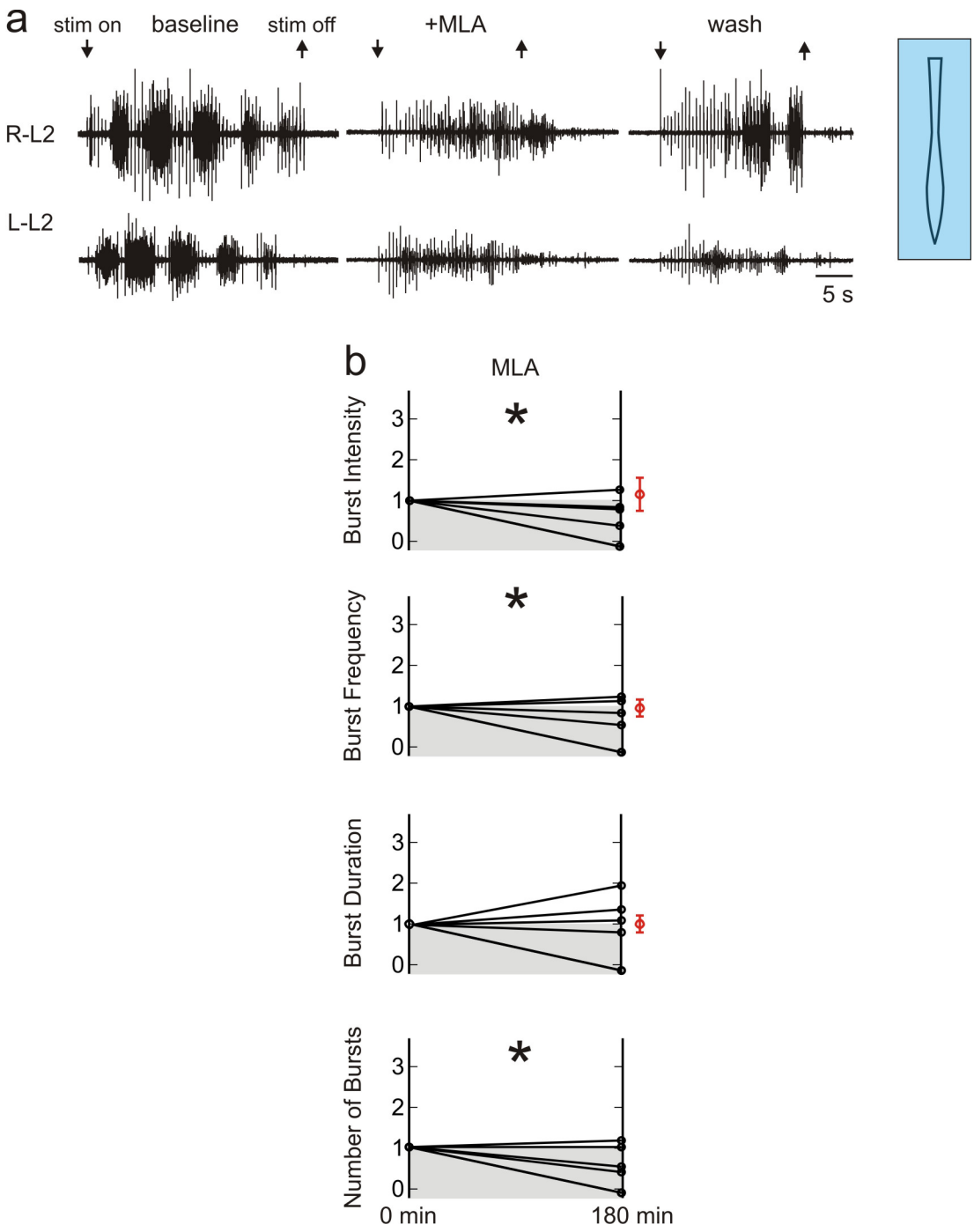

Figure 4.8: Effects of methyllycaconitine on sDC- and ACh-induced rhythms
Application of the α_7-nAChR antagonist, methyllycaconitine (MLA), attenuated or blocked sDC-evoked rhythms (n=5/7) and attenuated ACh/neo induced rhythms (n=3/3). (a) Representative example of MLA effects on sDC-evoked rhythms. MLA had significant effects on burst frequency and number of bursts resulting from sDC-stimulation. Normalized values for each experiment's individual L2 root parameters are shown in (b) for MLA's effects on sDC-evoked rhythms (n=7). Significant changes ($p<0.05$) from a one-sample t-test comparing percent changes to zero are indicated by an asterisk (*). Because these effects were irreversible, control experiments with no drug application were performed and analyzed, shown as mean±S.D. in red for the same time period.

Overall, the results of this section suggest that combining antagonists for both nAChRs and mAChRs was more effective than block of nAChRs or mAChRs on their own indicating that there is redundancy in the system where no one receptor subtype is critical to the pattern generation.

4.3.2 Split bath experiments

To isolate the effects of the ACh receptor antagonists to a particular location within the spinal cord, partitioned bath experiments separating the sacral segments from the thoracolumbar segments were conducted. Previous research postulated that sacral cholinergic interneurons were projecting to lumbar segments to modulate SCA-evoked rhythms (Anglister et al. 2008). However, here co-application of DHBE, atropine, and mecamylamine to the sacral segments had no significant effect on sDC-evoked rhythms (Table 4.8; Figure 4.9a). Burst intensity was decreased slightly (n=2/3) but all remaining parameters were virtually unchanged on average (n=3/3). These effects were not statistically different from time-matched control experiments (n=3). Figure 4.9b shows individual changes for the analyzed roots. Burst intensity and burst duration had a tendency to decrease while burst frequency and number had a slight tendency to increase in value, but due to the variability, the changes were not significant.

Application of DHBE, atropine, and mecamylamine to thoracolumbar segments significantly affected sDC-evoked rhythmic bursting in lumbar segments (n=5/5; Figure 4.9). Rhythms were blocked (n=3/5) or attenuated (n=2/5) in all experiments. Burst intensity, frequency, duration, and number of bursts were all significantly reduced (Table 4.8). These effects were partially reversible. Figure 4.9c shows a clear tendency for reduction in the normalized parameter values. This result implies that the cholinergic

receptor containing terminals responsible for modulating the sDC-evoked rhythms are located in the thoracolumbar cord close to the CPG.

Table 4.8: Effects of DHBE, atropine, and mecamylamine on sDC-evoked rhythms applied to split bath with partition at S1

	Caudal to S1(n=3)		*Rostral to S1 (n=5)*		
	0 min	**45 min**	**0 min**	**45 min**	**wash**
Burst Intensity (μV)	6.07 ± 4.50	4.90 ± 3.84	3.46 ± 3.50	0.34 ± 0.49*	1.24 ± 0.91
Burst Frequency (Hz)	0.38 ± 0.08	0.39 ± 0.09	0.42 ± 0.15	0.09 ± 0.15*	0.26 ± 0.23
Burst Duration (s)	1.43 ± 0.60	1.35 ± 0.47	1.27 ± 0.37	0.28 ± 0.43*	0.95 ± 0.62
Number of Bursts	5.33 ± 1.44	5.67 ± 0.57	4.00 ± 1.58	1.30 ± 2.17*	2.70 ± 2.05

Burst intensity, frequency, duration, and number were calculated before and 180 minutes after application of MLA. Values are presented as mean±S.D. for five experiments (10 L2 ventral roots). Statistical significance from a one-sample t-test comparing percent changes to zero ($p<0.05$) is indicated by an asterisk (*).

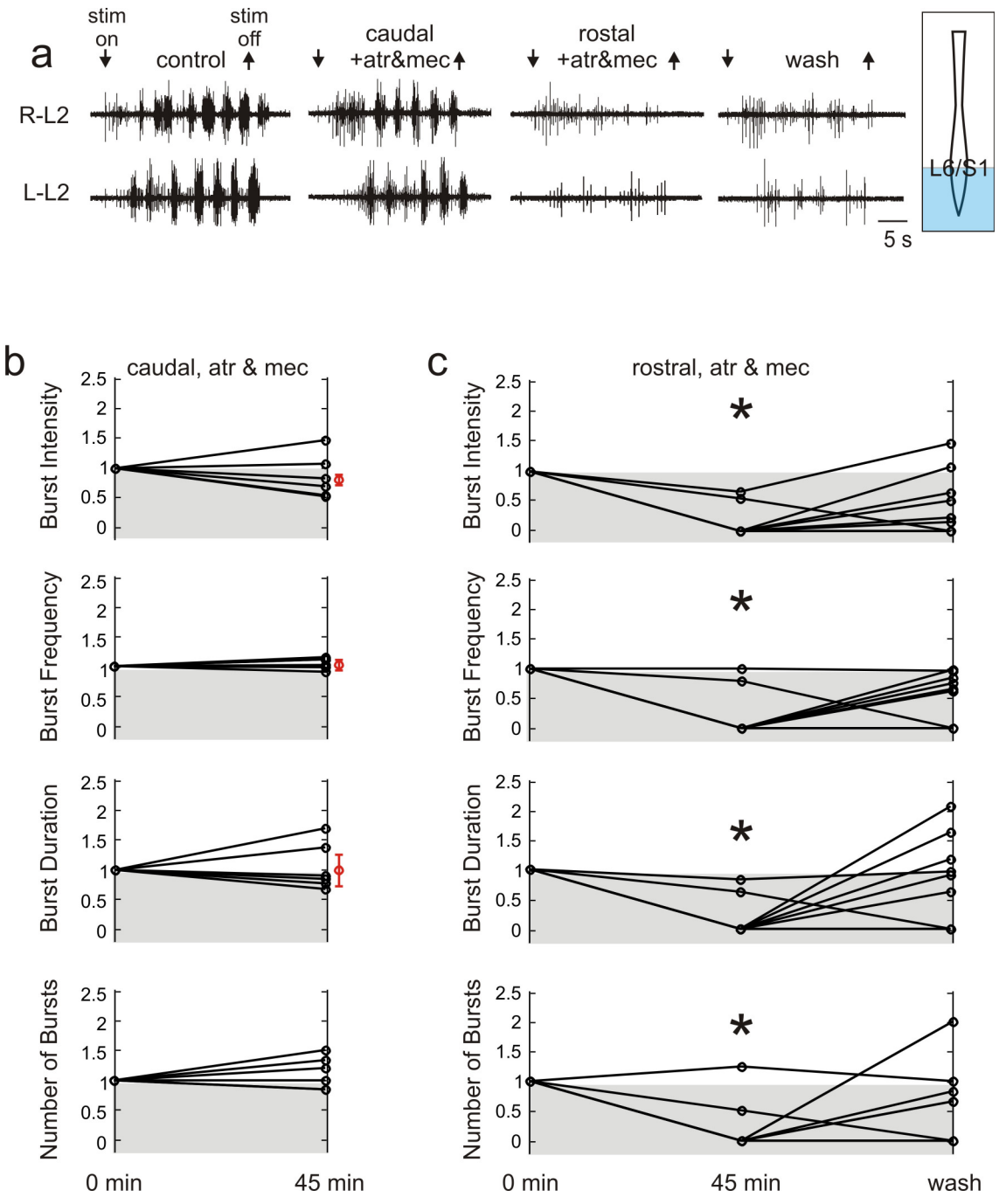

Figure 4.9: Effects of AChR antagonists on sDC-evoked rhythms using split bath
Application of nAChR and mAChR antagonists selectively to sacral segments did not alter the rhythm significantly, but application to thoracolumbar segments affected all measured parameters. A representative example of the combined effects of DHBE, mecamylamine, and atropine is shown in (a) for sequential application of mecamylamine and atropine to separate segments. Normalized changes from baseline values for each experiment's individual L2 root parameters are show in (b) for caudal application and (c) rostral application (n=5 experiments, 10 roots). Significant changes ($p<0.05$) from a one-sample t-test comparing percent changes to zero are indicated by an asterisk (*). Because these effects were irreversible, control experiments with no drug application were performed and analyzed, shown as mean±S.D. in red.

Figure 4.10 contains boxplot summaries of the percent changes from baseline for burst intensity, burst frequency, burst duration, and number of bursts with cholinergic receptor antagonist application. Significant differences in the groups of pooled percent changes were identified by Student's t-test. Overall, the effects seen from bath application of cholinergic receptor antagonists cannot be attributed only to nAChRs or mAChRs, and likely result from a combination of cholinergic co-activation of the two subclasses. However, the selective α_7-nAChR antagonist MLA did significantly reduce burst intensity, frequency and number of bursts generated by sDC-stimulation, and the location of α_7-nAChRs in the upper lumbar spinal cord is amenable to modulation of the CPG output and not just on motoneurons. The actions of AChR antagonists on burst frequency and burst duration indicate possible actions at the level of the CPG rather than on general motoneuron excitability and correlates with the actions of AChR antagonists being restricted to the thoracolumbar segments.

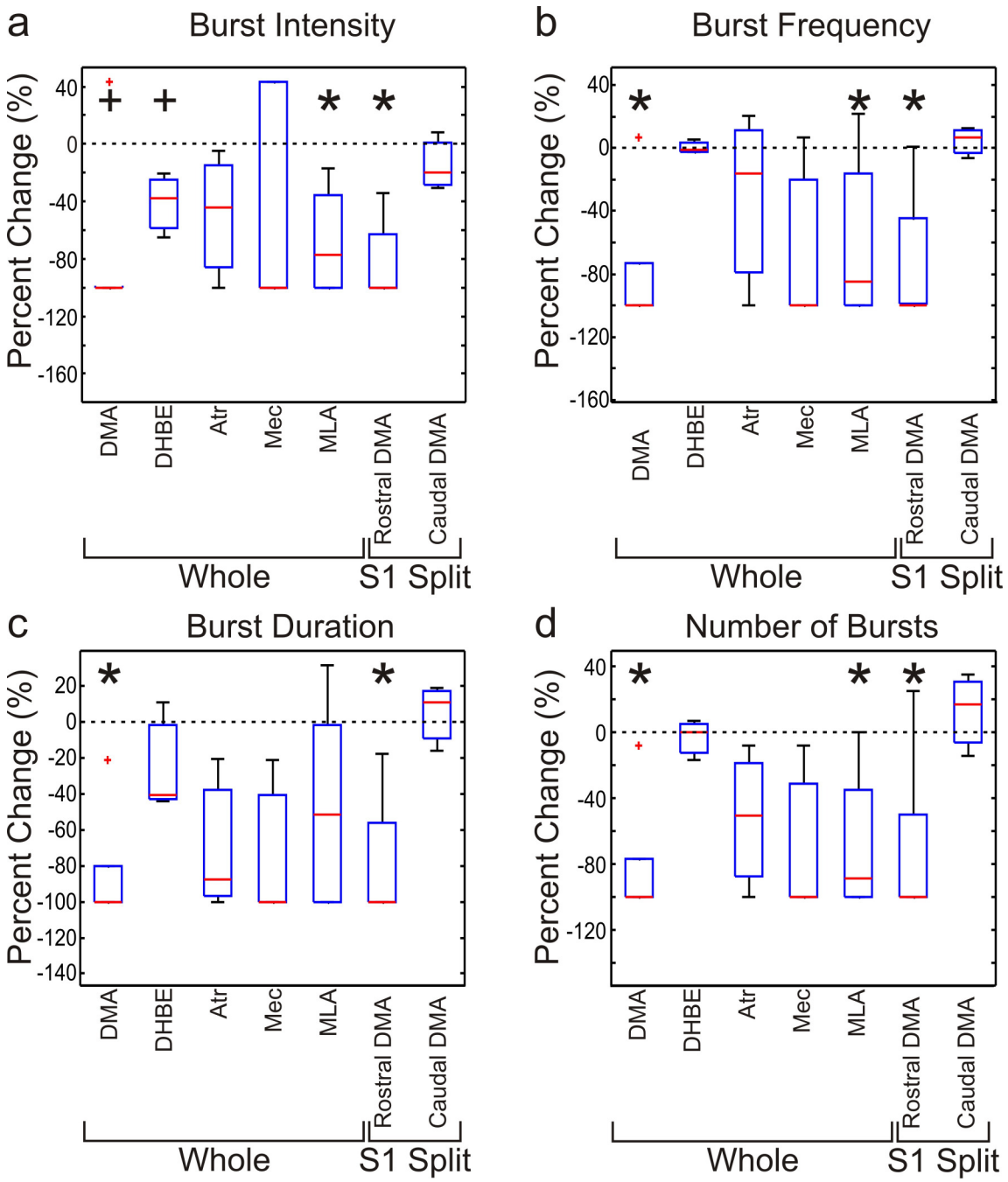

Figure 4.10: Summary of cholinergic receptor antagonist effects on sDC-evoked lumbar rhythms
Percent changes for each condition and parameter are presented as box plots. Medians are shown as red lines. Boxes outline the 25th and 75th percentiles with whiskers indicating the range. Extreme outliers are individually shown. Significant changes ($p<0.05$) from a one-sample t-test comparing percent changes to zero are indicated by an asterisk (*). Changes with $0.05<p<0.1$ are indicated by plus sign (+). Significant changes were observed with application of DHBE, mecamylamine, atropine, and MLA, and effects were selective to the thoracolumbar segments of the spinal cord. DMA =DHBE/mec/atr applied in combination.

4.4 Summary and perspective

The overall findings of this chapter support a requirement for purinergic, adrenergic, and cholinergic actions in sDC-evoked lumbar rhythms. The following observations support this conclusion:

The P2X receptor antagonist suramin abolished bursting rhythms evoked by sDC stimulation when applied to all segments of the spinal cord. While effects on sacral segments were reversible, effects of suramin on thoracolumbar segments were not, indicating potential actions on different P2X receptor subtypes based on location. Application of the α_1-AR antagonist prazosin significantly reduced burst intensity of sDC-evoked rhythms. The actions of the α_1-AR antagonist differed from those previously reported with SCA evoked rhythms (Strauss and Lev-Tov 2003) and may reflect a difference between activating lumbar rhythms via the subset of afferents traveling in the dorsal column versus the entire dorsal root. While the possibility of β-AR involvement in sDC-evoked rhythms cannot be excluded here, the actions of the α-AR antagonists on sDC-evoked rhythms were significant, and restricted to the sacral segments of the cord suggesting actions on sacral propriospinal projection neurons. In contrast to the α_1-AR antagonist, nAChR and mAChR antagonists had effects selective to thoracolumbar segments of the spinal cord. The actions of cholinergic receptor antagonists in lumbar segments suggest actions on interneurons that project to the pattern generating circuitry and/or via direct actions on the pattern generator. As cholinergic and adrenergic actions are the predominant signaling mechanisms of the autonomic nervous system, their involvement here further supports the overall proposition that autonomic visceral afferents activate spinal autonomic pathways to recruit lumbar pattern generating

circuitry. These results confirm that multiple neurotransmitter pathways contribute to the sacral afferent evoked lumbar patterns with differing spatial selectivity among the receptors tested in this research.

CHAPTER 5

EFFERENT OUTPUT PATTERNS RESULTING FROM SACRAL DORSAL COLUMN STIMULATION

Lumbar rhythms recorded in ventral roots and hindlimb musculature resulting from sacral afferent stimulation have revealed noteworthy distinctions from pharmacologically induced lumbar rhythms. In contrast to rhythms generated with serotonin (5-HT) and N-methyl-D-aspartate (NMDA) (Kudo and Yamada 1987; Smith et al. 1988; Kiehn and Kjaerulff 1996), previous research has demonstrated that sacrocaudal afferent (SCA) induced lumbar rhythms do not always recruit essential elements of the central pattern generator (CPG) resulting in an incomplete expression of lumbar ventral root bursting patterns with extensor-related L5 ventral root activity being noticeably absent (Whelan et al. 2000; Strauss and Lev-Tov 2003). Phase relationships between pairs of certain hindlimb muscles and muscle compartment recruitment have also been demonstrated as differing for pharmacologically-induced and SCA-evoked locomotion in the neonatal mouse with significant changes noted based on the method of locomotor recruitment (Klein et al. 2010).

In addition, high frequency epidural spinal cord stimulation is an effective method for activating the locomotor CPG (Edgerton and Roy 2002; Gerasimenko et al. 2006). Combined with application of 5-HT agonists, the efficacy of epidural stimulation improves locomotor stepping and weight bearing in the adult spinal rat demonstrating

that there are interactions between stimulation and pharmacological activation that may be beneficial for future rehabilitative therapies for patients with spinal cord injury (Ichiyama et al. 2008). Clinically, it is important to understand all of the effects of a rehabilitation strategy in order to anticipate potential side effects. In addition to motor responses due to spinal cord stimulation, autonomic effects can also occur. High frequency epidural spinal cord stimulation is commonly used for relief from intractable and ischemic pain and for peripheral vasodilation (Linderoth et al. 1994; Augustinsson et al. 1995; Linderoth et al. 1995, 1995).

In this work, the efferent patterns generated by sacral dorsal column stimulation were characterized. Here I demonstrate that sDC stimulation preferentially recruits rhythmic ventral root activity in autonomic efferent-containing spinal segments. Moreover, I show that GABAergic mechanisms mediate, in part, the coupling strength for rostral lumbar sympathetic rhythms to recruit hindlimb locomotor rhythm generating circuits.

5.1 $GABA_A$ receptors limit expression of the central pattern generator

The most surprising finding in the aforementioned results is the low incidence and relatively weak recruitment of L5 rhythmic motor activity. GABAergic circuits are known to limit activity in hindlimb locomotor CPG circuits, including the coupling of activity in L2 to L5 motor output (Cazalets et al. 1998). To examine whether GABAergic actions similarly limited the rhythmic motor output induced by sDC stimulation, I tested the actions of reduced GABA-mediated actions by applying the $GABA_A$ receptor antagonist bicuculline. Since doses of bicuculline greater than 5 μM may induce spontaneous, synchronous, seizure-like activity across all ventral roots (Bracci et al.

1996; Bracci et al. 1996), I used a dose of 1 μM. This dose has been shown to block ~50% of $GABA_A$ receptors (IC_{50} = 0.58 μM; (Jonas et al. 1998)). Bicuculline reduced pattern fatigability, by significantly increasing motor pattern expression time by 39±25% (n=4/6, $p<0.05$). Rhythm frequency also increased significantly (33±28%; n=5/6, $p<0.05$), as did motor burst intensity (32±40%; n=5/6, $p<0.05$). Importantly, previously non-bursting L5 activity was converted to locomotor-like bursting in three out of five experiments (i.e. Figure 5.1). The bursting produced in the L5 ventral roots was still noticeably weaker than the L2 ventral roots. This can be explained by the rostrocaudal gradient of the lumbar CPG, with the L2 segment having stronger rhythmogenic capacity than the L5 segment (Kjaerulff and Kiehn 1996). Additionally, the L5 extensor-related rhythmic output may be inhibited by sacral afferents, as found previously in the tail musculature (Delvolve et al. 2001; Strauss and Lev-Tov 2003). These results suggest that sDC evoked actions on CPG circuits are limited by ongoing $GABA_A$ receptor activation.

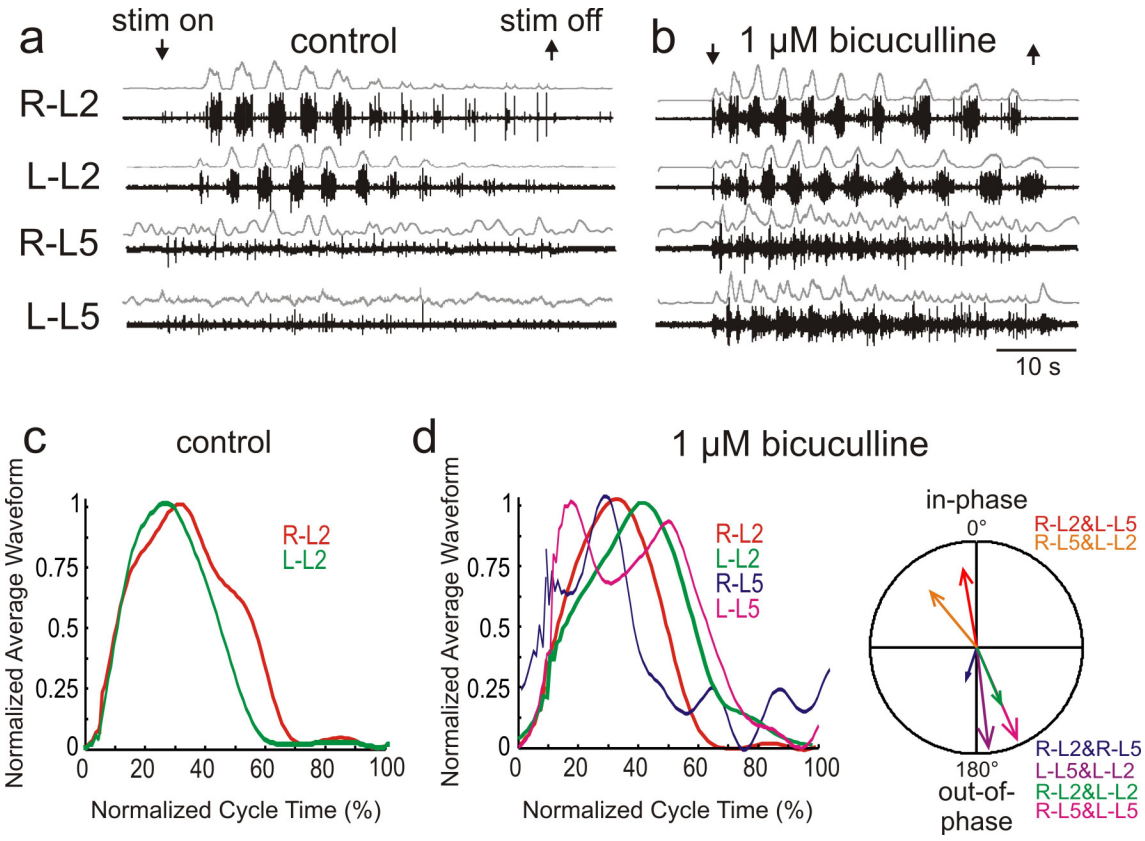

Figure 5.1: $GABA_A$ receptor antagonists facilitate sDC evoked rhythms
Application of the $GABA_A$ receptor antagonist bicuculline in small doses had dramatic effects on the sDC evoked motor patterns. (a) Before application of bicuculline, rhythmic activity was observed in the L2 ventral roots. (b) After application of bicuculline, patterned output from the L5 ventral roots was increased, as was the frequency, intensity, and duration of the stimulus evoked motor output. Average waveforms for bursting signals (c) before and (d) after bicuculline application. Mean resultant phase vectors for all root pairs in (b) are shown in (d). The rhythm was classified as locomotor-like based on phase relationships.

To more fully explore the segmental ventral root activity profile recruited following sDR or sDC stimulation, recordings from T11 to S2 ventral roots were collected. Since no differences were observed in rhythmic profile for the ventral roots using sDC or sDR stimulation, data were combined. Table 5.1 summarizes the rhythmicity of the ventral roots among six animals, with those ventral roots exhibiting bursting phase coupled to L2 ventral root activity in ≥50% of experiments highlighted in boldface type. An example of the ventral root activity observed within one animal is shown in Figure 5.2. Ventral roots T11-L2, which contain sympathetic preganglionic efferents, had rhythmic motor output along with ventral roots L6-S2, of which L6 and S1 contain parasympathetic preganglionic efferents. Overall, ventral roots L3-L5 were least likely to display rhythmic motor activity and only displayed reflex activation even though they are the largest ventral roots. This is consistent with the caudal lumbar segments' lower rhythmogenic capacity (Kjaerulff and Kiehn 1996) and consistent with sacral afferent suppressing rhythmic output from extensor related segments (Delvolve et al. 2001; Strauss and Lev-Tov 2003); however, it is surprising that almost no rhythmicity was observed in L3-L5 since these ventral roots, while predominantly containing extensor-related information, also contain flexor-related information, and should not be suppressed by sacral afferents. As only these roots are unique in their absence of autonomic preganglionic efferents (also see Figure 1.2) the efferent activity pattern supports a preferential recruitment of rhythmic autonomic efferent activity.

Table 5.1: Summary of sacral afferent evoked rhythmic ventral root activity

Animal	*Rhythmic activity*	*Non-rhythmic activity*
1	**L1, L2, L6, S1**	**T13**, *L3, L4, L5*
2	**T11, T13, L1, L2**, *L4*, **L6, S1**	*L3, L5*, **S2**
3	**L1, L2, L6, S1, S2**	**T13**, *L3, L4, L5*
4	**T12, T13, L1, L2**	N/A
5	**T12, T13, L1, L2, L6**	**T11**, *L4, L5*
6	**T12, L1, L2**, *L3*, **L6, S1, S2**	**T13**, *L4, L5*

In six animals, rhythmic activity was recorded from a wide range of ventral roots to determine the extent of rhythmicity resulting from sDC or sDR stimulation. For each animal, roots were categorized as rhythmic or non-rhythmic. Roots that were rhythmic in ≥50% of animals are in **bold** while roots that were rhythmic in <50% are in *italic*.

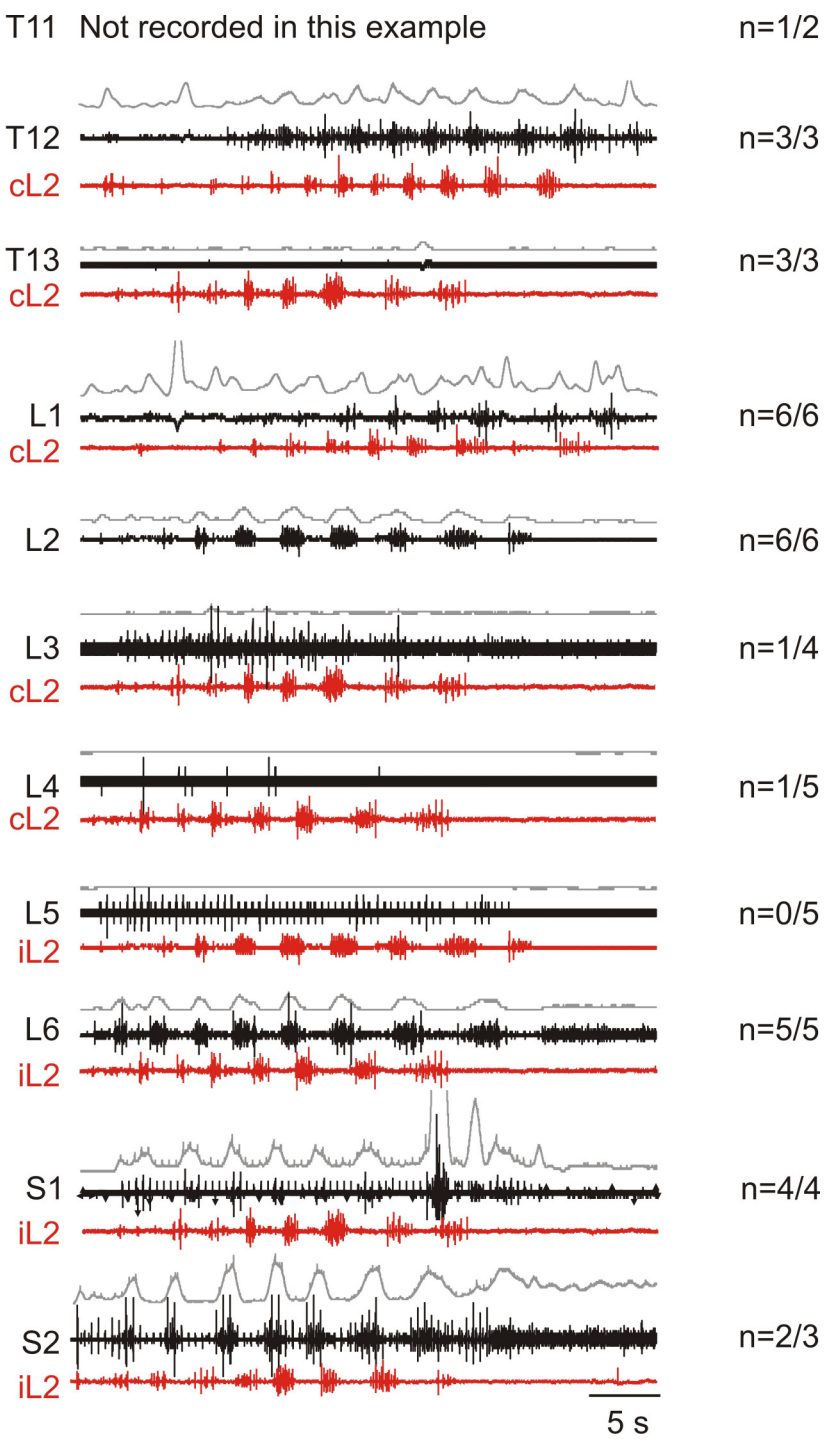

Figure 5.2: Ventral root efferent activity aligns with autonomic efferent distribution
Sacral dorsal column stimulation evoked rhythmic bursting from ventral roots in thoracic, lumbar, and sacral segments. Here a representative sample of bursting output within one animal is shown. Mid-lumbar segments (L3-L5), which have no autonomic efferents, were noticeably non-bursting in many cases. Recordings came from many trials. Red traces are for either ipsilateral (i) or contralateral (c) L2 ventral root recordings from the same trial as its paired ventral root to aid in visualizing relative timing. Total n's for rhythmic activity are shown to the right of each recording.

5.1.1 Separating autonomic from somatic activity: recordings from sympathetic chain

Ventral root activity reflects a mixture of somatic and autonomic efferent activity; therefore, studies examining the efferent output activated by sDC stimulation were conducted using more intact preparations: one with attached paravertebral ganglia and one with attached hindlimbs.

To determine if sDC or sDR CPG recruitment activated autonomic circuitry in addition to the somatic system, a hybrid preparation leaving the sympathetic chain intact was used. Recording electrodes were positioned between the sympathetic ganglia along the sympathetic chain, which contains efferents from sympathetic preganglionic fibers (Kayalioglu 2009) as well as sympathetic postganglionic fibers (Zimmerman et al. 2011). Rhythmic activity in the sympathetic chain was observed in five out of eight experiments (Figure 5.3a, left, and b). Of these five, three had robust rhythmic activity corresponding to the ventral root activity, one had rhythmic membrane fluctuations recorded as DC shirts but no spiking activity, and one preparation had rhythmic activity that transitioned to spontaneous non-bursting activity during the recording session. Additionally, in two out of the eight experiments 5-HT/NMDA (50 μM/5 μM) was applied to pharmacologically induce locomotor-like activity for comparison to the sDC rhythms. In one out of the two experiments, rhythmic activity was observed in the sympathetic chain recordings (Figure 5.3a, right). These results are consistent with previous experiments (Lohr and Hochman 2010). Rhythmic autonomic activity, similar to what is shown here, has been observed previously (Schomburg et al. 2003). Here, the sympathetic activity recorded in the lumbar segments may reflect phasic changes in vasodilation being

transmitted to the hindlimbs since phasic changes in blood pressure are seen during muscle contraction and relaxation (Lutjemeier et al. 2005; Lutjemeier et al. 2008).

In order to verify that the sympathetic recordings were truly of sympathetic origin and not EMG activity from neighboring rib muscles, the sympathetic recordings were verified as preganglionic by stimulating the homonymous ventral root and observing a compound action potential in the recording. Of the five rhythmic sympathetic recordings, only two were verified by stimulating the ventral root. Of the original eight experiments, the three that were not rhythmic had the recordings verified by ventral root stimulation. It is possible that by attaching *en passant* to the ventral root for the stimulation resulted in damage to the small number of efferent sympathetic fibers that could potentially be rhythmic, leading to an absence of rhythmic activity.

In several experiments, the neuromuscular junction antagonist, pancuronium, was used in an effort to eliminate the possibility of cross-talk with muscle activity in the neighboring rib muscles. However, in the three experiments with pancuronium applied at the beginning of the experiment, rhythmic alternation could not be recorded or recruited in the sympathetic chain. Additionally, in two experiments with pancuronium applied in the middle of the experiments while recording alternating activity from the sympathetic chain, the sympathetic chain activity would eventually be abolished. Previous studies identifying pancuronium as a neuromuscular junction antagonist were performed in *in vivo* preparations (Su et al. 1979; Weindlmayr-Goettel et al. 1993), and it has been shown to not penetrate the blood brain barrier (Weindlmayr-Goettel et al. 1993). Therefore, the actions previously reported to only occur at the neuromuscular junction may be

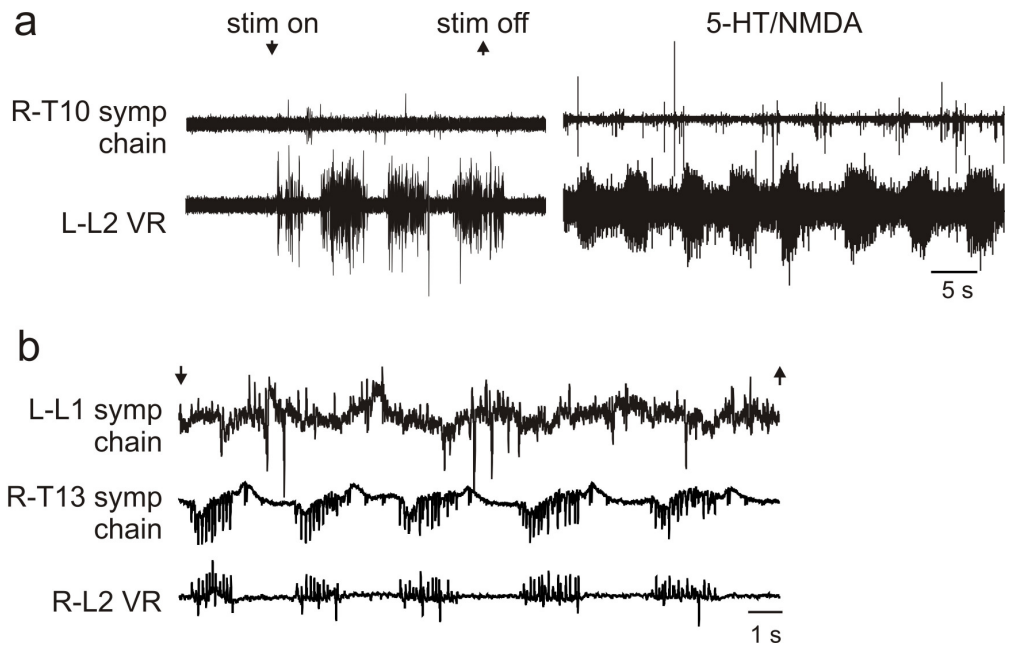

Figure 5.3: Efferent activity recorded at the sympathetic level
Stimulation of the sDC in (a) revealed weak rhythmicity of the sympathetic chain, which was out of phase with the contralateral L2 ventral root. Subsequent addition of 5-HT/NMDA strengthened the sympathetic rhythmicity and maintained the phase relationship with the ventral root. In a separate experiment (b), recordings from the sympathetic chain and corresponding ventral root had in-phase bursting activity.

inaccurate when using an *in vitro* preparation lacking a blood brain barrier, which may allow pancuronium to have central actions and affect cholinergic transmission.

5.1.2 Separating autonomic from somatic activity: recordings from muscle

An *in vitro* spinal cord with hindlimbs attached preparation was used to record from individual hindlimb muscles, with particular focus on muscles projecting from the L2 ventral root. Muscles accessible for recording with the spinal cord dorsal up included the vastus lateralis (VL), lateral gastrocnemius (LG), semimembranosus (SM), and tibialis anterior (TA). The location of the motoneuron pools identified for these muscles are summarized in Table 5.2 along with incidence of observed bursting during sDC stimulation. Rhythmic bursting in muscles was evoked by sDC stimulation or

Table 5.2: Location of motoneuron pools for recorded muscles

Muscle	*Location of motor pool (Stavroula Nicolopoulos-Stournaras 1983)*	*sDC evoked bursting*
VL	L2, L3	n=3/4
TA	L2, L3	n=1/2
SM	L3, L4	n=2/2
LG	L4	n=0/3

Hindlimb muscles recorded during sDC stimulation are shown below with the segmental location of the motor pools projecting to the specified muscle along with the incidence of rhythmicity observed in that muscle. VL-vastus lateralis, knee extensor; TA-tibialis anterior, ankle flexor; SM-semimembranosus, knee flexor; LG-lateral gastrocnemius, ankle extensor.

5-HT/NMDA application (n=4/4, n=1/1, respectively). VL had the strongest bursting of all muscles recorded (Figure 5.4a), while LG was never found to be bursting (Figure 5.4b). TA and SM had weak bursting detected in at least one experiment (Figure 5.4c and d). TA and SM were also found to be out of phase with the contralateral L2 while VL was found to be out of phase with the ipsilateral L2. This phase relationship for VL was of interest since previous reports indicated its motor pool was located in L2 and L3. However, it has been demonstrated that VL can have flexor- or extensor-like activation depending on the transmitter used to induce the rhythm (Kiehn and Kjaerulff 1996). Likewise, the bursting in SM may be explained by L3 segment's rhythmicity variability; however, LG's tonic activity was consistent with its motor pool being located in a typically non-bursting segment. In one experiment, 5-HT/NMDA was applied after stimulation of the sDC. The LLA induced by 5-HT/NMDA changed the phase relationship between SM and L2 and greatly strengthened the bursting output in SM (Figure 5.4d). In contrast to the sympathetic activity recordings described above,

activation of all recorded muscles was, in two out of three cases, delayed relative to onset of L2 activation by an average of 0.80±0.28 cycles. This includes VL, which has a portion of its motor pool in the L2 spinal segment.

Overall, the above two sections suggest that sacral afferent stimulation preferentially recruits autonomic efferent pathways, and their activity subsequently recruits somatic efferent motor rhythms that entrain to the autonomic pattern generator. Alternatively, sacral afferent stimulation recruits central pattern generating circuitry which produces both autonomic and somatic output that are entrained to one another with the threshold for autonomic output being slightly lower than that for the somatic output.

5.2 Efferent output characterization

5.2.1 Relating sacral dorsal column stimulation frequency to recruitment of lumbar ventral root bursts

To explore the stimulus-input/burst-output properties of sDC electrical activation, stimulus trains of varying frequencies were applied. Stimulation frequencies less than 0.2 Hz resulted in little motor activity and no bursting (n=6), while stimulation frequencies above 0.5 Hz produced a regular periodic rhythm which tended toward a maximal burst frequency of 0.31±0.07 Hz (n=53; Figure 5.5d and e).

Stimulation frequencies between 0.2 and 0.5 Hz were sufficient to evoke bursting in a single L2 ventral root. These bursts were initiated with and synchronized to the stimulus train (n=6). Successive stimulus pulses generally initiated a burst in the contralateral L2 ventral root resulting in a ratio of 0.5 left–right burst pairs per stimulus pulse (Figure 5.5a and b). The bursting did not persist for the entirety of the time between stimulus pulses leaving a silent period between each consecutive burst. Since

the duty cycle was less than 50% of the cycle period for both L2 ventral roots, bursting did not represent recruitment of a regular periodic rhythmic behavior. Nonetheless, as bursts alternated between sides, they may reflect recruitment of individual components of a half-center network.

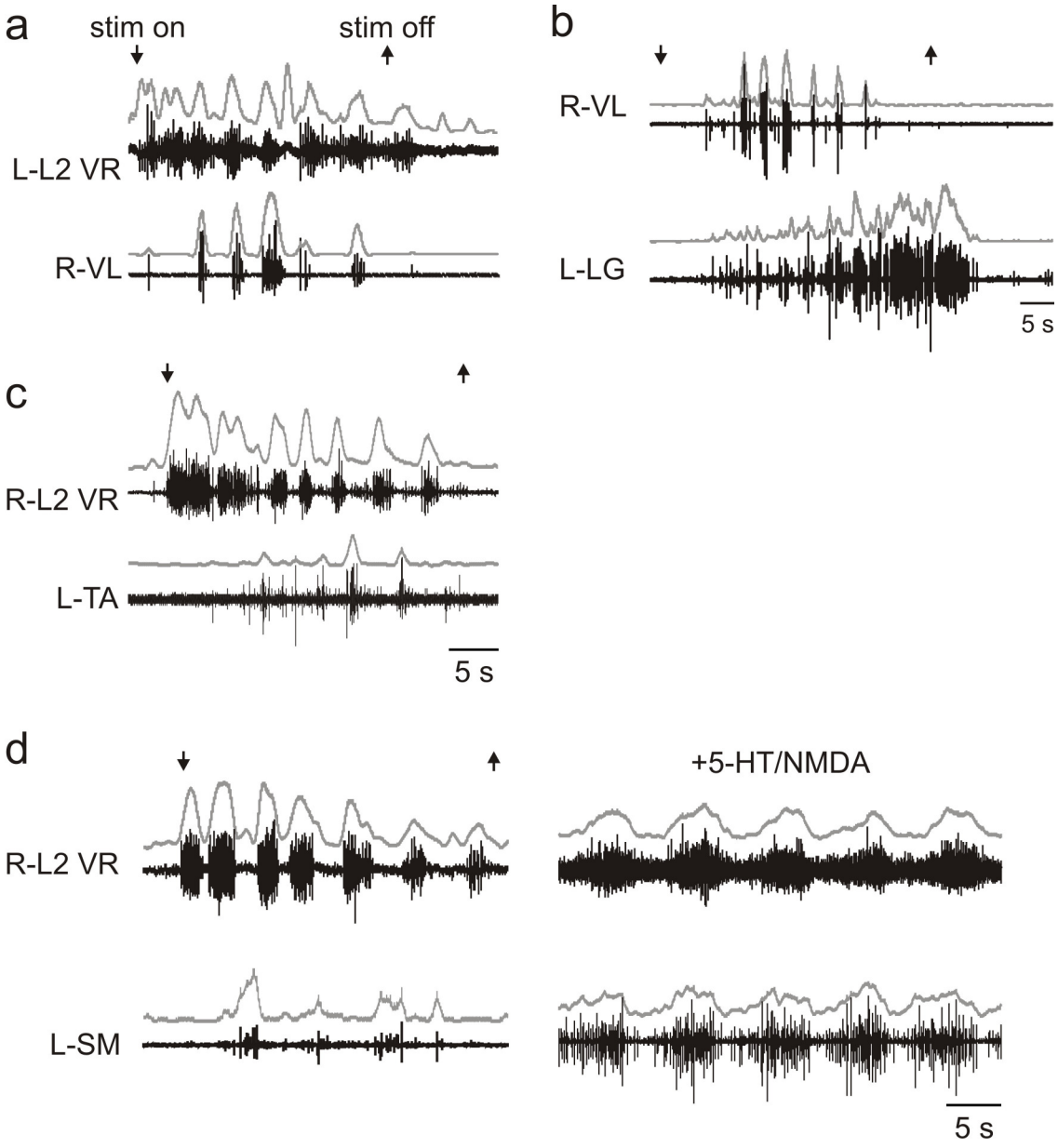

Figure 5.4: Efferent activity recorded at the muscle level
Stimulation of the sDC recruited rhythmic muscle activity in muscles associated with L2 VRs. In (a) stimulation of the sDC produced alternation between VL and contralateral L2 VR. However, in (b), no clear rhythmicity was seen in LG. In (c), bursting was also seen in TA, with the contralateral TA out of phase with the L2 VR. In (d), weak rhythmic bursting was seen in SM, out of phase with the contralateral L2 VR; however, when 5-HT/NMDA was applied, the rhythm was strengthened and SM was in phase with the contralateral L2 VR.

To explore this further, low frequency stimuli (0.1-0.25 Hz) were combined with a double-pulse protocol (2 pulses at 50 Hz). Under these conditions the previous single burst converted into a double burst of left–right alternation (Figure 5.5b and c). These data imply that the greater excitatory drive provided by the double pulses is of sufficient strength for one half-center to subsequently recruit the other half-center but was still insufficient for a full pattern of continuous alternation as quiescent gaps in the rhythm persisted. Incomplete but coupled half-center expression is consistent with the observation that the magnitude of the second burst was proportionally dependent on the magnitude of the first burst with a mean normalized burst intensity ratio of 0.92±0.33 (range 0.31-2.17) for the 2^{nd} burst relative to the 1^{st} burst of a cycle pair (n=2). Moreover, at no time did left L2 burst activity overlap with right L2 activity (and vice versa), supporting mutual inhibitory interactions. These results suggest that sDC-stimulation activates left–right half-centers whose modular substructure can be unmasked using low frequency stimulation protocols.

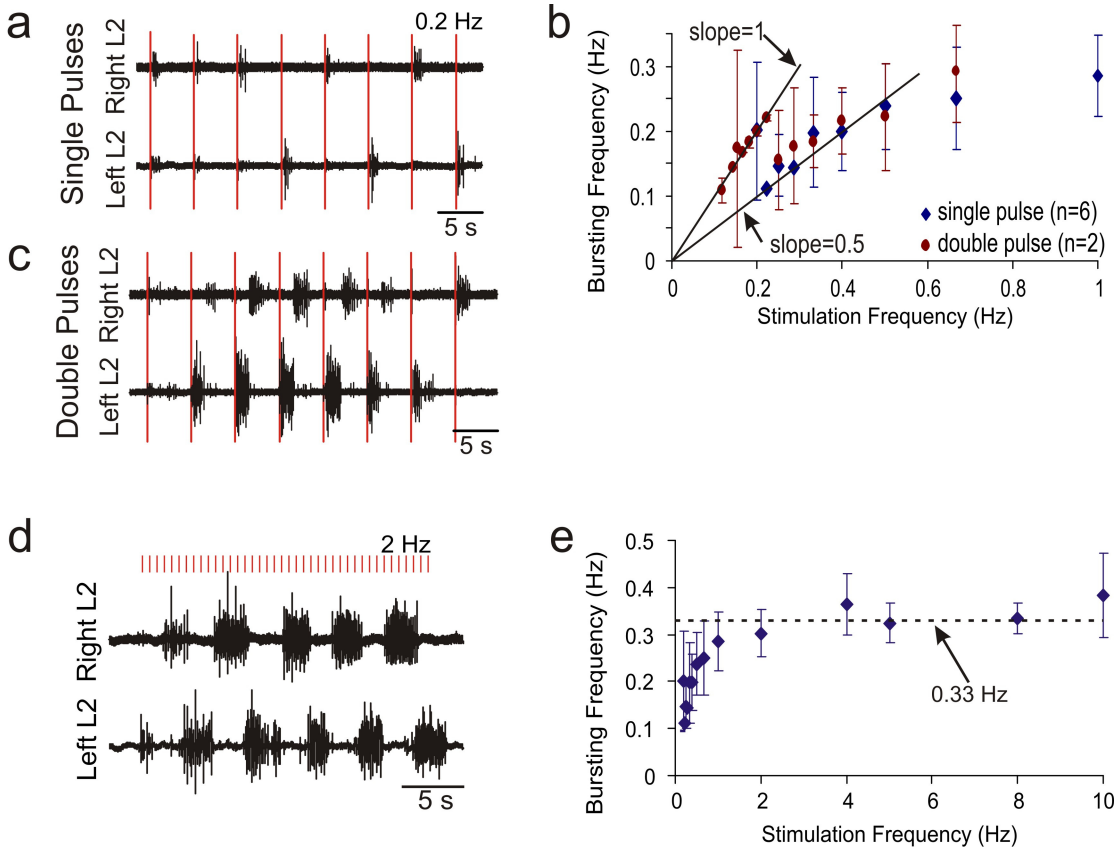

Figure 5.5: Effects of stimulation frequency on L2 bursting

Stimulation frequencies below 1 Hz (a and b) entrain burst timing to the stimulation in a ratio of 1 burst per stimulus pulse. (b and c) Double pulses (50 Hz) at low frequencies alter this ratio from 1 burst per stimulus pulse to 2 alternating bursts per stimulus double pulse. These stimulation protocols result in quiescent periods in the generated rhythms. (d and e) Stimulation frequencies above 1 Hz maximally activate the CPG to generate continuous rhythmic activity, which has a maximal bursting frequency independent of stimulation frequency.

5.2.2 Comparison of sDC rhythms to 5-HT/NMDA induced rhythms

The efferent activity recorded by ventral roots during sDC or sDR stimulation was rhythmic but the observed pattern was generally not consistent with activation of LLA. Therefore sDC evoked lumbar patterns were compared to those produced by 5-HT/NMDA since it is well established that 5-HT/NMDA evoked rhythms activate the locomotor CPG (Cazalets et al. 1992; Kiehn and Kjaerulff 1996; Cina and Hochman 2000).

In the present research, the frequencies of locomotor-like rhythms induced by 5-HT/NMDA generally ranged from 0.06-0.25 Hz (n=15). In comparison, with sDC stimulation, the frequencies of bursting fell in the range of 0.25-0.4 Hz with stimulation train frequencies greater than or equal to 1 Hz (n=53).

The bursts produced by 5-HT/NMDA-application and sDC-stimulation were noticeably different (Figure 5.6a and b). The 5-HT/NMDA rhythms had greater amount of background activity evident between bursting, as clearly seen in the STFT spectrograms (Figure 5.6c). Cycle normalized average waveforms of the bursting envelope from 5-HT/NMDA and sDC rhythms also differed (Figure 5.6a and b) sDC rhythms had statistically sharper transitions into the bursts ($p<0.05$; Table 5.3) with an average slope of 5.3±1.2% of the normalized amplitude per 1% cycle period. Burst offset slopes were similar between the two methods.

Table 5.3: Summary of burst onset and offset slopes for normalized sDC and 5-HT/NMDA average waveforms

Slope (%NormAmp/%Cycle)	*sDC-evoked rhythms n=16*	*5-HT/NMDA evoked rhythms n=14*
Burst onset*	5.3 ± 1.2	3.7 ± 1.0
Burst offset	-2.2 ± 0.6	-2.4 ± 0.6

The average slope of burst onset and offset were calculated for sDC- and 5-HT/NMDA-evoked L2 bursts. The bursts were normalized for amplitude and cycle period. Onset and offset slope were calculated as depicted in Figure 5.7d. Statistical significance (unpaired t-test, $p<0.05$) is denoted by an asterisk (*).

Because the normalization for cycle period may mask temporal differences between sDC- and 5-HT/NMDA-evoked bursts, comparisons between the time to peak burst amplitude and bursting period were also made. The 5-HT/NMDA induced rhythms had a time to peak amplitude that varied linearly with the bursting period (Figure 5.6d). In comparison sDC-evoked rhythms showed almost no linear relationship to bursting period, suggesting that sDC-evoked rhythms discretely transition from a non-bursting to bursting state independent of bursting frequency. Together, these results suggest that ensemble output properties from these two rhythms are overtly different.

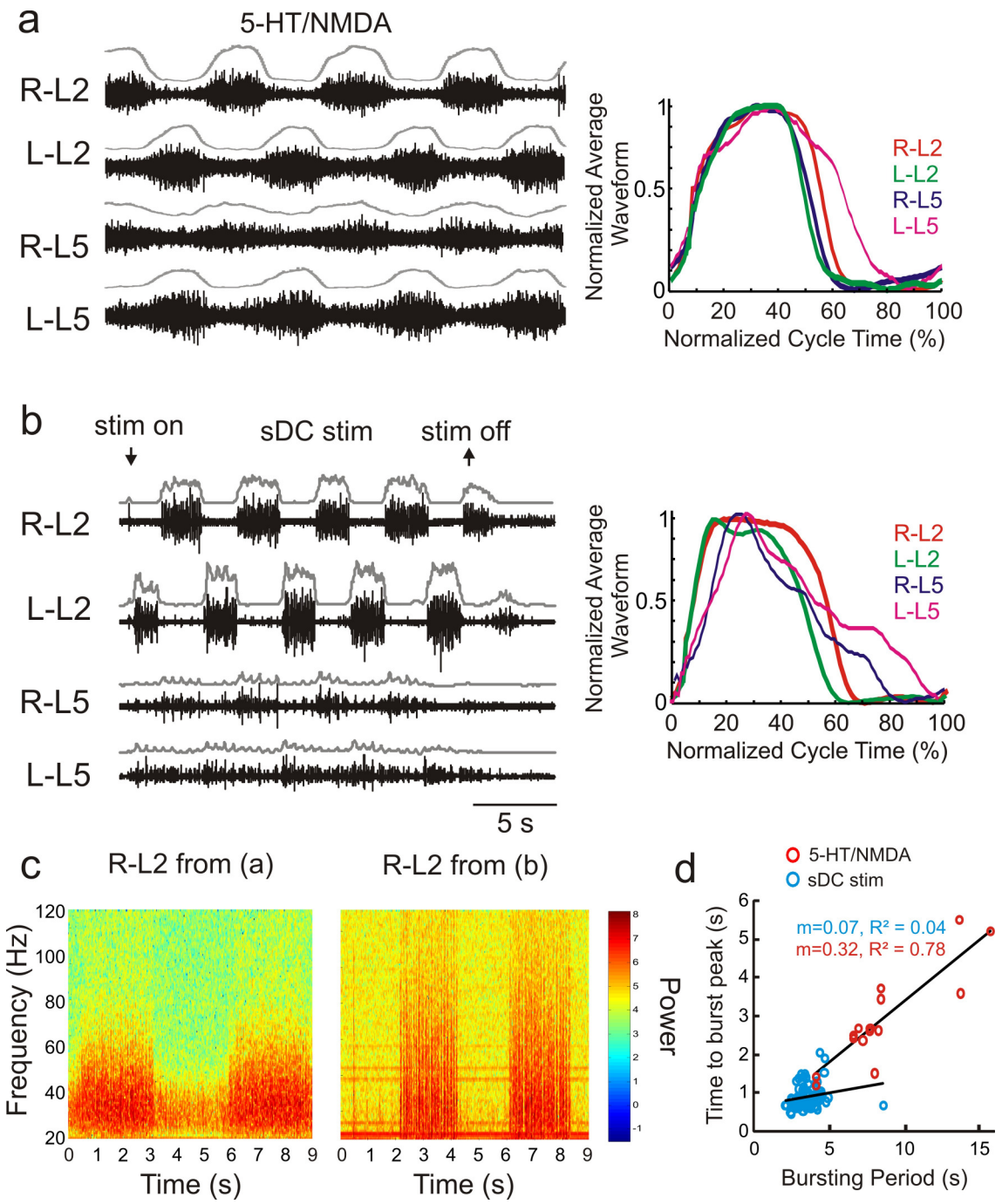

Figure 5.6: Comparison of pharmacological and dorsal column activated lumbar rhythms
Different methods of evoking lumbar motor rhythms produce differences in bursting shapes. In (a), locomotor-like activity was induced pharmacologically. In (b), lumbar rhythms were induced with sDC stimulation. Both produce rhythms of similar frequency. Differences in the average waveform shape are not obvious; however, the frequency components within the bursts are quite distinct, as seen in (c) using overlapping windows of short-time Fourier transforms (STFTs) to examine frequency components present in the signal over time. (d) Plot of time to peak burst amplitude vs. bursting period for sDC and 5-HT/NMDA induced rhythms with linear regression fits. Time to peak amplitude varies linearly for 5-HT/NMDA rhythms with a slope of 0.32 s/s (n=15), but not for sDC rhythms, which have a slope of 0.07 s/s (n=53).

To determine whether sDC-recruited pathways interact with neurochemically-recruited LLA, sDC-stimuli were given during ongoing 5-HT/NMDA LLA. The stimulus intensity typically used for sDC stimulation (200 μA amplitude, 200 μs pulse duration) affected 5-HT/NMDA LLA in some cases (n=2/3), but in one case this intensity had no effect on 5-HT/NMDA LLA (n=1/3); therefore, higher stimulus intensities were used in this experiment. Slow trains of sDC stimuli (0.1-1 Hz, 500 μA amplitude, 200-500 μs pulse duration) delivered to the sDC were found to alter LLA with the effects dependent on the stimulation frequency used (n=3; Figure 5.7a and c). In general, stimulus pulses resulted in significant increases in bursting frequency and burst intensity, which persisted for the duration of the stimulus train (Figure 5.7e and f). Additionally, the vast majority (87%) of stimulus pulses resulted in a phase advance in both the right and left ventral roots, regardless of phase time of stimulation (n=3 combined data). Stimulus trains ≥0.2 Hz had no evidence of resetting or entrainment of the 5-HT/NMDA rhythm (n=3/3; Figure 5.7b, c, d); however, stimulus trains at 0.2 Hz did result a sigmoidal relationship of calculated phase pairs on the phase response curve in one experiment (Figure 5.7b). In this one experiment, the phase response curve exhibits a differential response of the rhythm depending on the phase at which stimuli were applied. This suggests that at most stimulation frequencies, sDC stimulus pulses provide excitatory drive to the locomotor CPG to support a brief locomotor frequency increase, but do not contribute to phase-dependent alterations in timing. However, there was a narrow range of frequencies, 0.1-0.2 Hz, which resulted in phase-dependent modulation and entrainment of the ongoing rhythm. Figure 5.7d plots the 5-HT/NMDA period during perturbed cycles as it relates to the stimulation period. From this, stimulation

frequencies >0.2 Hz (stimulation period <5 s) tended to not entrain the rhythm, whereas stimulation frequencies ≤0.2 Hz (stimulation period ≥5 s) did have a relationship with the bursting rhythm's frequency. Overall, sDC stimulation-induced frequency changes support phase-independent excitatory actions on the locomotor CPG to increase frequency. Amplitude increases could occur due to overlapping reflex actions and/or through a stronger synaptic drive from the CPG.

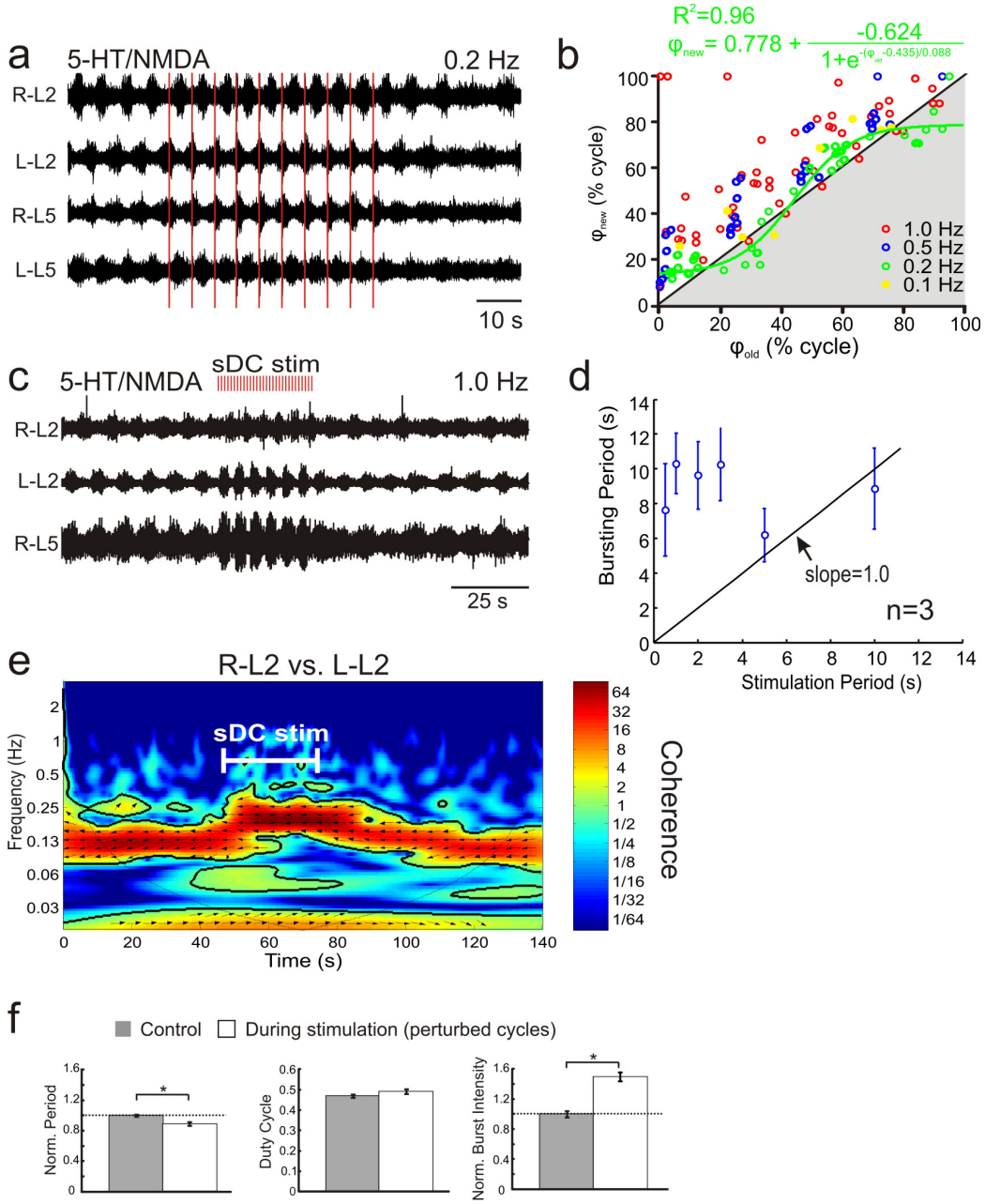

Figure 5.7: Effect of sDC-stimulation on ongoing 5-HT/NMDA LLA

(a) Trains of sDC stimulation (0.2 Hz) during 5-HT/NMDA-induced LLA entrained the rhythms in this example. Each stimulus pulse generated a pair of phases (φ_{old},φ_{new}), which were plotted as a phase response curve (n=3). (b) Example of phase response curve at different stimulation frequencies generated for one experiment with sigmoidal fit to cycles perturbed with 0.2 Hz stimulation. Shading indicates phase delay region. In (c), stimulus trains (2 Hz) significantly changed the cycle period and burst amplitude of the 5-HT/NMDA LLA. (d) Effects of stimulation period on bursting period. Stimulation periods of 5 and 10 s (stimulation frequencies of 0.2 and 0.1 Hz) entrained bursting (shown mean ± S.D.). (e) Wavelet spectral analysis of coherence between R-L2 and L-L2 for data in (c). Phase arrows on the spectrogram pointing to the left indicate out-of-phase activity between R-L2 and L-L2. Combined burst parameter analyses of three experiments are shown in (f). Due to inter-animal variability in bursting period and intensity, values were normalized. Data is displayed as mean ± S.E.M. Asterisks indicate significance with $p<0.05$.

5.3 Summary and perspective

A detailed examination of ventral root segments expressing evoked motor rhythms supported weakest expression in the only roots not containing autonomic efferents (L3-L5). Motor rhythmicity in L5 ventral roots was either absent or weak, did not typically recruit an activity pattern consistent with LLA, but was strengthened by partial block of $GABA_A$ receptors. That autonomic efferent pathways were recruited was supported by a preference for rhythmic activity in thoracolumbar roots containing sympathetic efferents and sacral root containing parasympathetic efferents. This was further confirmed with corresponding sympathetic efferent activity observed in the paravertebral sympathetic chain. In comparison, EMG recordings of several hindlimb muscles supported a cycle-delayed and incomplete secondary recruitment of somatic motor efferents. A half-center organization of this autonomic pattern generator emerged at lower frequency sDC stimulation where left and right burst generators could be independently recruited, or in alternating doublets. Their strict history dependence for left–right alternation without activity overlap supports a half-center organization coupled by mutual inhibition. The L2 autonomic pattern generator operated over a limited frequency range, with a discrete burst structure of fast-onset, frequency-independent peaks. In comparison, neurochemically-induced locomotor bursts operated over a wide frequency range and had slower time to peaks that varied with burst frequency. During ongoing 5-HT/NMDA induced LLA, stimuli from sacral afferent actions appeared to provide a phase-dependent excitatory drive at the same stimulation frequencies that revealed the half-center organization. Stimulation frequencies outside of this range increased burst frequency but did not entrain or reset the rhythm.

CHAPTER 6

DISCUSSION

6.1 Summary of key findings

The goal of this thesis was to identify a novel spinal cord surface site for evoking rhythmic behavior and characterize the fibers used for activating this behavior, the pathways mediating the behavior, and the resultant efferent output behaviors. In doing so, the findings presented in Chapters 3 support the existence of an autonomic pattern generator recruited by visceral C fiber afferents. Based on afferent compound action potential recordings in relation to the emergence of rhythmic activity and selective block of A and C fiber components, C fibers were found to be necessary and sufficient for sacral afferent generated lumbar rhythms. The generated L2 ventral root activity was robust and exhibited left–right alternation, which deteriorated usually in less than one minute. Rhythmicity in other locomotor-related ventral roots was generally absent or weak, with locomotor-like activity comprising a small percentage of observed patterns. These rhythms could be strengthened by partial block of $GABA_A$ receptors, which resulted in increased frequency and incidence of L5 rhythmicity consistent with locomotion. C fibers found in the sDC originate in the viscera and comprise a population of autonomic afferents. These C fibers contain the nociception encoding peripheral TRPV1 and P2X receptors, which are also on presynaptic afferent terminals in the spinal cord. Additionally, P2X receptors are found postsynaptically in all spinal segments. The sDC-evoked rhythms were found to be sensitive to both TRPV1 agonists and P2X

receptor antagonists, with P2X receptor activation being important in sacral and thoracolumbar segments, implying activation of postsynaptic P2X receptors.

In Chapter 4, pharmacological studies on spinal projection pathways involved in sDC-evoked lumbar rhythms implicated a requirement of sacral adrenergic and thoracolumbar cholinergic receptor activation. Sacral segments were found to be sensitive to α_1-adrenergic receptor antagonists by reducing all bursting parameters measured. Thoracolumbar segments were found to be sensitive to a mixture of nicotinic and muscarinic receptor antagonists with significant effects seen with the application of an α_7-nicotinic receptor antagonist. Since noradrenaline and acetylcholine are essential neurotransmitters in the autonomic nervous system, the involvement of adrenergic and cholinergic receptor-containing spinal neurons further supports the existence of an autonomic pattern generator activated by visceral afferents.

In Chapter 5, an examination of efferents activated by sDC stimulation found that of the ventral roots recorded (T11-S2), the only roots not expressing rhythmic activity (L3-L5) were those that do not contain autonomic afferents. Further, autonomic efferents recorded in the paravertebral sympathetic chain responded rhythmically to sDC stimulation, while EMG recordings from hindlimb musculature exhibited delayed activation of bursting that was an incomplete secondary recruitment of somatic motor efferents.

The circuit organization of this autonomic left–right rhythm generator materialized at very low frequencies of sDC stimulation (Chapter 5). Independent recruitment of left and right burst generators was possible, and alternating left–right burst doublets could also be recruited with certain stimulation parameters. These bursts

exhibited history dependent alternation with no evidence of activity overlap, supporting a half-center, mutually inhibited organization.

Compared to 5-HT/NMDA rhythms, sDC generated rhythms (i) were produced over a limited frequency range, and (ii) had sharper transitions to peak burst amplitude that were (iii) independent of overall bursting frequency. Chapter 5 demonstrated that during ongoing 5-HT/NMDA LLA, sDC stimulation provided excitatory drive since it increased burst frequency and amplitude. Phase-dependent actions were observed at the lower stimulation frequency range, including evidence of entrainment. The frequency range for observing entrainment of 5-HT/NMDA rhythms coincided with the frequency range of entrainment for sDC-stimulation induced bursts (see Figure 5.5b and Figure 5.7d)

The Discussion below is organized into three sections pertaining to the aforementioned three Results chapters. Then, I discuss the proposed circuitry relating sDC-evoked rhythms and recruitment of an autonomic left–right half-center organization to locomotion and its implications.

6.2 Sacral C fiber visceral afferents are required for generating lumbar ventral root rhythms

6.2.1 Afferents in the sacral dorsal column tract are necessary for evoked rhythms

Establishing the dorsal columns tract as the white matter pathway responsible for evoking lumbar rhythms during sacral dorsal columns (sDC) stimulation was of critical importance to this research. Previous studies using sacrocaudal afferent (SCA)-stimulation concluded that SCA-evoked rhythms did not require the dorsal columns for transmission of signals to the central pattern generator (CPG) through lesion studies

(Strauss and Lev-Tov 2003; Etlin et al. 2010; Lev-Tov et al. 2010). These studies indicated that every other white matter tract—ranging from dorsolateral funiculus to the ventral funiculus—had an observable impact on SCA-evoked rhythms due to the considerable amount of redundancy in the system as various neuronal populations were recruited (Etlin et al. 2010; Lev-Tov et al. 2010). Here, dorsal column lesions one segment rostral to the site of stimulation significantly affected the sDC-evoked lumbar rhythms, and stimulation current spread was shown to only recruit fibers in the dorsal columns tract. These results indicate that the afferents travelling via the sacral dorsal columns tract can activate lumbar pattern generators. The differences between this result and the previous research may lie in the location of the lesion. A previous study, which deemed the dorsal columns pathway as nonessential for long-projecting fibers, generally lesioned the cord 3-5 segments rostral to the stimulation site. In support of my observations, this group later determined that a subpopulation of the SCAs involved in SCA-evoked CPG activation travel briefly in the dorsal columns before entering the gray matter and synapsing onto interneurons (Etlin et al. 2010). Thus, the dorsal columns pathway is involved in SCA-evoked rhythms but only for one or two segments before afferents terminate in the gray matter. Dorsal columns afferents terminate in all laminae of the spinal cord (Ramon y Cajal 1909; Willis and Coggeshall 1991), and specifically visceral afferents terminate in laminae I, II, IV, V, and X (Sugiura and Tonosaki 1995). Therefore sDC stimulation provides an access point on the spinal cord surface for activating a subpopulation of the afferents involved in accessing a lumbar CPG.

The patterns evoked with sDC stimulation are transient and easily deteriorated, generally lasting less than one minute. In contrast serotonin (5-HT) and N-methyl-D-

aspartate (NMDA) evoked rhythms can last for hours (Kiehn and Kjaerulff 1996; Cina and Hochman 2000). This fatiguing rhythm was comparable to that seen with previously reported studies on afferent stimulation of both sacral (Strauss and Lev-Tov 2003) and lumbar (Marchetti et al. 2001) dorsal roots, implying a common fatigue mechanism. The deterioration seen with sDC-stimulation is not due to afferent action potential conduction failures since the afferent compound action potentials recorded in the DR or the DC remain the same even after the lumbar ventral root rhythms have subsided. Motor pattern depression may be due to synaptic vesicle depletion (Lev-Tov and Pinco 1992) but may also include fatigue or depression of subsequently activated spinal circuits. Evidence supporting afferent fatigue, presumably due to vesicle depletion, as the predominant mechanism through the recruitment of additional fiber populations was demonstrated by preventing deterioration using either alternating stimulation of left–right sites (Strauss and Lev-Tov 2003) or by recruiting previously unused afferents by increasing stimulation intensity (Figure 3.8).

6.2.2 Locomotor-like patterns are not the most prevalent pattern produced by sDC stimulation

Like other strategies studied for activating the hindlimb CPG networks, stimulation of the sacral dorsal column elicited rhythms comparable in many ways to those observed with and left–right alternation from the L2, purportedly flexor-reporting, ventral roots as SCA stimulation; however, notable differences were seen with regards to the rhythmicity of the extensor, motor-reporting L5 segment. Stimulation of the sDC typically did not produce a pattern of coordination consistent with locomotor-like activity (LLA), and when it did, L5 extensor-related activity was weak. An absence of extensor-

related rhythmic activity induced by SCA stimulation has been noted in some cases (Whelan et al. 2000; Strauss and Lev-Tov 2003), but the rhythms were still classified as locomotor-like. The lack of L5 alternation was postulated to arise due to SCA inhibition of extensor musculature as seen in the tail (Delvolve et al. 2001; Strauss and Lev-Tov 2003). While this explanation is plausible, another explanation might be that sDC stimulation-induced rhythms activate different pattern generating elements than those used for producing LLA.

While it remains possible that the lack of bursting in more caudal lumbar roots may be due to incomplete activation of the locomotor CPG, it should be noted that increasing afferent drive by increasing stimulation intensity or frequency did not unmask or strengthen bursting in these segments. This phenomenon suggests two possible explanations: (i) the increased intensity likely increased both excitatory and inhibitory drives to the lumbar segments, which resulted in rhythmic bursting in the L2 segments and inhibition of the L3-L5 segments by the sacral afferents or (ii) the sDC stimulation was preferentially activating a L2 ventral root pattern generator that may be largely uncoupled or actively inhibited by other spinal mechanisms. The role of inhibition in pattern generators has been widely studied, and the effects of $GABA_A$ receptors on locomotion include actions on the interneuronal CPG circuitry due to its demonstrated effects on bursting frequency (Cazalets et al. 1994; Cazalets et al. 1998).

The L5 extensor-related activity, as previously discussed, generally did not produce a coordination pattern with L2 flexor-related activity consistent with locomotion in most cases. The majority of the time, L5 extensor-related activity presented a pattern similar to that seen with the application of acetylcholine (ACh) and edrophonium to the

spinal cord (Cowley and Schmidt 1994). With this pattern, left–right alternation was maintained, but ipsilateral ventral roots were synchronous. The evidence that two very different rhythms, one that is locomotor-like and one that is consistent with ACh-induced rhythms, can be generated with the same sDC-stimulation supports the theory of reorganization of unit burst generators in the L5 segments dependent on the state of the neuronal system. The flexibility observed in the system may result from subtle differences in the afferent populations being recruited due to the nature of stimulating electrode placement, which would generate different types of sensory input, or may depend on the general excitability of the neuronal elements connected within the central pattern generator. The ability to generate a variety of rhythmic patterns by presumably overlapping neural elements depending on the state of the system or sensory feedback is consistent with transitions necessary to locomote in different directions (i.e. forward, backward, or sideways) as previously shown in the spinalized adult rat (Courtine et al. 2009). Cases without bursting activity observed in the L5 ventral roots could be transformed into the locomotor-like pattern by disinhibiting the sacral afferents suppressing extensor expression (Delvolve et al. 2001) or disinhibiting other inhibitory GABAergic pathways involved pattern generation.

6.2.3 Threshold is an inaccurate measure of recruitment of afferent fiber populations

The previous research concerning SCA-stimulation maintains that because the threshold required to activate the CPG is low (typically 1.3-3 times threshold), the afferent fiber populations recruited must be the larger diameter propriospinal pathways (Marchetti et al. 2001; Strauss and Lev-Tov 2003; Gordon and Whelan 2006; Mandadi et

al. 2009). This conclusion is highly dependent on how threshold is defined and the range of conduction velocities of different fiber subpopulations. For many SCA studies, threshold was defined as the stimulus amplitude (for a given pulse duration) required to evoke a reflex in a lumbar ventral root (Mandadi et al. 2009; Etlin et al. 2010) or a homonymous sacral ventral root (Whelan et al. 2000; Marchetti et al. 2001; Strauss and Lev-Tov 2003). These methods are indirect and do not determine threshold based on actual recruitment of afferent volleys, relying instead on transmission through synaptic circuits to define threshold. The only reliable method for determining stimulation threshold and which afferent fiber populations are recruited is to record the compound action potentials (CAPs) propagating within the activated axons directly, as classically used in the vast majority of *in vivo* work (Wall 1958; Eccles and Lundberg 1959; Schouenborg and Sjolund 1983). Using this direct approach for defining stimulation threshold, evoked reflexes were observed at ~2xT for dorsal root afferent volley threshold, suggesting that the thresholds determined in earlier studies could be multiplied by two to get an approximate estimate of afferent threshold.

Axon diameters of myelinated axons in P1-P7 rats are between the 1-2 μm Aδ phenotype (Vejsada et al. 1985; Nussbaumer et al. 1989). Thus, "low-threshold" stimuli in the neonatal rat recruit what would be considered slower-conducting, high-threshold Aδ fibers in the adult rat. This, coupled with limited amounts of myelination in the first week after birth, results in little variability in conduction velocities between myelinated afferent subtypes and between group A and C fibers (Fulton 1987). I observed that stimulation intensity could not be reliably used to separate recruitment of A and C fibers, which made the recoding of afferent CAPs essential to make this distinction. As

consistent with an earlier report, I found A and C fiber components to be clearly separable in the neonatal rodent (Nussbaumer et al. 1989). The current thresholds for sDC stimulation were higher than that for sDR stimulation. These differences may be attributed to the same afferents having a smaller diameter axon in the dorsal column due to axon collateralization (Joyner et al. 1978; Struijk et al. 1992). Additionally, afferents in the dorsal columns are not simple, straight fibers as they are in the dorsal root. Dorsal columns fibers have many collaterals entering the gray matter, which run perpendicular to white matter tract (Ramon y Cajal 1909; Willis and Coggeshall 1991). These morphological differences contribute to sDC afferents requiring a higher stimulus intensity to reach threshold, is consistent with modeling studies of dorsal column afferent stimulation (Struijk et al. 1992), and is also consistent with observed slower conduction velocities due to reduced axon diameters in axon collaterals (Rall 1959; Joyner et al. 1978).

6.2.4 High-threshold, nociceptive sacral fibers are necessary and sufficient for recruiting lumbar pattern generators

With this work, the appearance of the slowest C fiber component of the compound action potential (CAP) coincided with the recruitment of L2 ventral root rhythmicity with either sDC- or SCA-stimulation, implying that the recruitment of these fibers is necessary for CPG activation using these stimulation sites. Additional experiments indicated that these presumed C fibers, were sufficient for CPG activation by sDC-stimulation and also confirmed that the faster A fibers were neither necessary nor sufficient.

Thus, sDC- and SCA-stimulation activated C fiber pathways, which project rostrally and recruit, via direct or indirect actions, the L2 pattern generator. One candidate afferent population for these C fibers are those containing thermoceptors since noxious heat stimuli have been shown to activate short bouts of locomotor rhythms (Blivis et al. 2007). The TRPV1 receptor is found in peripheral free nerve endings as well as on presynaptic afferent terminals in the dorsal horn (Julius and Basbaum 2001; Levine and Alessandri-Haber 2007; Willis Jr 2007; Mandadi et al. 2009). TRPV1 receptor transiently activated then blocked the sDC- and SCA- evoked rhythms due to excessive receptor activation. This Ca^{2+}-dependent desensitization subsequently blocks spiking by keeping the neuron in a depolarized state (Szolcsányi 2004; Tominaga and Tominaga 2005). As shown previously (Mandadi et al. 2009), this desensitization resulted in a selective absence of the C fiber volley from dorsal root recordings. Select C fiber loss in DC volleys could not be determined due to the complexity of ascending and descending afferent populations of various orders of branching as well as contamination from post-synaptic dorsal column tract cell axons. Previous work in the mouse found a similar requirement of TRPV1 fibers for modulating SCA-evoked rhythms (Mandadi et al. 2009). However their assumption that "low-threshold" stimulation meant selective activation of Aβ fibers led to the erroneous assumption that the TRPV1 effects were due to long-range fibers projecting from sacral to lumbar cord to modulate the SCA-evoked rhythms (Mandadi et al. 2009). Another receptor class I tested was the purinergic P2X receptor family. These receptors were chosen for study because they are involved in spinal nociceptive signaling and usually colocalize with TRPV1 receptors on afferent fibers (Gu and Heft 2004). In Chapter 4, I demonstrated that block of postsynaptic P2X

receptors in the thoracolumbar cord and either pre- or postsynaptic P2X receptors in the sacral cord blocked sacral afferent evoked lumbar rhythms. However, unlike the TRPV1 receptors which are only found in primary afferents (Julius and Basbaum 2001; Levine and Alessandri-Haber 2007; Willis Jr 2007; Mandadi et al. 2009), P2X receptors are also found postsynaptically on spinal neurons throughout all segments (Nakatsuka and Gu 2006). The activation of postsynaptic P2X receptors suggests a release of ATP within the spinal cord. ATP can be released from primary afferent central terminals (Burnstock 2006) in response to nerve injury, it can also be released as a co-transmitter with GABA, dopamine, 5-HT, and NA (Burnstock 2004), and it can be released by astrocytes in response to nociceptive substance P or glutamate signaling in the spinal cord (Werry et al. 2006). Interestingly, the effects of the P2X receptor antagonist suramin was only reversible when used on sacral segments, suggesting that the antagonist may be acting on different subpopulations of P2X receptors distributed in the spinal cord. For example, *in situ* hybridization performed by the Allen Institute Mouse Spinal Cord Database, $P2X_2$ receptors have a stronger distribution in the rostral (cervical through lumbar) segments compared to the sacral segments, but $P2X_3$ receptors have a stronger distribution in lumbar and sacral segments compared to upper lumbar and thoracic (see Appendix A)(Allen_Institute_for_Brain_Science 2009). Both $P2X_2$ and $P2X_3$ are found on presynaptic afferent terminals in lamina II of the spinal cord, whereas only $P2X_2$ receptors are found postsynaptically in the dorsal horn (Chizh and Illes 2001). The concentration of suramin, a P2X receptor antagonist, used in these studies could have activated either $P2X_2$ or $P2X_3$ receptor subtypes (Chizh and Illes 2001). Given this knowledge, it is probable that suramin was acting on presynaptic $P2X_3$ receptors in the

sacral cord, which had reversible effects, and suramin acted on postsynaptic $P2X_2$ receptors in the thoracolumbar cord, which had irreversible effects. If suramin was acting on $P2X_2$ receptors in the sacral cord, these receptor-containing interneurons were not involved in the sacral afferent evoked lumbar rhythm.

Since sDC-stimulation evoked lumbar rhythms seem to be mediated by a nociceptive, high-threshold pathway, it is important to consider the types of information transmitted through the dorsal column. The dorsal column was historically viewed as a non-pain pathway, but recent research clearly demonstrated that it is also an important projection system for visceral nociceptive information (Al-Chaer et al. 1996; Hirshberg et al. 1996; Al-Chaer et al. 1998; Willis et al. 1999; Palecek 2004). The visceral nociceptive information transmitted by the dorsal columns is thought to travel via the post-synaptic dorsal column neurons rather than the primary afferents travelling in the dorsal column (Al-Chaer et al. 1996; Palecek 2004). However, those studies examined the effects of thoracic lesions to sacral visceral pain information, and it has been shown that visceral afferents only travel 2-3 segments within the dorsal columns before terminating (Sugiura and Tonosaki 1995). Thus, at the thoracic level, there would be no sacral visceral afferents in the dorsal columns. It has also been shown that up to 20% of the visceral afferent fibers terminate in the dorsal columns (Sugiura and Tonosaki 1995), and stimulation of the dorsal column definitely activates primary afferents since antidromic CAPs can be recorded in the dorsal root resulting from sDC stimulation. Interestingly, one study demonstrated that SCA-activated primary afferents enter the dorsal column, travel a short distance, and then synapse onto interneurons in the spinal gray matter (Etlin et al. 2010), which is a very similar route just described for visceral

afferents. My research demonstrated that sDC- and SCA-stimulation activated overlapping pathways with similar fatigue, threshold, and pharmacological properties. Therefore, sDC- and SCA-stimulation both activate high-threshold afferents, with the sDC afferents belonging to a class of visceral sensation. Visceral afferents, which are generally thinly or unmyelinated and thus higher-threshold (Ness and Gebhart 1990), have been found in the dorsal column originating from the pelvic nerves, which enter the spinal cord in the sacral region (Kawatani et al. 1986; McKenna and Nadelhaft 1986). These nerves innervate the bladder, rectum, and genital region and so are associated with excretory and sexual function. The pelvic nerve is a parasympathetic nerve (McKenna and Nadelhaft 1986). Therefore, stimulation of high-threshold visceral afferents projecting through the dorsal columns is likely activating autonomic pattern generating circuitry associated with activation of one or more of these territories in the neonatal rat. Stimulation of the dorsal column has been shown previously to have effects on autonomic function. High frequency dorsal column stimulation (>30Hz) is used therapeutically for relief from ischemic pain and intractable pain and also causes peripheral vasodilation (Linderoth et al. 1994; Augustinsson et al. 1995; Linderoth et al. 1995, 1995; Oakley and Prager 2002). Thus activation of both somatic and autonomic circuitry is likely occurring by sacral dorsal column stimulation. In this regard it is interesting that studies on spinal locomotor mechanisms in the cat use perineal stimulation to help recruit locomotor circuits (Belanger et al. 1996; Chau et al. 2002) since both noxious and innocuous cutaneous perineal afferents converge on interneurons also receiving input from nociceptive visceral afferents (Foreman et al. 1981; Cervero 1982; Cervero and Tattersall 1985; Kasparov 1992). These viscerosomatic interneurons

ascend in the spinothalamic tract, which runs in the ventrolateral funiculus (Al-Chaer et al. 1996; Katter et al. 1996). Since there are no interneurons that receive purely visceral input (Cervero and Tattersall 1985), these interneurons may represent important relays to an autonomic pattern generator. Since the autonomic and somatic rhythms generated by sacral dorsal column stimulation are entrained to one another, an alternative explanation is that sacral dorsal column stimulation is activating a central pattern generator, which produces alternating rhythms in both somatic and autonomic targets, thereby coordinating the two systems to one another. This coordination between autonomic and somatic rhythms may serve as a way for the body to cope with the dramatic changes occurring in the limbs as they locomote, particularly with regards to vascular function and metabolic demands. As such, it would not be surprising for there to be a significant overlap, or even shared pattern generators, between autonomic and somatic pattern generating circuitry.

6.3 Pharmacological dissection of spinal pathways involved in afferent evoked rhythms

6.3.1 Adrenergic receptor involvement in sDC evoked rhythms

The previous research concerning the adrenergic system's role in CPG activation has demonstrated an ability of the adrenergic system to activate the sacrococcygeal CPG network of the rodent (Gabbay et al. 2002) and the cat (Forssberg and Grillner 1973; Barbeau and Rossignol 1991; Chau et al. 1998) but not the lumbar of the neonatal rodent CPG network (Kiehn et al. 1999; Sqalli-Houssaini and Cazalets 2000). In the lumbar segments of the rodent, noradrenaline alone produces slow, non-locomotor rhythms with a period of 80-90 s (Sqalli-Houssaini and Cazalets 2000) and fast rhythms with an

average period of 2.7 s (Gabbay and Lev-Tov 2004) both mediated by α_1-adrenergic receptor (AR) activation. The non-locomotor rhythm induced by noradrenaline had left-right alternation with ipsilateral L2 and L5 co-contracting (Sqalli-Houssaini and Cazalets 2000), which is a similar rhythm generated in the majority of sDC-evoked lumbar rhythms with L5 bursting. For the fast rhythm reported by Gabbay and Lev-Tov, recordings were not collected from L5 ventral roots, so the activated rhythm was not conclusively locomotor-like (Gabbay and Lev-Tov 2004). Noradrenaline's effects on locomotor-like activity in the neonatal rodent can be neuromodulatory, with α_1-AR activation increasing frequency and α_2-AR activation decreasing frequency of LLA induced by NMDA (Sqalli-Houssaini and Cazalets 2000). My research (Chapter 4) demonstrated that application of α_1-AR antagonists to sacral segments reduced burst intensity, frequency and number. The reduction in frequency produced by α_1-AR antagonists would be expected since the modulatory actions of α_1-AR agonists increase frequency of LLA. Since these effects are isolated to the sacral segments more caudal to those containing the CPG elements, they cannot be direct actions on the L2 segment's motoneurons or sympathetic preganglionic neurons (SPNs) located in the intermediolateral (IML) cell column.

Immunocytochemical staining for dopamine-β-hydroxylase, the enzyme required for production of noradrenaline and adrenaline, has shown descending noradrenergic projections in the dorsal horn, ventral horn, IML, and around the central canal in the spinal cord in all segments studied (Westlund et al. 1983). Adrenergic α_1 receptors have been shown to be homogeneously distributed throughout the cord by autoradiography using the specific α_1-AR antagonist [^{3}H]Prazosin as a ligand (Roudet et al. 1993) and

throughout cervical, thoracic, lumbar, and sacral segments (Roudet et al. 1993; Day et al. 1997; Smith et al. 1999). Density of α_1-ARs varied somewhat throughout various areas of the cord: the highest concentration of α_1-ARs was around the central canal, and the dorsal horn displayed the lowest density of receptors (Roudet et al. 1993). The effects of α_1-AR activation are widespread and involve autonomic, somatosensory, and motor functions, which is not surprising given the widespread distribution of α_1-ARs in the spinal cord (Roudet et al. 1993; Smith et al. 1999; Schwinn and Michelotti 2000). This makes it difficult to determine exactly how the α_1-ARs are modulating the CPG through sDC stimulation, but there are several possibilities. Stimulation of the sDC may activate interneurons containing α_1-ARs (i) in the dorsal horn of the sacral cord or (ii) around the central canal of the sacral cord, which project to lumbar segments and activate the CPG. These locations are likely termination points for the afferents traveling in the dorsal columns (Willis et al. 1999), and given the α_1-AR sensitivity in the sacral segments, these are potential sites for synapses to form.

However, since the only source of noradrenaline to the spinal cord originates in the brain (Westlund et al. 1983), and since primary afferents cannot synthesize noradrenaline (Mouchet et al. 1986; Vega et al. 1991; Brumovsky et al. 2006), and since there are no adrenergic neurons in the spinal cord (Westlund et al. 1983), it is not obvious how α_1-AR activity would be recruited. One possibility is that there are α_1-ARs in the spinal cord that are constitutively active (active in the absence of neurotransmitter). Constitutive activity of adrenergic receptors has been shown in single cell systems (Rossier et al. 1999; Seifert and Wenzel-Seifert 2002) and after spinal cord injury (Rank et al. 2011). Inverse agonists, as opposed to competitive antagonists, can block

constitutively active receptors. Prazosin, which was used in this study, has been shown to act as a potent inverse agonist of α_1-ARs (Noguera et al. 1996; Rossier et al. 1999; Seifert and Wenzel-Seifert 2002), and in particular, the α_1-ARs, not α_2-ARs, have been shown to be constitutively active after spinal cord injury (Rank et al. 2011). Another source of adrenergic activation may be descending adrenergic projections continuing to release adrenaline even after being separated from their cell body. If so, these projections would then be tonically activating α_1-ARs on the spinal neurons, which would then project to lumbar segments and modulate pattern generating circuitry.

6.3.2 Cholinergic receptor involvement in sDC evoked rhythms

In addition to the monoamines, the role of cholinergic neurotransmission in generation of locomotor patterns has been widely studied in the mammalian nervous system (Atsuta et al. 1991; Cowley and Schmidt 1994; Miles et al. 2007; Anglister et al. 2008; Kwan et al. 2009). Acetylcholine was initially described as an endogenous neurochemicals capable of activating the CPG but not critical to CPG activation (Smith et al. 1988). Application of ACh in combination with the acetylcholinesterase inhibitor edrophonium (EDRO) can produce bouts of LLA in the rat (Cowley and Schmidt 1994; Anglister et al. 2008) but is more likely to produce non-locomotor rhythmic activity. This non-locomotor activity typically involves electroneurographically-measured co-activation of ipsilateral flexors and extensors and may have left–right alternation (Cowley and Schmidt 1994). In this research, the typical pattern of activity evoked with sDC stimulation resembled that seen in the rat with application of ACh/EDRO suggesting that the circuitry recruited by ACh can also be activated by sDC afferent stimulation. This suggestion corresponds with previous research demonstrating the existence of cholinergic

relay interneurons activated by SCA stimulation (Anglister et al. 2008). These relay interneurons are located in the sacral segments of the spinal cord, identified by vesicular acetylcholine transporter labeling, and project in the ventral funiculus to the lumbar segments. Another population of medium and large-sized cholinergic neurons are located in the dorsal root ganglia suggesting that a subpopulation of primary afferents may also release ACh within the spinal cord (Olave et al. 2002). Since it's been demonstrated here and previously (Strauss and Lev-Tov 2003) that sDC- and SCA-evoked lumbar rhythms require the activation of an spinal neurons in the sacral segments, it is unlikely that the cholinergic primary afferents are a major source of modulation on sDC-evoked rhythms. The cholinergic receptor antagonists investigated in the present work had selective effects on bath-partitioned thoracolumbar segments and modulated parameters related to CPG activation, suggesting they had direct effects on the CPG. There is evidence supporting direct modulation of the CPG by acetylcholine by c-fos and choline acetyltransferase labeling after prolonged fictive locomotion in the decerebrate cat (Huang et al. 2000) and frequency reduction after application of ACh on SCA-evoked rhythms (Anglister et al. 2008). Candidate cholinergic interneurons for this direct modulation are found throughout the rostrocaudal extent of the spinal cord, primarily located in laminae III, IV, VII, VIII, and X (Olave et al. 2002; Brownstone and Wilson 2008), and the cholinergic interneurons activated during CPG activation have been localized to medial lamina VII and lamina X, which are areas believed to be partition interneurons (Barber et al. 1991), in the cat (Huang et al. 2000) and the rat (Brownstone and Wilson 2008). These cholinergic interneurons make connections with motoneurons through C-boutons and cholinergic varicosities and are thought to modulate motoneuron activation through M2-

mAChR activation (Zagoraiou et al. 2009). The present work demonstrated that broad-spectrum muscarinic receptor antagonists modulate sDC-evoked rhythms by having a tendency to reduce burst intensity, burst frequency burst duration, and the number of evoked bursts, though not significantly.

Nicotinic acetylcholine receptors (nAChRs) are widespread in the spinal cord (Khan et al. 1994; Hellstrom-Lindahl et al. 1998), with a higher density of nAChRs in the dorsal half of the lumbosacral rat spinal cord (Khan et al. 1994) and the presence of α_3-, α_4-, α_5-, and α_7-nAChR subunits in the human spinal cord (Hellstrom-Lindahl et al. 1998). In the Allen Brain Atlas Database (see Appendix A) labeling for α_3- and α_7-nAChR subunits was found in the thoracic and upper lumbar segments of the mouse spinal cord, with α_3-selective labeling on motoneurons and in the dorsal horn, and α_7-selective labeling in the dorsal horn, around the central canal, and in intermediate lamina III associated with Clark's column. These areas, especially around the central canal and in lamina III, are areas associated with pattern generation in the lumbar segment; therefore it is possible that at least a subpopulation of the cholinergic relay interneurons is nicotinic and contains α_7-nAChRs.

Neurons around the central canal, which are implicated in locomotor rhythmogenesis (Miles et al. 2007; Anglister et al. 2008), project to the IML where SPNs are located (Wilson et al. 2005), and also receive a large amount of descending modulatory monoaminergic input (Loewy and McKellar 1981; Westlund et al. 1983; Milner et al. 1988; Ridet et al. 1992). Descending monoaminergic systems are behavioral drive systems also implicated in locomotor rhythmogenesis (Sillar et al. 1998; Kiehn et al. 1999; Schmidt and Jordan 2000; Sqalli-Houssaini and Cazalets 2000; Ballion et al.

2002; Branchereau et al. 2002; Jordan and Schmidt 2002; Allain et al. 2005; Liu and Jordan 2005).

Functionally, the application of nAChR agonists to the spinal cord results in increased pressor responses and excites behavioral responses (Khan et al. 1994). Additionally, the cholinergic system is known to affect the coordination of movements (Carlin et al. 2006) and level of excitability of motoneurons (Miles et al. 2007). Muscarinic receptors $M_{2\text{-}4}$ have been shown to mediate antinociception, similar to α-adrenergic receptors (Hoglund and Baghdoyan 1997). Given the widespread distribution of acetylcholine receptors in the spinal cord, it is likely that both locomotor and sympathetic function in the lumbar cord are being modulated with application of ACh, which may explain the non-locomotor, co-activated flexor-extensor behaviors seen in the spinal cord due to sDC-stimulation. The non-locomotor patterns generated may somehow be a result of reorganization of the circuitry by exciting a different subset of receptors on the interneurons, which then produces non-locomotor, co-contracting rhythms.

6.4 Efferent output patterns resulting from sacral dorsal column stimulation

6.4.1 Rhythmic efferent output is via an autonomic pattern generator

The involvement of visceral afferents combined with the absence of rhythmicity in the L3-L5 segments in sDC-evoked rhythms indicates involvement of the autonomic nervous system as described below. The autonomic nervous system efferents originate from thoracic, lumbar, and sacral segments, but not all lumbar segments are included. Of the recorded segments in this work (T11-S2), segments T11-L2 have sympathetic efferents, with T13-L2 projecting to the hindlimbs; segments L3-L5 have no autonomic

innervations; and segments L6-S2 have parasympathetic efferents (McLachlan et al. 2009). It is curious that the sDC-evoked rhythms lacked rhythmicity the majority of the time in segments L3-L5. In Chapter 5, recordings from the sympathetic chain and hindlimb musculature revealed that sDC-stimulation activated both autonomic and somatic efferents. The difficulty in detecting rhythmic bursting in the sympathetic chain was likely due to the relatively small number of axons travelling in between the sympathetic ganglia in the chain in the neonates as compared to ventral roots (Fraher and O'Sullivan 1989). With so few fibers to potentially be activated, successful recordings were difficult to obtain, but when successfully recorded evidence of rhythmicity was observed, and the sympathetic chain bursting clearly alternated from left to right. Generally, the sympathetic nervous system is not thought to have bilateral differences in activation, but in the case of locomotion, it is plausible that alternating activation may result due to the differential needs of the limbs at different points in the step cycle. For example, changes in blood vessel dilation may be changing in a phase-dependent manner to deliver the appropriate amount of oxygen to active muscles (Walløe and Wesche 1988; Lutjemeier et al. 2005; Lutjemeier et al. 2008). However, the kinetics of autonomic output from the spinal cord to the hindlimbs may impede the ability for autonomic outflow to sustain higher locomotor speeds, such as a gallop, but stimulus induced autonomic junction potentials can keep up with moderate stimulus frequencies between 2 and 15 Hz (Burnstock and Holman 1961). Additionally, the vasculature within a limb can adapt relatively rapidly to skeletal muscle contractions. In particular, changes in contraction intensity result in immediate effects on vasodilation within the contracted muscle, but these effects cannot be maintained for contractile frequencies greater than 1

Hz (Rogers et al. 2006), thus demonstrating differences between stimulus induced and naturally occurring frequency entrainment. With regard to the data presented in this dissertation, the relatively small range of frequencies generated by sacral dorsal column stimulation may be indicative of the autonomic information being generated. Because the frequency range is so narrow for sacral dorsal column evoked rhythms, this may suggest that an autonomic pattern generator is in control of both the autonomic and somatic output. Alternatively, sacral dorsal column stimulation may be preferentially activating a mode of the central pattern generator, which supports rhythmic activity in both the autonomic and somatic nervous systems. In contrast, the locomotor frequency range generated by 5-HT/NMDA is much greater, and indicates that this method of activating locomotor-like activity only activates both somatic and autonomic rhythmicity within the range overlapping with that produced by sacral dorsal column stimulation. However, the possibility that autonomic outflow generated by the spinal cord continues to entrain with the somatic outflow at greater locomotor frequencies cannot be eliminated at this time as no recordings for locomotor rhythms at greater frequencies have also had recordings from autonomic nerves.

When hindlimb muscle activity was recorded electromyographically, sDC-stimulation induced activity tended to be stronger in muscles from motor pools with axons exiting from the more rostral lumbar segments, consistent with the ventral root patterns observed. Interestingly, unlike the co-initiation of L2 and sympathetic chain bursts, muscle recruitment was seldom seen in the early burst cycles. This indicates that either rhythmicity of sympathetic targets precedes and therefore entrains motor rhythmicity and supports the presence of an independent pattern generator that serves as

the “clock” for the locomotor CPG or the threshold for activating somatic output, perhaps due to the subset of afferents being activated, is slightly lower than that required for activating the autonomic rhythmicity even though both autonomic and somatic rhythms are generated by a shared “clock”.

Thus far, the activation of the central pattern generator has only been discussed in terms of activation by more caudal afferents or global excitation by pharmacological agents, but descending supraspinal systems clearly play a large role in both the initiation and control of spinal pattern generating circuitry, which is especially evident after a spinal cord injury. Even at the supraspinal level there is evidence for an overlap between autonomic and somatic-related areas of the brain in the activation of lumbar central pattern generation. Several areas of the brain are capable of being stimulated to activate locomotor activity, including the mesencephalic locomotor region (MLR) and hypothalamic locomotor region (HLR). The MLR is the most prevalent area stimulated to induce robust locomotor activity in decerebrate cats since this area is located in the midbrain and remains intact after decerebration. The MLR projects to the spinal cord with projections travelling in the ventrolateral funiculus (Whelan 1996), which is also capable of being stimulated to activate locomotor-like activity (Magnuson and Trinder 1997). This descending system is under monoaminergic control, with strong evidence for dopaminergic and/or noradrenergic pathways playing significant roles in the activation of locomotion (Whelan 1996). Stimulation of the HLR is also capable of activating locomotion, and it has been proposed that different subsets of neurons are activated depending on the behavioral context of the locomotion being generated with the behaviors being separated into exploratory, appetitive, and defensive categories

(Sinnamon 1993; Jordan 1998). The hypothalamus and mesencephalon are connected through both the medial and lateral hypothalamus (Swanson et al. 1984; Whelan 1996; Jordan 1998). The lateral hypothalamus is responsible for the autonomic sensations of thirst and hunger and the medial hypothalamus is responsible for blood pressure, heart rate, and satiety (Kandel et al. 2000). Stimulation of the lateral hypothalamus produces appetitive locomotor behaviors, whereas stimulation of the medial hypothalamus produces defensive locomotor behaviors (Sinnamon 1993). Lesions to the medial hypothalamus, specifically the suprachiasmatic nucleus, can disrupt circadian-related locomotor behaviors in the rat (Stephan and Zucker 1972) revealing a strong connection between the hypothalamus and locomotion. Thus, the autonomic and somatic nervous systems are tightly interwoven even in supraspinal centers with regard to locomotion, which is consistent with the results from stimulating the sacral dorsal columns. How the autonomic control generated by the hypothalamus relates to the rhythmic autonomic output generated by sacral dorsal column stimulation remains unclear at this time. Potentially, activation of the medial hypothalamus may generate signals for changes in blood pressure related to the initiation of locomotor defensive behaviors, which are transmitted via the MLR to the spinal cord to the lumbar central pattern generator. Another plausible scenario would instead activate the lateral hypothalamus to generate the sensation of hunger, which travels through the MLR to the spinal cord through the ventrolateral funiculus to the lumbar central pattern generator creating foraging locomotor behaviors along with the requisite autonomic functions, such as vasodilation, necessary for nourishing the musculature during this task. Thus it is probable that

descending autonomic centers can activate the same central pattern generating circuitry associated with sacral dorsal column stimulation.

6.4.2 Half center organization of the autonomic pattern generator

While higher frequencies of sDC stimulation induced continuous alternating left-right L2 efferent actions, lower stimulation frequencies (<1 Hz) induced rhythms that displayed unique bursting properties. At these low frequencies, motor rhythms became entrained to the stimuli. The slow stimuli provided a sufficient input to shift the excitability of one side to burst, but the single pulse was insufficient for generating a full cycle of alternation. The next stimulus pulse then activated the alternate side since the balance of excitation between the two sides was shifted, and the previously activated side was in a refractory state. The alternation from left to right resulted from approximately equal excitatory activation from the sDC stimulation with intrinsic fatigability as proposed by Lundberg and colleagues (Jankowska et al. 1967). The double pulse stimuli results also supported a half-center organization. Double pulses temporally summated to provide sufficient excitation to produce an entire cycle of left-right alternation, but there was insufficient excitation to continue the rhythm beyond one cycle. These results suggest that (i) bursting reflects activity in half-centers; (ii) activation of a half-center produces a history-dependent fatigue for a long period after its recruitment so that subsequent stimuli are more likely to recruit the other half-center, and this fatigue may be rate-limiting to maximal frequency; and (iii) one half-center provides synaptic drive to the other half-center, which must be inhibitory to prevent co-activation, suggesting that recruitment of the CPG is mediated by post inhibitory rebound.

6.4.3 Comparison of sacral afferent stimulation-evoked rhythms to 5-HT/NMDA evoked locomotor-like activity

The ventral root activity evoked by sDC stimulation had noticeable differences from 5-HT/NMDA induced rhythms, such as the lack of L5 bursting to produce locomotor-like activity as previously discussed. The two types of bursting also differed in the sharpness of burst onsets/offsets and the quiescent periods between bursts. The sDC-evoked bursts were more consistent in reaching peak amplitude independent of bursting frequency while 5-HT/NMDA bursts had a time to peak burst amplitude that varied with the bursting frequency, which had a narrower range with sDC stimulation rhythms than 5-HT/NMDA evoked rhythms. The greater background activity observed in the 5-HT/NMDA rhythms between bursts, relative to sDC-evoked rhythms, at least partly resulted from direct depolarization of the motoneurons by 5-HT and NMDA (Hochman and Schmidt 1998). In comparison, the sDC-evoked rhythms may have little to no background activity because the activation was more selective and transient.

The combination of 5-HT/NMDA LLA with sDC stimulation supports the existence of multiple central pattern generating networks in the lumbar spinal cord by showing that sDC stimulation generally increased LLA frequency, and at certain stimulation frequencies the rhythm was altered in a phase-dependent manner, indicating that sDC stimulation can control the CPG activated by 5-HT. Interestingly, subsequent to stimulation termination, 5-HT rhythm became disorganized for many cycles, demonstrating that the pathways activated by sDC stimulation can powerfully interact with that generating 5-HT LLA.

The actions of sDC stimulation of 5-HT/NMDA LLA may be complicated by indirect effects as 5-HT known to profoundly depress afferent input (Garraway and Hochman 2001), including visceral afferent input (Zimmerman and Hochman 2011), making it difficult to independently assess afferent actions on locomotion. Indeed in at least one animal, sDC stimulation intensity increases were required to produce actions on lumbar circuits during 5-HT/NMDA LLA.

6.4.4 On the organization of the locomotor CPG

As mentioned earlier, Cowley and Schmidt (1994) demonstrated that neurochemical application of acetylcholine in the presence of a cholinesterase inhibitor usually generated in-phase activation of flexors and extensors from one hindlimb, which rhythmically alternated with extensors/flexors from the contralateral hindlimb. Interestingly, I found that this was the most common output observed following sDC stimulation when L5 bursting was present. This pattern is also consistent with the type of rhythm generated during sideways stepping (Courtine et al. 2009). The variability of patterns produced by sacral dorsal column stimulation may be a result of subtle differences in the state of the spinal cord with regard to the neuronal excitability or channel conductances, and the variability is a testament to the immense flexibility of the neural circuitry within the spinal cord whereby many different patterns can be produced with slight reorganization to the neural circuitry. Assuming that the majority of the activity observed in the L2 ventral roots resulting from sDC-stimulation is motor-related, spinal circuit organizations that explain these differences in motor coordination include: (i) that there are multiple independent hindlimb CPGs which are activated by different means (i.e. 5-HT, ACh, SCA stimulation); or (ii) the CPG is comprised of unit burst

generators which reorganize their firing properties depending on the situation (i.e. neurochemical environment, activity history).

To date, several studies have attempted to identify neuronal components comprising the locomotor CPG following genetic deletion/disruption of transcriptionally defined classes of spinal interneurons, but coordinated albeit altered rhythmic motor patterns remain. These transcriptionally defined interneurons are putative "core" CPG interneurons and are called V0, V1, V2, and V3. Selective knockout of V0 and V2a result in a loss of left–right coupling with V0 knockouts exhibiting hopping patterns (Lanuza et al. 2004) and V2a knockouts having increased variability in period and increased burst amplitude (Crone et al. 2008); V1 knockout resulted in a prolonged step cycle due to loss of inhibition (Gosgnach et al. 2006); and V3 inhibitory interneurons are responsible for symmetrical motor output (Zhang et al. 2008). This may indicate rhythmicity is an emergent property of a redundant and distributed network, and therefore, no single developmental subpopulation of interneurons can block rhythmicity. Alternatively there may be multiple parallel locomotor CPGs recruited under different behavioral conditions, and no single class of interneurons contributes essentially to the operation of all CPGs.

In analogy to our understanding of motor network reconfiguration by neuromodulators in invertebrate pattern generating circuits neurons (Marder and Calabrese 1996), it seems plausible that the differential actions of 5-HT and sDC-stimulation or ACh-induced rhythms may be due to a transmitter-dependent reconfiguration of the CPG. This was observed between 5-HT and dopamine associated with neonatal rat hindlimb locomotion (Kiehn and Kjaerulff 1998). Phasing differences

in rhythmic hindlimb muscle activation by 5-HT/NMDA and SCA stimulation, have been demonstrated here and previously after deafferentation. In Chapter 5, during sDC stimulation, the semimembranosus muscle was out of phase with the contralateral L2 ventral root, but during 5-HT/NMDA semimembranosus was in phase with the contralateral L2 ventral root. Similarly, Klein and Tresch demonstrated that during stimulation of the cauda equina, rectus femoris was active during extension and semitendinosus was active during flexion, but during 5-HT/NMDA rhythms, the phases during which these muscles were active switched and persisted even after deafferentation, indicating that these phase shifts were due to differences in central circuitry (2010).

6.5 Could the autonomic pattern generator be the clock for the locomotor CPG?

The research presented in this dissertation leaves an interesting question. Could the autonomic pattern generator be the clock for the locomotor CPG? This seems likely as the autonomic pattern generator (i) is rhythmic and active prior to locomotion, (ii) couples rhythmically to locomotor patterns, (iii) is exactly located where previous studies identified as critical for locomotor rhythmogenesis, and (iv) has a half-center organization. While the evidence for a half-center organization was provided in Section 6.4.2 above, support for points (i-iii) are elaborated further below.

(i) Studies of spontaneous fictive locomotion in the paralyzed, decorticate cat observed that centrally-mediated cardiorespiratory autonomic actions always preceded and were an integral part of fictive locomotion (Eldridge et al. 1985).

(ii) Others have shown sympathetic and hindlimb muscle activity are coupled in spinalized preparations during locomotion in the acutely spinalized L-dopa cat preparation (Schomburg et al. 2003) and during application of NMDA in an adult mouse spinal cord hindlimb preparation (Chizh et al. 1998). Thus, descending systems are not necessary for such synchronization. Moreover, purported "sympathetic" interneurons project both to sympathetic preganglionic neurons as well as motoneurons (Deuchars 2007).

(iii) The aforementioned "sympathetic" interneurons are located in segments with sympathetic innervation (McLachlan et al. 2009) and found around the central canal. This corresponds to the level at which progressive dorsal-to-ventral horizontal lesions abolished locomotor-like activity (Kjaerulff and Kiehn 1996). Intriguingly, this horizontal level (lamina X) is also where the entire sympathetic nervous system neurons are located with a mediolateral and rostrocaudal ladder-like distribution (Markham et al. 1991). Such a system would allow for a redundant system resistant to many levels of partial lesioning along the thoracic and rostral lumbar cord (Cowley and Schmidt 1997). Lesioning studies have also identified T13-L2 spinal segments as containing the core essential neural network for locomotion, with L2 being particularly important (Cazalets et al. 1996; Kjaerulff and Kiehn 1996; Cowley and Schmidt 1997). Intriguingly, these segments also correspond rather strikingly to the part of the sympathetic system responsible for control of hindlimb function (McLachlan et al. 2009) and demonstrated that L2 contains an autonomic pattern generator.

The brain does not treat the autonomic and somatic nervous systems as independent entities as their integrated actions are required to provide coordinated outputs to meet the needs of a given behavior. Rather these patterns represent a behavior comprised of autonomic and somatic components, a fact demonstrated by concurrent recordings of locomotion and sympathetic efferents, which show that behaviorally, the brain recruits changes in autonomic circuitry as if to prepare the body for the onset of locomotion (Eldridge et al. 1985). Further support for autonomic ties to central pattern generator are found in the hypothalamic innervation of the MLR and the ability to initiate locomotion by stimulating the hypothalamus itself (Swanson et al. 1984; Sinnamon 1993; Whelan 1996; Jordan 1998).

The reasoning behind having the "clock" under control of supposed visceral afferents is a less clear. Potentially, these afferents may play a role in the defensive locomotor behaviors related to the perineal region of an animal since strong stimulation of this region in cats can generate locomotion on treadmill, and stimulation of the perineum may activate a mixture of both somatic and autonomic afferents given their close proximity (Belanger et al. 1996; Chau et al. 2002). Also, both the autonomic and somatic afferents in this region converge on the same set of interneurons, which may be in the pathway either to supraspinal centers for further processing and/or the lumbar pattern generating circuitry (Foreman et al. 1981; Cervero 1982; Cervero and Tattersall 1985; Kasparov 1992).

6.6 Proposed circuitry

Based on the research presented here combined with the previous studies, Figure 6.1 illustrates the proposed circuitry for sDC-evoked activation of spinal autonomic and motor CPGs. In the proposed pathway, afferent C fibers entering by dorsal roots travel in the dorsal column a short distance (1-3 segments) before terminating in the sacral spinal gray matter. The high-threshold visceral afferent C-fibers possess TRPV1, $GABA_A$, and P2X receptors on their presynaptic terminals. These afferents have synaptic actions on spinal neurons in the superficial dorsal horn and elsewhere (lamina I, II, IV, V, X) (Sugiura et al. 1989) with their excitability under descending noradrenergic control from the brain. These spinal neurons project directly or synapse onto other spinal neurons that project to the lumbar cord, likely including cholinergic projections in the ventral, ventrolateral, or lateral funiculi (Borges and Iversen 1986; Anglister et al. 2008) and sacral pattern generator. In the lumbar cord, cholinergic actions, mediated by a combination of nAChR and mAChR receptor activation, are necessary to activate the sympathetic autonomic CPG. Sacral C fibers also activate a sacral parasympathetic CPG that couples to the sympathetic autonomic CPG (Gabbay et al. 2002; Strauss and Lev-Tov 2003). The sympathetic autonomic CPG, organized as a half-center oscillator, comprises the purported locomotion rhythm generator (Rybak et al. 2006). The coupling of this CPG to flexor and extensor somatic pattern generating modules is dependent on the system and can result in either in-phase or alternating patterns. The strength of this coupling is modulated by GABAergic inhibitory interneurons that contribute to overall burst frequency. The extensor-related segments also receive inhibitory connections from sacral afferents (Delvolve et al. 2001), which explains the absence of extensor activity in

many scenarios. The strong autonomic drive originating in the hypothalamus also activates the autonomic pattern generator by sending command signals through the MLR and the ventrolateral funiculus of the spinal cord.

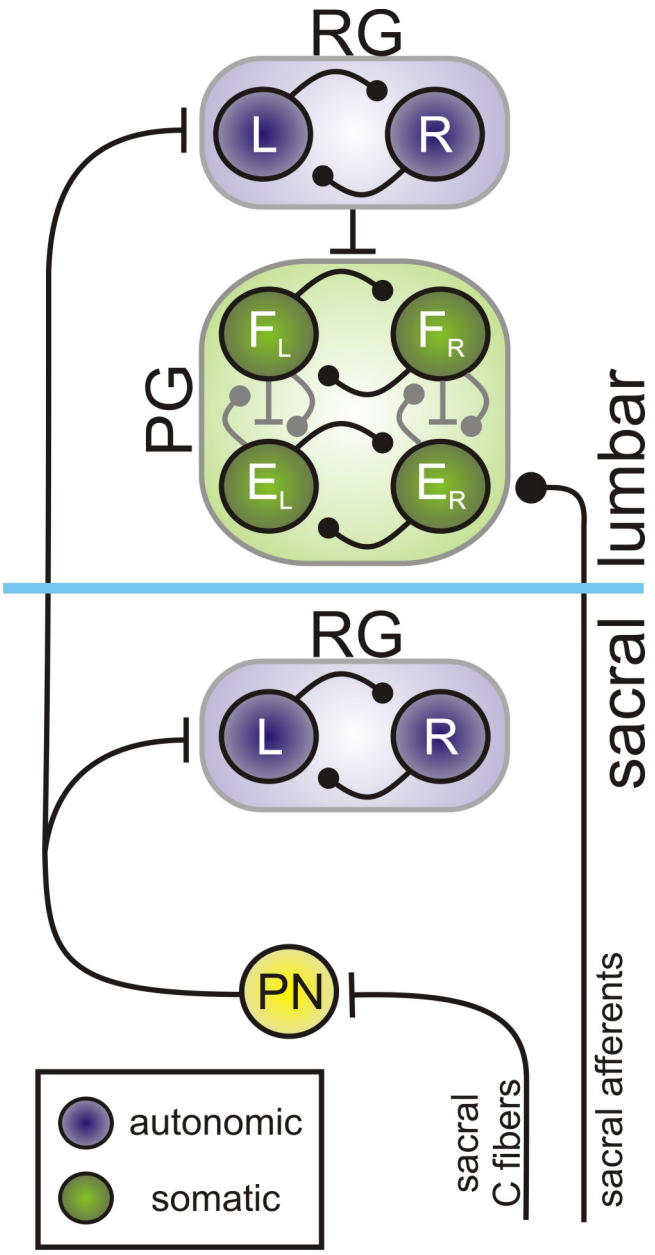

Figure 6.1: Schematic for relating sDC stimulation to autonomic pattern generator activation Sacral C fiber afferents enter the spinal cord and travel in the dorsal column briefly (2-3 segments) before terminating in the spinal gray onto projecting neurons (PN), which possess α_1-adrenergic receptors activated by descending systems. These PNs project rostrally in the white matter tracts, are likely cholinergic, and synapse either directly onto the lumbar sympathetic rhythm generator (RG) or onto other spinal neurons which then synapse onto the sympathetic RG. The sympathetic RG, under cholinergic control, acts as the clock for the locomotor pattern generator (PG), which depending on the state of the system can produce in-phase or alternating hindlimb rhythms. A parasympathetic RG is located in sacral cord, and previous research demonstrated connectivity between it and the sympathetic RG (Gabbay et al. 2002; Strauss and Lev-Tov 2003) which is believed to be through connectivity of the PN.

6.7 Alternative interpretations and limitations

While the proposed circuitry presented here is plausible, it is by no means the only interpretation of the data presented. Of greatest importance, it is possible that the central pattern generator retains a two-level organization, but that the "clock" is neither autonomic nor somatic. With this organization, the pattern generating level could be either a shared network for establishing autonomic and somatic patterns or composed of two separate networks for the two branches of the nervous system. Based on the data presented, the most likely alternative scenario would be the existence of a shared clock with separate pattern generating circuitry (Figure 6.2). Having one "clock" for both would ensure that the two rhythms could remain entrained to one another as needed and could account for the phase-dependent changes seen in 5-HT/NMDA rhythms by sacral afferent stimulation. With at least a portion of the pattern formation network separate between the two systems, this could account for the delay seen between autonomic and somatic onset of activity by allowing for differences in threshold between the two networks. In order to confirm or refute either of these interpretations, additional experiments isolating the effects of the proposed autonomic pattern generator would have to be performed to verify its existence. If the autonomic pattern generator is truly the "clock", then its elimination would result in the inability to generate rhythms in both the somatic and autonomic targets. If there is an independent "clock", then the somatic pattern generation would not be affected by elimination of the autonomic circuitry.

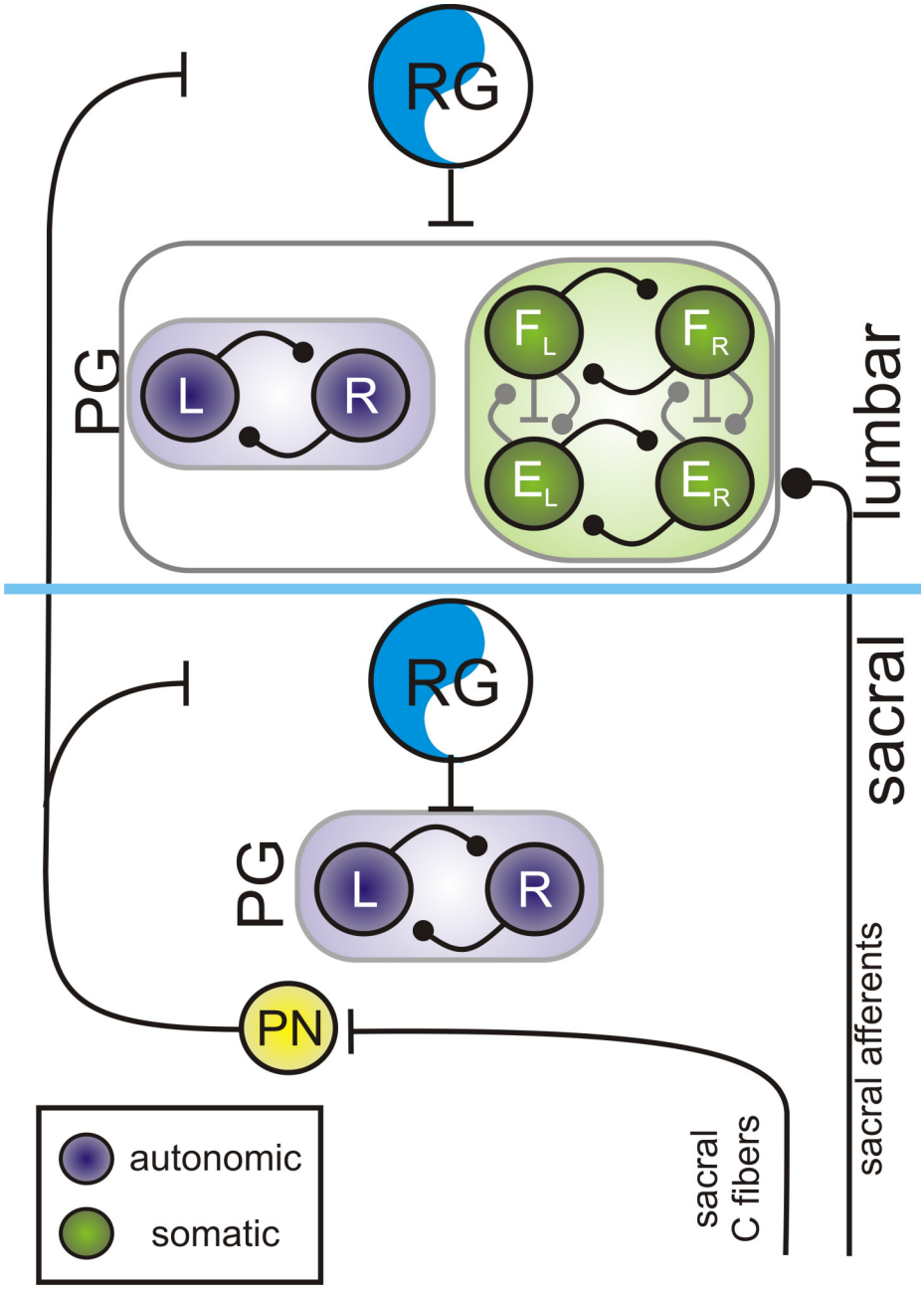

Figure 6.2: Alternative schematic for relating sDC stimulation to lumbar pattern generation
Sacral C fiber afferents enter the spinal cord and travel in the dorsal column briefly (2-3 segments) before terminating in the spinal gray onto projecting neurons (PN), which possess α_1-adrenergic receptors activated by descending systems. These PNs project rostrally in the white matter tracts, are likely cholinergic, and synapse either directly onto the lumbar rhythm generator (RG) or onto other spinal neurons which then synapse onto the lumbar RG. The RG clock activates locomotor and autonomic pattern generators (PGs). The locomotor PG can produce state-dependent patterns of in-phase or alternating hindlimb rhythms. A RG is also located in sacral cord, and previous research demonstrated connectivity between it and the lumbar RG (Gabbay et al. 2002; Strauss and Lev-Tov 2003), which is believed to be through connectivity from the PN.

6.8 Concluding remarks

This research has built upon past work using SCA-stimulation to activate the locomotor CPG. I investigated more fully the populations of afferents required for CPG activation along with demonstrating reorganization of the CPG to produce a variety of outputs with the same stimuli. The major contributions of this research are two-fold: (i) there may exist an autonomic pattern generator which acts as the clock for locomotor rhythms which can be accessed by activating sacral C fiber afferents and potentially by descending supraspinal centers (i.e. MLR), and (ii) the autonomic pattern generator has a half-center organization which can be dissected and used for entraining bursts generated by sacral afferent stimulation or locomotor rhythms generated by neurochemicals. That spinal cord stimulation has both autonomic and somatic efferent effects is not new; however, this work provides a greater understanding of how the two divisions of the nervous system interact to generate behaviors, which is of critical importance in understanding their dysfunction following injury. The characterization presented here shows the interaction of the somatic and autonomic systems in generating rhythmic patterns in the lumbar spinal cord of the neonatal rat. Furthermore, I have shown that this identified autonomic pattern generator can be accessed to modulate existing motor rhythms. In this model, the ability to access and modulate both somatic and autonomic systems and their output in a single location indicates that the sacral dorsal columns may be an ideal location for intervention following injury. It is hoped that this research and future investigations will lead to improved understanding of the critical interplay of the somatic and autonomic systems within the spinal cord, ultimately leading to more specific and targeted therapies for functional recovery following spinal cord injury.

APPENDIX A

APPENDIX A: ALLEN SPINAL CORD ATLAS

The Allen Spinal cord Atlas (http://mousespinal.brain-map.org) gives an extensive database of RNA *in situ* hybridization images for specific gene expression in juvenile (postnatal day 4) mouse spinal cord (Allen_Institute_for_Brain_Science 2009). Spinal cord *in situ* hybridization expression patterns collected from the Allen Spinal Cord Atlas for α_1-adrenoceptors, $P2X_2$ and $P2X_3$ receptors, $\alpha_{6,7,9}$-nicotinic acetylcholine receptors, and M1-5 muscarinic acetylcholine receptors are found in the following figures. The Allen Spinal Cord Atlas also determines the presence or absence of gene expression for different laminae and white or gray matter. However, reaction product indicating gene expression is observed in some neurons even though they are marked as absent.

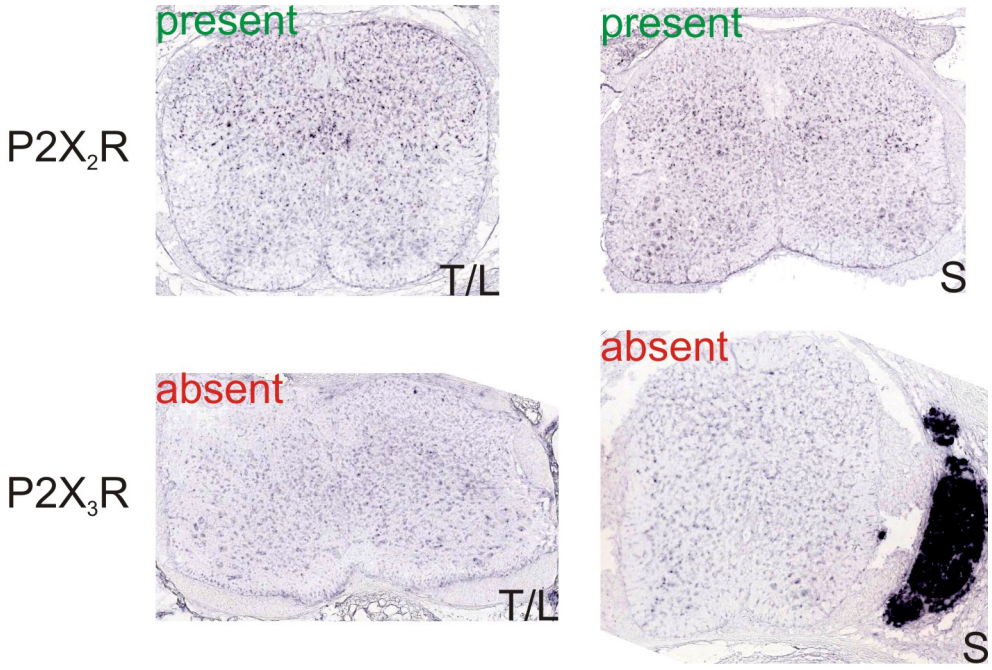

Figure A.1: Allen Spinal Cord Atlas of *in situ* hybridization of $P2X_2$ and $P2X_3$ receptors
Sections from P4 mouse spinal cord at thoracolumbar (T/L) and sacral segments (S) for $P2X_2$ and $P2X_3$ receptors. $P2X_2$ is found in laminae I-VI. $P2X_3$ is marked as absent but reaction product is seen in lamina I of the T/L section. Additionally, paravertebral ganglion is strongly labeled near sacral cord.

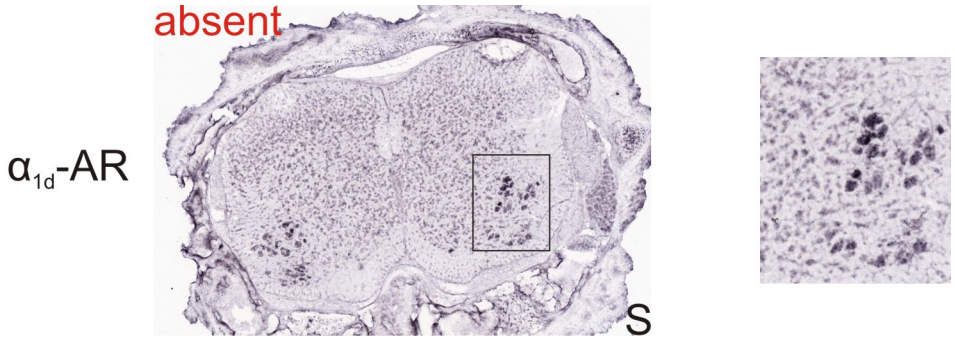

Figure A.2: Allen Spinal Cord Atlas *in situ* hybridization of α_{1d}-adrenoceptors
Sections from P4 mouse spinal cord from sacral segments with *in situ* hybridization of α_{1d}-adrenoceptors. The atlas labeled this receptor as absent, but there is clear reaction product in lamina IX and throughout the spinal cord.

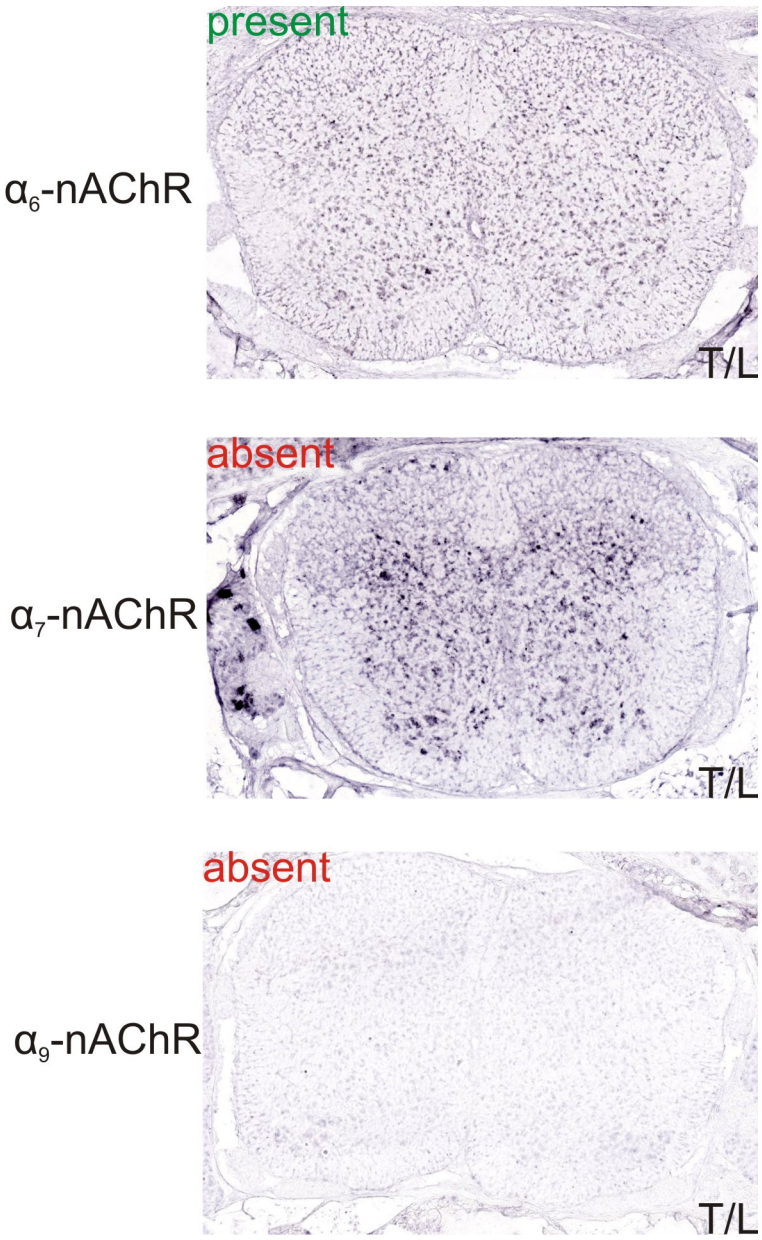

Figure A.3: Allen Spinal Cord Atlas *in situ* hybridization for $\alpha_{6,7,9}$-nicotinic receptors
Sections from P4 mouse thoracolumbar spinal cord with *in situ* hybridization for $\alpha_{6,7,9}$-nicotinic acetylcholine receptors. α_6-nicotinic receptors are found in laminae IV-VI. α_7-nicotinic receptors, marked as absent, are obvious throughout spinal, and especially in motoneurons and near Clark's column with additional labeling in a subpopulation of paravertebral ganglion neurons. α_9-nicotinic receptors are not found in thoracolumbar spinal cord.

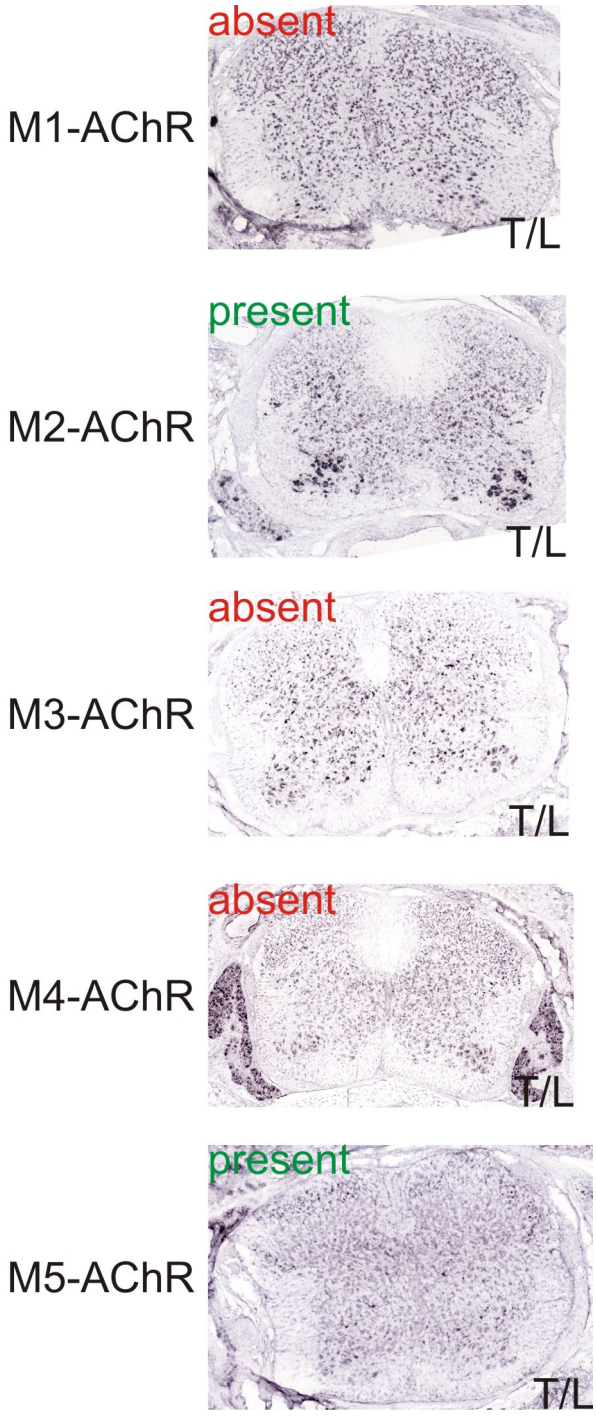

Figure A.4: Allen Spinal Cord Atlas *in situ* hybridization for M1-5-muscarinic receptors
Sections from P4 mouse thoracolumbar spinal cord with *in situ* hybridization for M1-5-nicotinic acetylcholine receptors. M1-muscarinic receptors, marked absent, are found throughout the cord. M2 receptors are in lamina IX and intermediate laminae. M3 receptors are found throughout, but are denser in ventral horn. M4 receptors are not found except in paravertebral ganglia. M5 receptors are found in laminae I-III and also in ventral horn.

REFERENCES

Al-Chaer, E. D., Y. Feng, et al. (1998). "A Role for the Dorsal Column in Nociceptive Visceral Input Into the Thalamus of Primates." J Neurophysiol **79**(6): 3143-3150.

Al-Chaer, E. D., N. B. Lawand, et al. (1996). "Pelvic visceral input into the nucleus gracilis is largely mediated by the postsynaptic dorsal column pathway." J Neurophysiol **76**(4): 2675-2690.

Al-Chaer, E. D., N. B. Lawand, et al. (1996). "Visceral nociceptive input into the ventral posterolateral nucleus of the thalamus: a new function for the dorsal column pathway." J Neurophysiol **76**(4): 2661-2674.

Alexander, S. P., A. Mathie, et al. (2008). "Guide to Receptors and Channels (GRAC), 3rd edition." Br J Pharmacol **153 Suppl 2**: S1-209.

Allain, A.-E., P. Meyrand, et al. (2005). "Ontogenic Changes of the Spinal GABAergic Cell Population Are Controlled by the Serotonin (5-HT) System: Implication of 5-HT1 Receptor Family." The Journal of Neuroscience **25**(38): 8714-8724.

Allen_Institute_for_Brain_Science (2009). "Allen Mouse Spinal Cord Atlas." 2011, from http://mousespinal.brain-map.org.

Anglister, L., A. Etlin, et al. (2008). "Cholinesterases in development and disease." Chemico-Biological Interactions **175**(1-3): 92-100.

Atsuta, Y., P. Abraham, et al. (1991). "Control of locomotion in vitro: II. Chemical stimulation." Somatosens Mot Res **8**(1): 55-63.

Augustinsson, L. E., B. Linderoth, et al. (1995). "Spinal cord stimulation in cardiovascular disease." Neurosurg Clin N Am **6**(1): 157-165.

Ballion, B., P. Branchereau, et al. (2002). "Ontogeny of descending serotonergic innervation and evidence for intraspinal 5-HT neurons in the mouse spinal cord." Brain Res Dev Brain Res **137**(1): 81-88.

Barbeau, H. and S. Rossignol (1987). "Recovery of locomotion after chronic spinalization in the adult cat." Brain Research **412**(1): 84-95.

Barbeau, H. and S. Rossignol (1991). "Initiation and modulation of the locomotor pattern in the adult chronic spinal cat by noradrenergic, serotonergic and dopaminergic drugs." Brain Res **546**(2): 250-260.

Barber, R. P., P. E. Phelps, et al. (1991). "Generation patterns of immunocytochemically identified cholinergic neurons at autonomic levels of the rat spinal cord." The Journal of Comparative Neurology **311**(4): 509-519.

Barthelemy, D., H. Leblond, et al. (2006). "Nonlocomotor and Locomotor Hindlimb Responses Evoked by Electrical Microstimulation of the Lumbar Cord in Spinalized Cats." J Neurophysiol **96**(6): 3273-3292.

Belanger, M., T. Drew, et al. (1996). "A comparison of treadmill locomotion in adult cats before and after spinal transection." J Neurophysiol **76**(1): 471-491.

Berecek, K. H. and M. J. Brody (1982). "Evidence for a neurotransmitter role for epinephrine derived from the adrenal medulla." American Journal of Physiology - Heart and Circulatory Physiology **242**(4): H593-H601.

Berthelsen, S. and W. A. Pettinger (1977). "A functional basis for classification of [alpha]-adrenergic receptors." Life Sciences **21**(5): 595-606.

Blivis, D., G. Z. Mentis, et al. (2007). "Differential Effects of Opioids on Sacrocaudal Afferent Pathways and Central Pattern Generators in the Neonatal Rat Spinal Cord." J Neurophysiol **97**(4): 2875-2886.

Bonnot, A., D. Morin, et al. (1998). "Genesis of spontaneous rhythmic motor patterns in the lumbosacral spinal cord of neonate mouse." Developmental Brain Research **108**(1-2): 89-99.

Bonnot, A., D. Morin, et al. (1998). "Organization of Rhythmic Motor Patterns in the Lumbosacral Spinal Cord of Neonate Mouse." Ann NY Acad Sci **860**(1): 432-435.

Borges, L. F. and S. D. Iversen (1986). "Topography of choline acetyltransferase Immunoreactive Neurons and fibers in the rat spinal cord." Brain Research **362**(1): 140-148.

Bracci, E., L. Ballerini, et al. (1996). "Localization of Rhythmogenic Networks Responsible for Spontaneous Bursts Induced by Strychnine and Bicuculline in the Rat Isolated Spinal Cord." J. Neurosci. **16**(21): 7063-7076.

Bracci, E., L. Ballerini, et al. (1996). "Spontaneous rhythmic bursts induced by pharmacological block of inhibition in lumbar motoneurons of the neonatal rat spinal cord." J Neurophysiol **75**(2): 640-647.

Branchereau, P., J. Chapron, et al. (2002). "Descending 5-hydroxytryptamine raphe inputs repress the expression of serotonergic neurons and slow the maturation of inhibitory systems in mouse embryonic spinal cord." J Neurosci **22**(7): 2598-2606.

Brown, A. G., P. B. Brown, et al. (1983). "Receptive field organization and response properties of spinal neurones with axons ascending the dorsal columns in the cat." J Physiol **337**: 575-588.

Brown, T. G. (1911). "The Intrinsic Factors in the Act of Progression in the Mammal." Proceedings of the Royal Society of London. Series B, Containing Papers of a Biological Character **84**(572): 308-319.

Brown, T. G. (1914). "On the nature of the fundamental activity of the nervous centres; together with an analysis of the conditioning of rhythmic activity in progression, and a theory of the evolution of function in the nervous system." The Journal of Physiology **48**(1): 18-46.

Brownstone, R. M. and J. M. Wilson (2008). "Strategies for delineating spinal locomotor rhythm-generating networks and the possible role of Hb9 interneurones in rhythmogenesis." Brain Research Reviews **57**(1): 64-76.

Brumovsky, P., M. J. Villar, et al. (2006). "Tyrosine hydroxylase is expressed in a subpopulation of small dorsal root ganglion neurons in the adult mouse." Experimental Neurology **200**(1): 153-165.

Buchanan, J. T. and S. Grillner (1987). "Newly Identified `Glutamate Interneurons' and their Role in Locomotion in the Lamprey Spinal Cord." Science **236**(4799): 312-314.

Burnstock, G. (2004). "Cotransmission." Current Opinion in Pharmacology **4**(1): 47-52.

Burnstock, G. (2006). "Purinergic P2 receptors as targets for novel analgesics." Pharmacol Ther **110**(3): 433-454.

Burnstock, G. and M. E. Holman (1961). "The transmission of excitation from autonomic nerve to smooth muscle." The Journal of Physiology **155**(1): 115-133.

Carlin, K. P., Y. Dai, et al. (2006). "Cholinergic and Serotonergic Excitation of Ascending Commissural Neurons in the Thoraco-Lumbar Spinal Cord of the Neonatal Mouse." Journal of Neurophysiology **95**(2): 1278-1284.

Carr, P. A., A. Huang, et al. (1995). "Cytochemical characteristics of cat spinal neurons activated during fictive locomotion." Brain Research Bulletin **37**(2): 213-218.

Cazalets, J., M. Borde, et al. (1995). "Localization and organization of the central pattern generator for hindlimb locomotion in newborn rat." The Journal of Neuroscience **15**(7): 4943-4951.

Cazalets, J. R., S. Bertrand, et al. (1998). "GABAergic control of spinal locomotor networks in the neonatal rat." Ann N Y Acad Sci **860**: 168-180.

Cazalets, J. R., M. Borde, et al. (1996). "The synaptic drive from the spinal locomotor network to motoneurons in the newborn rat." J. Neurosci. **16**(1): 298-306.

Cazalets, J. R., Y. Sqalli-Houssaini, et al. (1992). "Activation of the central pattern generators for locomotion by serotonin and excitatory amino acids in neonatal rat." J Physiol **455**(1): 187-204.

Cazalets, J. R., Y. Sqalli-Houssaini, et al. (1994). "GABAergic inactivation of the central pattern generators for locomotion in isolated neonatal rat spinal cord." J Physiol **474**(1): 173-181.

Cervero, F. (1982). "Noxious intensities of visceral stimulation are required to activate viscerosomatic multireceptive neurons in the thoracic spinal cord of the cat." Brain Res **240**(2): 350-352.

Cervero, F. and J. E. Tattersall (1985). "Cutaneous receptive fields of somatic and viscerosomatic neurones in the thoracic spinal cord of the cat." J Comp Neurol **237**(3): 325-332.

Changfeng, T. and J. Dazong (1994). "Selective stimulation of smaller fibers in a compound nerve trunk with single cathode by rectangular current pulses." Biomedical Engineering, IEEE Transactions on **41**(3): 286-291.

Chau, C., H. Barbeau, et al. (1998). "Early Locomotor Training With Clonidine in Spinal Cats." J Neurophysiol **79**(1): 392-409.

Chau, C., H. Barbeau, et al. (1998). "Effects of intrathecal alpha1- and alpha2-noradrenergic agonists and norepinephrine on locomotion in chronic spinal cats." J Neurophysiol **79**(6): 2941-2963.

Chau, C., N. Giroux, et al. (2002). "Effects of Intrathecal Glutamatergic Drugs on Locomotion I. NMDA in Short-Term Spinal Cats." J Neurophysiol **88**(6): 3032-3045.

Chizh, B. A., P. M. Headley, et al. (1998). "Coupling of sympathetic and somatic motor outflows from the spinal cord in a perfused preparation of adult mouse in vitro." J Physiol **508 (Pt 3)**: 907-918.

Chizh, B. A. and P. Illes (2001). "P2X receptors and nociception." Pharmacol Rev **53**: 553 - 568.

Christianson, J. A., K. Bielefeldt, et al. (2009). "Development, plasticity and modulation of visceral afferents." Brain Research Reviews **60**(1): 171-186.

Chung, S. K., K. T. McVary, et al. (1988). "Sexual reflexes in male and female rats." Neuroscience Letters **94**(3): 343-348.

Cina, C. and S. Hochman (2000). "Diffuse distribution of sulforhodamine-labeled neurons during serotonin-evoked locomotion in the neonatal rat thoracolumbar spinal cord." The Journal of Comparative Neurology **423**(4): 590-602.

Civantos Calzada, B. and A. Aleixandre de Artiñano (2001). "Alpha-adrenoceptor subtypes." Pharmacological Research **44**(3): 195-208.

Contreras, R. J., M. M. Gomez, et al. (1980). "Central origins of cranial nerve parasympathetic neurons in the rat." The Journal of Comparative Neurology **190**(2): 373-394.

Conway, B. A., H. Hultborn, et al. (1987). "Proprioceptive input resets central locomotor rhythm in the spinal cat." Experimental Brain Research **68**(3): 643-656.

Courtine, G., Y. Gerasimenko, et al. (2009). "Transformation of nonfunctional spinal circuits into functional states after the loss of brain input." Nat Neurosci **12**(10): 1333-1342.

Cowley, K. C. and B. J. Schmidt (1994). "A comparison of motor patterns induced by , acetylcholine and serotonin in the in vitro neonatal rat spinal cord." Neuroscience Letters **171**(1-2): 147-150.

Cowley, K. C. and B. J. Schmidt (1997). "Regional Distribution of the Locomotor Pattern-Generating Network in the Neonatal Rat Spinal Cord." J Neurophysiol **77**(1): 247-259.

Crone, S. A., K. A. Quinlan, et al. (2008). "Genetic Ablation of V2a Ipsilateral Interneurons Disrupts Left-Right Locomotor Coordination in Mammalian Spinal Cord." Neuron **60**(1): 70-83.

Dai, X., B. R. Noga, et al. (2005). "Localization of Spinal Neurons Activated During Locomotion Using the c-fos Immunohistochemical Method." Journal of Neurophysiology **93**(6): 3442-3452.

Day, H. E. W., S. Campeau, et al. (1997). "Distribution of [alpha]1a-, [alpha]1b- and [alpha]1d-adrenergic receptor mRNA in the rat brain and spinal cord." Journal of Chemical Neuroanatomy **13**(2): 115-139.

Delvolve, I., H. Gabbay, et al. (2001). "The Motor Output and Behavior Produced by Rhythmogenic Sacrocaudal Networks in Spinal Cords of Neonatal Rats." J Neurophysiol **85**(5): 2100-2110.

Deuchars, S. A. (2007). "Multi-tasking in the spinal cord – do 'sympathetic' interneurones work harder than we give them credit for?" The Journal of Physiology **580**(3): 723-729.

Dimitrijevic, M. R., Y. Gerasimenko, et al. (1998). "Evidence for a Spinal Central Pattern Generator in Humans." Annals of the New York Academy of Sciences **860**(1): 360-376.

Duysens, J., D. McCrea, et al. (2006). "How deletions in a model could help explain deletions in the laboratory." Journal of Neurophysiology **95**(1): 562-565.

Eccles, R. M. and A. Lundberg (1959). "Supraspinal control of interneurones mediating spinal reflexes." J Physiol **147**: 565-584.

Edgerton, V. R. and R. R. Roy (2002). "Paralysis recovery in humans and model systems." Current Opinion in Neurobiology **12**(6): 658-667.

Eldridge, F. L., D. E. Millhorn, et al. (1985). "Stimulation by central command of locomotion, respiration and circulation during exercise." Respir Physiol **59**(3): 313-337.

Enevoldson, T. P. and G. Gordon (1989). "Postsynaptic dorsal column neurons in the cat: a study with retrograde transport of horseradish peroxidase." Exp Brain Res **75**(3): 611-620.

Etlin, A., D. Blivis, et al. (2010). "Long and Short Multifunicular Projections of Sacral Neurons Are Activated by Sensory Input to Produce Locomotor Activity in the Absence of Supraspinal Control." The Journal of Neuroscience **30**(31): 10324-10336.

Fitzgerald, M. (1987). "Cutaneous primary afferent properties in the hind limb of the neonatal rat." The Journal of Physiology **383**(1): 79-92.

Foreman, R. D., M. B. Hancock, et al. (1981). "Responses of spinothalamic tract cells in the thoracic spinal cord of the monkey to cutaneous and visceral inputs." Pain **11**(2): 149-162.

Forssberg, H. and S. Grillner (1973). "The locomotion of the acute spinal cat injected with clonidine i.v." Brain Research **50**(1): 184-186.

Fraher, J. P. and V. R. O'Sullivan (1989). "Age changes in axon number along the cervical ventral spinal nerve roots in rats." The Journal of Comparative Neurology **280**(2): 171-182.

Fucile, S. (2004). "Ca2+ permeability of nicotinic acetylcholine receptors." Cell Calcium **35**(1): 1-8.

Fulton, B. P. (1987). "Postnatal changes in conduction velocity and soma action potential parameters of rat dorsal root ganglion neurones." Neuroscience Letters **73**(2): 125-130.

Gabbay, H., I. Delvolve, et al. (2002). "Pattern Generation in Caudal-Lumbar and Sacrococcygeal Segments of the Neonatal Rat Spinal Cord." J Neurophysiol **88**(2): 732-739.

Gabbay, H. and A. Lev-Tov (2004). "Alpha-1 Adrenoceptor Agonists Generate a "Fast" NMDA Receptor-Independent Motor Rhythm in the Neonatal Rat Spinal Cord." J Neurophysiol **92**(2): 997-1010.

Garraway, S. M. and S. Hochman (2001). "Serotonin increases the incidence of primary afferent-evoked long-term depression in rat deep dorsal horn neurons." J Neurophysiol **85**(5): 1864-1872.

Gerasimenko, Y., R. R. Roy, et al. (2008). "Epidural stimulation: Comparison of the spinal circuits that generate and control locomotion in rats, cats and humans." Experimental Neurology **209**(2): 417-425.

Gerasimenko, Y. P., V. D. Avelev, et al. (2003). "Initiation of Locomotor Activity in Spinal Cats by Epidural Stimulation of the Spinal Cord." Neuroscience and Behavioral Physiology **33**(3): 247-254.

Gerasimenko, Y. P., I. A. Lavrov, et al. (2005). "Formation of locomotor patterns in decerebrate cats in conditions of epidural stimulation of the spinal cord." Neuroscience and Behavioral Physiology **35**(3): 291-298.

Gerasimenko, Y. P., I. A. Lavrov, et al. (2006). "Spinal cord reflexes induced by epidural spinal cord stimulation in normal awake rats." Journal of Neuroscience Methods **157**(2): 253-263.

Gerasimenko, Y. P., A. N. Makarovskii, et al. (2002). "Control of Locomotor Activity in Humans and Animals in the Absence of Supraspinal Influences." Neuroscience and Behavioral Physiology **32**(4): 417-423.

Giesler, G. J., Jr., R. L. Nahin, et al. (1984). "Postsynaptic dorsal column pathway of the rat. I. Anatomical studies." J Neurophysiol **51**(2): 260-275.

Gildenberg, P. L. and R. M. Hirshberg (1984). "Limited myelotomy for the treatment of intractable cancer pain." J Neurol Neurosurg Psychiatry **47**(1): 94-96.

Gillis, G. B. (1998). "Neuromuscular control of anguilliform locomotion: patterns of red and white muscle activity during swimming in the american eel anguilla rostrata." J Exp Biol **201 (Pt 23)**: 3245-3256.

Glass, L. and M. C. Mackey (1988). From Clocks to Chaos: The Rhythms of Life. Princeton, NJ, Princeton University Press.

Gordh, T., I. Jansson, et al. (1989). "Interactions between noradrenergic and cholinergic mechanisms involved in spinal nociceptive processing." Acta Anaesthesiologica Scandinavica **33**(1): 39-47.

Gordon, I. T. and P. J. Whelan (2006). "Monoaminergic Control of Cauda-Equina-Evoked Locomotion in the Neonatal Mouse Spinal Cord." J Neurophysiol **96**(6): 3122-3129.

Gosgnach, S., G. M. Lanuza, et al. (2006). "V1 spinal neurons regulate the speed of vertebrate locomotor outputs." Nature **440**(7081): 215-219.

Goulding, M. (2009). "Circuits controlling vertebrate locomotion: moving in a new direction." Nat Rev Neurosci **10**(7): 507-518.

Goupillaud, P., A. Grossmann, et al. (1984). "Cycle-octave and related transforms in seismic signal analysis." Geoexploration **23**(1): 85-102.

Gozal, E. A. (2010). Trace amines as novel modulators of spinal motor function. Atlanta, GA, Georgia Institute of Technology.

Graham, A., J. A. Court, et al. (2002). "Immunohistochemical localisation of nicotinic acetylcholine receptor subunits in human cerebellum." Neuroscience **113**(3): 493-507.

Gray, H. (1918). Anatomy of the human body. Philadelphia, Lea & Febiger.

Grillner, S. (1981). Control of Locomotion in Bipeds, Tetrapods, and Fish. Waverly, MD, American Physiol. Society.

Gu, J. and M. Heft (2004). "P2X receptor-mediated purinergic sensory pathways to the spinal cord dorsal horn." Purinergic Signalling **1**(1): 11-16.

Guertin, P., M. J. Angel, et al. (1995). "Ankle extensor group I afferents excite extensors throughout the hindlimb during fictive locomotion in the cat." The Journal of Physiology **487**(Pt 1): 197-209.

Guo, L., K. W. Meacham, et al. (2010). "A PDMS-Based Conical-Well Microelectrode Array for Surface Stimulation and Recording of Neural Tissues." Biomedical Engineering, IEEE Transactions on **57**(10): 2485-2494.

Hayes, H. B., Y.-H. Chang, et al. (2009). "An In Vitro Spinal Cord-Hindlimb Preparation for Studying Behaviorally Relevant Rat Locomotor Function." J Neurophysiol **101**(2): 1114-1122.

Hedo, G. and J. A. Lopez-Garcia (2001). "Alpha-1A adrenoceptors modulate potentiation of spinal nociceptive pathways in the rat spinal cord in vitro." Neuropharmacology **41**(7): 862-869.

Hellstrom-Lindahl, E., O. Gorbounova, et al. (1998). "Regional distribution of nicotinic receptors during prenatal development of human brain and spinal cord." Developmental Brain Research **108**(1-2): 147-160.

Hernandez, P., K. Elbert, et al. (1991). "Spontaneous and NMDA evoked motor rhythms in the neonatal mouse spinal cord: an in vitro study with comparisons to in situ activity." Exp Brain Res **85**(1): 66-74.

Hirshberg, R. M., E. D. Al-Chaer, et al. (1996). "Is there a pathway in the posterior funiculus that signals visceral pain?" Pain **67**(2-3): 291-305.

Hitchcock, E. (1974). "Stereotactic myelotomy." Proc. Roy. Soc. Med. **67**(8): 771-772.

Hochman, S. and B. J. Schmidt (1998). "Whole Cell Recordings of Lumbar Motoneurons During Locomotor-Like Activity in the In Vitro Neonatal Rat Spinal Cord." J Neurophysiol **79**(2): 743-752.

Hoglund, A. U. and H. A. Baghdoyan (1997). "M2, M3 and M4, but not M1, Muscarinic Receptor Subtypes are Present in Rat Spinal Cord." Journal of Pharmacology and Experimental Therapeutics **281**(1): 470-477.

Huang, A., B. R. Noga, et al. (2000). "Spinal Cholinergic Neurons Activated During Locomotion: Localization and Electrophysiological Characterization." Journal of Neurophysiology **83**(6): 3537-3547.

Hultborn, H., et al. (1998). "How do we approach the locomotor network in the mammalian spinal cord?" Ann NY Acad Sci **860**(1): 70-82.

Ichiyama, R. M., Y. Gerasimenko, et al. (2008). "Dose dependence of the 5-HT agonist quipazine in facilitating spinal stepping in the rat with epidural stimulation." Neuroscience Letters **438**(3): 281-285.

Ichiyama, R. M., Y. P. Gerasimenko, et al. (2005). "Hindlimb stepping movements in complete spinal rats induced by epidural spinal cord stimulation." Neuroscience Letters **383**(3): 339-344.

Itier, V. and D. Bertrand (2001). "Neuronal nicotinic receptors: from protein structure to function." FEBS Letters **504**(3): 118-125.

Iwahara, T., Y. Atsuta, et al. (1991). "Locomotion induced by spinal cord stimulation in the neonate rat in vitro." Somatosens Mot Res **8**(3): 281-287.

Iwahara, T., Y. Atsuta, et al. (1992). "Spinal cord stimulation-induced locomotion in the adult cat." Brain Research Bulletin **28**(1): 99-105.

Janig, W. (2006). The Integrative Action of the Autonomic Nervous System: Neurobiology of Homeostasis. Cambridge, UK, Cambridge University Press.

Jankowska, E. (1992). "Interneuronal relay in spinal pathways from proprioceptors." Prog Neurobiol **38**(4): 335-378.

Jankowska, E. and S. Edgley (1993). "Interactions between pathways controlling posture and gait at the level of spinal interneurones in the cat." Prog Brain Res **97**: 161-171.

Jankowska, E., M. G. M. Jukes, et al. (1967). "The Effect of DOPA on the Spinal Cord 6. Half-centre organization of interneurones transmitting effects from the flexor reflex afferents." Acta Physiologica Scandinavica **70**(3-4): 389-402.

Jankowska, E., J. Rastad, et al. (1979). "Segmental and supraspinal input to cells of origin of non-primary fibres in the feline dorsal columns." J Physiol **290**(2): 185-200.

Jiang, Z., K. P. Carlin, et al. (1999). "An in vitro functionally mature mouse spinal cord preparation for the study of spinal motor networks." Brain Research **816**(2): 493-499.

Johnson, D. S., J. Martinez, et al. (1995). "alpha-Conotoxin ImI exhibits subtype-specific nicotinic acetylcholine receptor blockade: preferential inhibition of homomeric alpha 7 and alpha 9 receptors." Mol Pharmacol **48**(2): 194-199.

Jonas, P., J. Bischofberger, et al. (1998). "Corelease of Two Fast Neurotransmitters at a Central Synapse." Science **281**(5375): 419-424.

Jones, D. J., D. E. Kendall, et al. (1982). "Adrenergic receptors in rat spinal cord." Neuropharmacology **21**(4): 367-370.

Jordan, L. M. (1998). "Initiation of Locomotion in Mammals." Annals of the New York Academy of Sciences **860**(1): 83-93.

Jordan, L. M. and B. J. Schmidt (2002). "Propriospinal neurons involved in the control of locomotion: potential targets for repair strategies?" Prog Brain Res **137**: 125-139.

Joyner, R. W., M. Westerfield, et al. (1978). "A numerical method to model excitable cells." Biophys J **22**(2): 155-170.

Julius, D. and A. I. Basbaum (2001). "Molecular mechanisms of nociception." Nature **413**(6852): 203-210.

Kalamida, D., K. Poulas, et al. (2007). "Muscle and neuronal nicotinic acetylcholine receptors. Structure, function and pathogenicity." FEBS J **274**(15): 3799-3845.

Kandel, E. R., J. H. Schwartz, et al. (2000). Principles of Neural Science. New York, NY, McGraw-Hill.

Kasparov, S. A. (1992). "[Viscerosomatic convergence on the lumbar interneurons of the dorsal horn of the spinal cord in cats and rats]." Neirofiziologiia **24**(1): 3-11.

Katter, J. T., R. J. Dado, et al. (1996). "Spinothalamic and spinohypothalamic tract neurons in the sacral spinal cord of rats. II. Responses to cutaneous and visceral stimuli." J Neurophysiol **75**(6): 2606-2628.

Kawatani, M., J. Nagel, et al. (1986). "Identification of neuropeptides in pelvic and pudendal nerve afferent pathways to the sacral spinal cord of the cat." The Journal of Comparative Neurology **249**(1): 117-132.

Kayalioglu, G. (2009). The spinal nerves. The Spinal Cord: A Christopher and Dana Reeve Foundation Text and Atlas. United States, Academic Press**:** 37-56.

Kerlavage, A. R., C. M. Fraser, et al. (1986). "Molecular structure and evolution of adrenergic and cholinergic receptors." Proteins: Structure, Function, and Bioinformatics **1**(4): 287-301.

Khan, I. M., T. L. Yaksh, et al. (1994). "Ligand specificity of nicotinic acetylcholine receptors in rat spinal cord: studies with nicotine and cytisine." J Pharmacol Exp Ther **270**(1): 159-166.

Kiehn, O. and S. J. B. Butt (2003). "Physiological, anatomical and genetic identification of CPG neurons in the developing mammalian spinal cord." Progress in Neurobiology **70**(4): 347-361.

Kiehn, O. and O. Kjaerulff (1996). "Spatiotemporal characteristics of 5-HT and dopamine-induced rhythmic hindlimb activity in the in vitro neonatal rat." Journal of Neurophysiology **75**(4): 1472-1482.

Kiehn, O. and O. Kjaerulff (1998). "Distribution of Central Pattern Generators for Rhythmic Motor Outputs in the Spinal Cord of Limbed Vertebrates." Ann NY Acad Sci **860**(1): 110-129.

Kiehn, O., K. T. Sillar, et al. (1999). "Effects of noradrenaline on locomotor rhythm-generating networks in the isolated neonatal rat spinal cord." J Neurophysiol **82**(2): 741-746.

Kirkup, A. J., A. M. Brunsden, et al. (2001). "Receptors and Transmission in the Brain-Gut Axis: Potential for Novel Therapies: I. Receptors on visceral afferents." Am J Physiol Gastrointest Liver Physiol **280**(5): G787-794.

Kjaerulff, O., I. Barajon, et al. (1994). "Sulphorhodamine-labelled cells in the neonatal rat spinal cord following chemically induced locomotor activity in vitro." The Journal of Physiology **478**(Pt 2): 265-273.

Kjaerulff, O. and O. Kiehn (1996). "Distribution of Networks Generating and Coordinating Locomotor Activity in the Neonatal Rat Spinal Cord In Vitro: A Lesion Study." J. Neurosci. **16**(18): 5777-5794.

Klein, D. A., A. Patino, et al. (2010). "Flexibility of Motor Pattern Generation Across Stimulation Conditions by the Neonatal Rat Spinal Cord." Journal of Neurophysiology **103**(3): 1580-1590.

Kremer, E. and A. Lev-Tov (1997). "Localization of the Spinal Network Associated With Generation of Hindlimb Locomotion in the Neonatal Rat and Organization of Its Transverse Coupling System." J Neurophysiol **77**(3): 1155-1170.

Kremer, E. and A. Lev-Tov (1998). "GABA-receptor-independent dorsal root afferents depolarization in the neonatal rat spinal cord." Journal of Neurophysiology **79**(5): 2581-2592.

Kriellaars, D. J., R. M. Brownstone, et al. (1994). "Mechanical entrainment of fictive locomotion in the decerebrate cat." J Neurophysiol **71**(6): 2074-2086.

Kudo, N. and T. Yamada (1987). "Locomotor activity in a spinal cord-hindlimb muscles preparation of the newborn rat studied in vitro." Neuroscience Letters **75**(1): 43-48.

Kwan, A. C., S. B. Dietz, et al. (2009). "Activity of Hb9 Interneurons during Fictive Locomotion in Mouse Spinal Cord." The Journal of Neuroscience **29**(37): 11601-11613.

Lafreniere-Roula, M. and D. A. McCrea (2005). "Deletions of Rhythmic Motoneuron Activity During Fictive Locomotion and Scratch Provide Clues to the Organization of the Mammalian Central Pattern Generator." Journal of Neurophysiology **94**(2): 1120-1132.

Lambrecht, G. (2000). "Agonists and antagonists acting at P2X receptors: selectivity profiles and functional implications." Naunyn-Schmiedeberg's Archives of Pharmacology **362**(4): 340-350.

Lanuza, G. M., S. Gosgnach, et al. (2004). "Genetic Identification of Spinal Interneurons that Coordinate Left-Right Locomotor Activity Necessary for Walking Movements." Neuron **42**(3): 375-386.

Lavrov, I., Y. P. Gerasimenko, et al. (2006). "Plasticity of Spinal Cord Reflexes After a Complete Transection in Adult Rats: Relationship to Stepping Ability." Journal of Neurophysiology **96**(4): 1699-1710.

Lazareno, S., A. Popham, et al. (2000). "Allosteric interactions of staurosporine and other indolocarbazoles with N-[methyl-(3)H]scopolamine and acetylcholine at muscarinic receptor subtypes: identification of a second allosteric site." Mol Pharmacol **58**(1): 194-207.

Lazareno, S., A. Popham, et al. (2002). "Analogs of WIN 62,577 define a second allosteric site on muscarinic receptors." Mol Pharmacol **62**(6): 1492-1505.

Lev-Tov, A., I. Delvolve, et al. (2000). "Sacrocaudal Afferents Induce Rhythmic Efferent Bursting in Isolated Spinal Cords of Neonatal Rats." J Neurophysiol **83**(2): 888-894.

Lev-Tov, A., A. Etlin, et al. (2010). "Sensory-induced activation of pattern generators in the absence of supraspinal control." Ann NY Acad Sci **1198**(Neurons and Networks in the Spinal Cord): 54-62.

Lev-Tov, A. and M. J. O'Donovan (1995). "Calcium imaging of motoneuron activity in the en-bloc spinal cord preparation of the neonatal rat." Journal of Neurophysiology **74**(3): 1324-1334.

Lev-Tov, A. and M. Pinco (1992). "In vitro studies of prolonged synaptic depression in the neonatal rat spinal cord." J Physiol **447**(1): 149-169.

Levine, J. D. and N. Alessandri-Haber (2007). "TRP channels: targets for the relief of pain." Biochim Biophys Acta **1772**(8): 989-1003.

Lindblom, U. and B. A. Meyerson (1975). "Influence on touch, vibration and cutaneous pain of dorsal column stimulation in man." PAIN **1**(3): 257-270.

Linderoth, B., G. Gherardini, et al. (1995). "Preemptive spinal cord stimulation reduces ischemia in an animal model of vasospasm." Neurosurgery **37**(2): 266-271; discussion 271-262.

Linderoth, B., G. Gherardini, et al. (1995). "Severe peripheral ischemia after vasospasm may be prevented by spinal cord stimulation. A preliminary report of a study in a free-flap animal model." Acta Neurochir Suppl **64**: 101-105.

Linderoth, B., P. Herregodts, et al. (1994). "Sympathetic Mediation of Peripheral Vasodilation Induced by Spinal Cord Stimulation: Animal Studies of the Role of Cholinergic and Adrenergic Receptor Subtypes." Neurosurgery **35**(4): 711-719.

Liu, J. and L. M. Jordan (2005). "Stimulation of the Parapyramidal Region of the Neonatal Rat Brain Stem Produces Locomotor-Like Activity Involving Spinal 5-HT7 and 5-HT2A Receptors." J Neurophysiol **94**(2): 1392-1404.

Loewy, A. D. and S. McKellar (1981). "Serotonergic projections from the ventral medulla to the intermediolateral cell column in the rat." Brain Research **211**(1): 146-152.

Lohr, K. and S. Hochman (2010). Rhythmic sympathetic efferents in response to 5-HT/NMDA in the neonatal rat spinal cord. Atlanta, GA.

Lutjemeier, B. J., L. F. Ferreira, et al. (2008). "Muscle microvascular hemoglobin concentration and oxygenation within the contraction-relaxation cycle." Respiratory Physiology & Neurobiology **160**(2): 131-138.

Lutjemeier, B. J., A. Miura, et al. (2005). "Muscle contraction-blood flow interactions during upright knee extension exercise in humans." Journal of Applied Physiology **98**(4): 1575-1583.

Machacek, D. W., S. M. Garraway, et al. (2001). "Serotonin 5-HT2 receptor activation induces a long-lasting amplification of spinal reflex actions in the rat." J Physiol **537**(1): 201-207.

Machacek, D. W. and S. Hochman (2006). "Noradrenaline Unmasks Novel Self-Reinforcing Motor Circuits within the Mammalian Spinal Cord." J. Neurosci. **26**(22): 5920-5928.

Magnuson, D. S. K. and T. C. Trinder (1997). "Locomotor Rhythm Evoked by Ventrolateral Funiculus Stimulation in the Neonatal Rat Spinal Cord In Vitro." J Neurophysiol **77**(1): 200-206.

Mandadi, S., S. T. Nakanishi, et al. (2009). "Locomotor networks are targets of modulation by sensory transient receptor potential vanilloid 1 and transient receptor potential melastatin 8 channels." Neuroscience **162**(4): 1377-1397.

Marchetti, C., M. Beato, et al. (2001). "Alternating rhythmic activity induced by dorsal root stimulation in the neonatal rat spinal cord in vitro." J Physiol **530**(1): 105-112.

Marcoux, J. and S. Rossignol (2000). "Initiating or Blocking Locomotion in Spinal Cats by Applying Noradrenergic Drugs to Restricted Lumbar Spinal Segments." J. Neurosci. **20**(22): 8577-8585.

Marder, E. and R. L. Calabrese (1996). "Principles of rhythmic motor pattern generation." Physiol Rev **76**(3): 687-717.

Markham, J. A., P. E. Phelps, et al. (1991). "Development of rostrocaudal dendritic bundles in rat thoracic spinal cord: analysis of cholinergic sympathetic preganglionic neurons." Brain Res Dev Brain Res **61**(2): 229-236.

McIntosh, J. M., N. Absalom, et al. (2009). "Alpha9 nicotinic acetylcholine receptors and the treatment of pain." Biochemical Pharmacology **78**(7): 693-702.

McKenna, K. E. and I. Nadelhaft (1986). "The organization of the pudendal nerve in the male and female rat." The Journal of Comparative Neurology **248**(4): 532-549.

McLachlan, E., J. Keast, et al. (2009). Spinal autonomic preganglionic neurons: the visceral efferent system of the spinal cord. The Spinal Cord: A Christopher and Dana Reeve Foundation Text and Atlas. United States, Academic Press**:** 115-129.

Meacham, K. W., R. J. Giuly, et al. (2008). "A lithographically-patterned, elastic multi-electrode array for surface stimulation of the spinal cord." Biomed Microdevices **10**(2): 259-269.

Mellen, N. M. and J. L. Feldman (2000). "Phasic lung inflation shortens inspiration and respiratory period in the lung-attached neonate rat brain stem spinal cord." Journal of Neurophysiology **83**(5): 3165-3168.

Meyerson, B. A., B. Ren, et al. (1995). "Spinal cord stimulation in animal models of mononeuropathy: effects on the withdrawal response and the flexor reflex." Pain **61**(2): 229-243.

Miles, G. B., R. Hartley, et al. (2007). "Spinal cholinergic interneurons regulate the excitability of motoneurons during locomotion." Proc Natl Acad Sci U S A **104**(7): 2448-2453.

Millan, M. J. (1992). "Evidence that an alpha 2A-adrenoceptor subtype mediates antinociception in mice." Eur J Pharmacol **215**(2-3): 355-356.

Millar, N. S. and C. Gotti (2009). "Diversity of vertebrate nicotinic acetylcholine receptors." Neuropharmacology **56**(1): 237-246.

Milner, T. A., S. F. Morrison, et al. (1988). "Phenylethanolamine N-methyltransferase-containing terminals synapse directly on sympathetic preganglionic neurons in the rat." Brain Research **448**(2): 205-222.

Mor, Y. and A. Lev-Tov (2007). "Analysis of rhythmic patterns produced by spinal neural networks." J Neurophysiol **98**(5): 2807-2817.

Mouchet, P., M. Manier, et al. (1986). "Immunohistochemical study of catecholaminergic cell bodies in the rat spinal cord." Brain Res Bull **16**(3): 341-353.

Nadelhaft, I. and A. M. Booth (1984). "The location and morphology of preganglionic neurons and the distribution of visceral afferents from the rat pelvic nerve: a horseradish peroxidase study." J Comp Neurol **226**(2): 238-245.

Naguib, M. and T. L. Yaksh (1997). "Characterization of muscarinic receptor subtypes that mediate antinociception in the rat spinal cord." Anesthesia & Analgesia **85**(4): 847-853.

Nakatsuka, T. and J. Gu (2006). "P2X purinoceptors and sensory transmission." Pflügers Archiv European Journal of Physiology **452**(5): 598-607.

Ness, T. J. and G. F. Gebhart (1990). "Visceral pain: a review of experimental studies." PAIN **41**(2): 167-234.

Nissl, F. (1894). Ueber die sogenannten Granula der Nervenzellen. Neurologisches Zentralblatt. E. Mendel. Leipzig, Veit and Comp. **13:** 781-789.

Noble, R. and J. S. Riddell (1988). "Cutaneous excitatory and inhibitory input to neurones of the postsynaptic dorsal column system in the cat." J Physiol **396**: 497-513.

Noguera, M. A., M. D. Ivorra, et al. (1996). "Functional evidence of inverse agonism in vascular smooth muscle." Br J Pharmacol **119**(1): 158-164.

Nussbaumer, J. C., M. Yanagisawa, et al. (1989). "Pharmacological properties of a C-fibre response evoked by saphenous nerve stimulation in an isolated spinal cord-nerve preparation of the newborn rat." Br J Pharmacol **98**(2): 373-382.

Oakley, J. C. and J. P. Prager (2002). "Spinal Cord Stimulation: Mechanisms of Action." Spine **27**(22): 2574-2583.

Oguz Kayaalp, S. and N. H. Neff (1980). "Regional distribution of cholinergic muscarinic receptors in spinal cord." Brain Research **196**(2): 429-436.

Olave, M. J., N. Puri, et al. (2002). "Myelinated and unmyelinated primary afferent axons form contacts with cholinergic interneurons in the spinal dorsal horn." Exp Brain Res **145**(4): 448-456.

Palecek, J. (2004). "The role of dorsal columns pathway in visceral pain." Physiol. Res. **53**(Suppl. 1): S125-S130.

Quevedo, J. (2011). Unknown mechanism for high intensity stimulation block of low-threshold afferent components. J. Anderson. Atlanta.

Rajaofetra, N., J. L. Ridet, et al. (1992). "Immunocytochemical mapping of noradrenergic projections to the rat spinal cord with an antiserum against noradrenaline." J Neurocytol **21**(7): 481-494.

Rall, W. (1959). "Branching dendritic trees and motoneuron membrane resistivity." Exp Neurol **1**: 491-527.

Ramon y Cajal, S. (1909). Histologie du Système Nerveux de l'Homme et des Vertébrés. Madrid, Consejo Sup. Invest. Cient. Tome I.

Rank, M. M., K. C. Murray, et al. (2011). "Adrenergic Receptors Modulate Motoneuron Excitability, Sensory Synaptic Transmission and Muscle Spasms After Chronic Spinal Cord Injury." Journal of Neurophysiology **105**(1): 410-422.

Ranson, S. W. (1914). "The tract of Lissauer and the substantia gelatinosa Rolandi." American Journal of Anatomy **16**(1): 97-126.

Reddy, S. V., J. L. Maderdrut, et al. (1980). "Spinal cord pharmacology of adrenergic agonist-mediated antinociception." Journal of Pharmacology and Experimental Therapeutics **213**(3): 525-533.

Richter, D. W. (1982). "Generation and maintenance of the respiratory rhythm." The Journal of experimental biology **100**: 93-107.

Ridet, J.-L., F. Sandillon, et al. (1992). "Spinal dopaminergic system of the rat: light and electron microscopic study using an antiserum against dopamine, with particular emphasis on synaptic incidence." Brain Research **598**(1-2): 233-241.

Rogers, A. M., N. R. Saunders, et al. (2006). "Rapid vasoregulatory mechanisms in exercising human skeletal muscle: dynamic response to repeated changes in contraction

intensity." American Journal of Physiology - Heart and Circulatory Physiology **291**(3): H1065-H1073.

Rossier, O., L. Abuin, et al. (1999). "Inverse agonism and neutral antagonism at alpha(1a)- and alpha(1b)-adrenergic receptor subtypes." Mol Pharmacol **56**(5): 858-866.

Roudet, C., M. Savasta, et al. (1993). "Normal distribution of alpha-1-adrenoceptors in the rat spinal cord and its modification after noradrenergic denervation: a quantitative autoradiographic study." J Neurosci Res **34**(1): 44-53.

Russo, R. E., R. Delgado-Lezama, et al. (2000). "Dorsal root potential produced by a TTX-insensitive micro-circuitry in the turtle spinal cord." J Physiol **528 Pt 1**: 115-122.

Rybak, I. A., N. A. Shevtsova, et al. (2006). "Modelling spinal circuitry involved in locomotor pattern generation: insights from deletions during fictive locomotion." J Physiol **577**(2): 617-639.

Schmidt, B. J. and L. M. Jordan (2000). "The role of serotonin in reflex modulation and locomotor rhythm production in the mammalian spinal cord." Brain Res Bull **53**(5): 689-710.

Schmidt, B. J. and L. M. Jordan (2000). "The role of serotonin in reflex modulation and locomotor rhythm production in the mammalian spinal cord." Brain Research Bulletin **53**(5): 689-710.

Schomburg, E. D., H. Steffens, et al. (2003). "Rhythmic phrenic, intercostal and sympathetic activity in relation to limb and trunk motor activity in spinal cats." Neuroscience Research **46**(2): 229-240.

Schouenborg, J. and B. H. Sjolund (1983). "Activity evoked by A- and C-afferent fibers in rat dorsal horn neurons and its relation to a flexion reflex." J Neurophysiol **50**(5): 1108-1121.

Schwinn, D. A. and G. A. Michelotti (2000). "alpha1-adrenergic receptors in the lower urinary tract and vascular bed: potential role for the alpha1d subtype in filling symptoms and effects of ageing on vascular expression." BJU Int **85 Suppl 2**: 6-11.

Seifert, R. and K. Wenzel-Seifert (2002). "Constitutive activity of G-protein-coupled receptors: cause of disease and common property of wild-type receptors." Naunyn Schmiedebergs Arch Pharmacol **366**(5): 381-416.

Sillar, K. T., C. A. Reith, et al. (1998). "Development and aminergic neuromodulation of a spinal locomotor network controlling swimming in Xenopus larvae." Ann N Y Acad Sci **860**: 318-332.

Sinnamon, H. M. (1993). "Preoptic and hypothalamic neurons and the initiation of locomotion in the anesthetized rat." Progress in neurobiology **41**(3): 323-344.

Smith, J. C., J. L. Feldman, et al. (1988). "Neural mechanisms generating locomotion studied in mammalian brain stem- spinal cord in vitro." FASEB J. **2**(7): 2283-2288.

Smith, M. S., U. B. Schambra, et al. (1999). "Alpha1-adrenergic receptors in human spinal cord: specific localized expression of mRNA encoding alpha1-adrenergic receptor subtypes at four distinct levels." Brain Res Mol Brain Res **63**(2): 254-261.

Sqalli-Houssaini, Y. and J.-R. Cazalets (2000). "Noradrenergic control of locomotor networks in the in vitro spinal cord of the neonatal rat." Brain Research **852**(1): 100-109.

Stavroula Nicolopoulos-Stournaras, J. F. I. (1983). "Motor neuron columns in the lumbar spinal cord of the rat." The Journal of Comparative Neurology **217**(1): 75-85.

Stephan, F. K. and I. Zucker (1972). "Circadian Rhythms in Drinking Behavior and Locomotor Activity of Rats Are Eliminated by Hypothalamic Lesions." Proceedings of the National Academy of Sciences **69**(6): 1583-1586.

Stone, L. S., C. Broberger, et al. (1998). "Differential Distribution of Œ±2A and Œ±2C Adrenergic Receptor Immunoreactivity in the Rat Spinal Cord." The Journal of Neuroscience **18**(15): 5928-5937.

Strack, A. M., W. B. Sawyer, et al. (1988). "Spinal origin of sympathetic preganglionic neurons in the rat." Brain Research **455**(1): 187-191.

Strauss, I. and A. Lev-Tov (2003). "Neural Pathways Between Sacrocaudal Afferents and Lumbar Pattern Generators in Neonatal Rats." J Neurophysiol **89**(2): 773-784.

Struijk, J. J., J. Holsheimer, et al. (1992). "Recruitment of dorsal column fibers in spinal cord stimulation: influence of collateral branching." IEEE Trans Biomed Eng **39**(9): 903-912.

Su, P. C., W.-h. L. Su, et al. (1979). "Pre- and Postsynaptic Effects of Pancuronium at the Neuromuscular Junction of the Mouse." Anesthesiology **50**(3): 199-204.

Su, X., R. E. Wachtel, et al. (1999). "Capsaicin sensitivity and voltage-gated sodium currents in colon sensory neurons from rat dorsal root ganglia." Am J Physiol Gastrointest Liver Physiol **277**(6): G1180-1188.

Sugaya, K. and W. C. De Groat (1994). "Micturition reflexes in the in vitro neonatal rat brain stem-spinal cord-bladder preparation." American Journal of Physiology - Regulatory, Integrative and Comparative Physiology **266**(3): R658-R667.

Sugiura, Y., N. Terui, et al. (1989). "Difference in distribution of central terminals between visceral and somatic unmyelinated (C) primary afferent fibers." Journal of Neurophysiology **62**(4): 834-840.

Sugiura, Y. and Y. Tonosaki (1995). Spinal organization of ynmyelinated visceral afferent fibers in comparison with somatic afferent fibers. Visceral Pain. G. F. Gebhart. **5**.

Swanson, L. W., G. J. Mogenson, et al. (1984). "Evidence for a projection from the lateral preoptic area and substantia innominata to the 'mesencephalic locomotor region' in the rat." Brain Research **295**(1): 161-178.

Szolcsányi, J. (2004). "Forty years in capsaicin research for sensory pharmacology and physiology." Neuropeptides **38**(6): 377-384.

Tominaga, M. and T. Tominaga (2005). "Structure and function of TRPV1." Pflügers Archiv European Journal of Physiology **451**(1): 143-150.

Torrence, C. and G. P. Compo (1998). "A practical guide to wavelet analysis." Bull Am Meterol Soc **79**: 61-78.

Vega, J. A., F. Amenta, et al. (1991). "Presence of catecholamine-related enzymes in a subpopulation of primary sensory neurons in dorsal root ganglia of the rat." Cell Mol Biol **37**(5): 519-530.

Vejsada, R., J. Palecek, et al. (1985). "Postnatal development of conduction velocity and fibre size in the rat tibial nerve." International Journal of Developmental Neuroscience **3**(5): 583-589, 591-595.

Vogelstein, R. J., N. V. Thakor, et al. (2005). Electrical Stimulation of a Spinal Central Pattern Generator for Locomotion. Proceedings of the 2nd International IEEE EMBS Conference on Neural Engineering, Arlington, Virginia.

von Euler, C. (1983). "On the central pattern generator for the basic breathing rhythmicity." Journal of applied physiology: respiratory, environmental and exercise physiology **55**(6): 1647-1659.

Wada, E., K. Wada, et al. (1989). "Distribution of alpha2, alpha3, alpha4, and beta2 neuronal nicotinic receptor subunit mRNAs in the central nervous system: A hybridization histochemical study in the rat." The Journal of Comparative Neurology **284**(2): 314-335.

Wada, T., T. Otsu, et al. (1996). "Characterization of [alpha]1-adrenoceptor subtypes in rat spinal cord." European Journal of Pharmacology **312**(2): 263-266.

Wall, P. D. (1958). "Excitability changes in afferent fibre terminations and their relation to slow potentials." The Journal of Physiology **142**(1): i3-21.

Walløe, L. and J. Wesche (1988). "Time course and magnitude of blood flow changes in the human quadriceps muscles during and following rhythmic exercise." The Journal of Physiology **405**(1): 257-273.

Wang, Z., L. Li, et al. (2008). "Early Postnatal Development of Reciprocal Ia Inhibition in the Murine Spinal Cord." Journal of Neurophysiology **100**(1): 185-196.

Weindlmayr-Goettel, M., H. Gilly, et al. (1993). "Lipid solubility of pancuronium and vecuronium determined by N-octnol/water partitioning." British Journal of Anaesthesia **70**(5): 579-580.

Weiss, L. and R. O. Greep (1977). Histology. New York, McGraw-Hill.

Werry, E. L., G. J. Liu, et al. (2006). "Glutamate-stimulated ATP release from spinal cord astrocytes is potentiated by substance P." Journal of Neurochemistry **99**(3): 924-936.

Westlund, K. N., R. M. Bowker, et al. (1983). "Noradrenergic projections to the spinal cord of the rat." Brain Research **263**(1): 15-31.

Whelan, P., A. Bonnot, et al. (2000). "Properties of Rhythmic Activity Generated by the Isolated Spinal Cord of the Neonatal Mouse." J Neurophysiol **84**(6): 2821-2833.

Whelan, P. J. (1996). "Control of locomotion in the decerebrate cat." Progress in neurobiology **49**(5): 481-515.

Willis Jr, W. D. (2007). "The somatosensory system, with emphasis on structures important for pain." Brain Research Reviews **55**(2): 297-313.

Willis, W. D., E. D. Al-Chaer, et al. (1999). "A visceral pain pathway in the dorsal column of the spinal cord." Proceedings of the National Academy of Sciences of the United States of America **96**(14): 7675-7679.

Willis, W. D. and R. E. Coggeshall (1991). Sensory mechanisms of the spinal cord. New York, Plenum Press.

Wilson, J. M., R. Hartley, et al. (2005). "Conditional rhythmicity of ventral spinal interneurons defined by expression of the Hb9 homeodomain protein." J Neurosci **25**(24): 5710-5719.

Winfree, A. T. (1980). The Geometry of Biological Time. New York, Springer-Verlag.

Zagoraiou, L., T. Akay, et al. (2009). "A cluster of cholinergic premotor interneurons modulates mouse locomotor activity." Neuron **64**(5): 645-662.

Zar, J. (1999). Biostatistical Analysis, Prentice Hall.

Zhang, Y., S. Narayan, et al. (2008). "V3 Spinal Neurons Establish a Robust and Balanced Locomotor Rhythm during Walking." Neuron **60**(1): 84-96.

Zhong, G., M. A. Masino, et al. (2007). "Persistent Sodium Currents Participate in Fictive Locomotion Generation in Neonatal Mouse Spinal Cord." The Journal of Neuroscience **27**(17): 4507-4518.

Zimmerman, A. and S. Hochman (2011). 5-HT depresses afferent input. J. Anderson. Atlanta, GA, Personal communication.

Zimmerman, A., M. Sawchuk, et al. (2011). Evidence for post-ganglionic fibers in paravertebral chain. J. Anderson. Atlanta, GA, Personal Communication.